

STEADY STATE STABILITY ANALYSIS OF AC-DC POWER SYSTEMS

by

© FAROOQ AHMAD QURESHY

A Thesis

Submitted to the School of Graduate Studies

in Partial Fulfilment of the Requirements

for the Degree of

Doctor of Philosophy

McMaster University

May 1985

STEADY STATE STABILITY ANALYSIS OF AC-DC POWER SYSTEMS

بِسْمِ اللَّهِ الرَّحْمَنِ الرَّحِيمِ

In the name of Allah, the Beneficent,
the Merciful.

Glory be to God, and
praise be to God! There is no
deity save God. God is Supreme.
There is no strength nor power
save in God.

سُبْحَانَ اللَّهِ وَالْحَمْدُ لِلَّهِ
وَلَا إِلَهَ إِلَّا اللَّهُ وَاللَّهُ أَكْبَرُ
وَلَا حَوْلَ وَلَا قُوَّةَ إِلَّا بِاللَّهِ.

DOCTOR OF PHILOSOPHY (1985)
(Electrical & Computer Engineering)

McMaster University,
Hamilton, Ontario

TITLE: STEADY STATE STABILITY ANALYSIS OF AC-DC POWER
SYSTEMS

AUTHOR: Farooq Ahmad Qureshy
B.Sc. (Elect. Eng., West Pakistan University of
Engineering & Technology, Lahore)
M.S. (Elect. Eng., Polytechnic Institute of New
York, New York)

SUPERVISOR: R.T.H. Alden, Ph.D., P.Eng.

NUMBER OF PAGES: xvi, 184

ACKNOWLEDGEMENTS

I would like to express my sincere appreciation and gratitude to Professor R.T.H. Alden for his guidance and encouragement and for having made this work a pleasurable exchange of information. Thanks are due to Professors N.K. Sinha, R.D. Findlay and Dr. P. Kundur for their continuing support and helpful advice.

Thanks are rightly due to my associates Dr. I. El-Nahas and Dr. M. El-Sobki for their useful discussions both on mathematical technique and physical interpretation.

The financial support of McMaster University, the Natural Sciences and Engineering Research Council of Canada and the Government of Ontario (Ontario Graduate Scholarship Program) is gratefully acknowledged.

I would like to thank Mrs. Dianne Crabtree of Dianne's Word Processing Service, Burlington, Ontario, for her typing and cheerful cooperation in the preparation of this manuscript.

Finally, I would like to express special thanks to my wife Shahnaz and parents Asrar and Mutahhira Qureshy for their love, encouragement and support. It is to them that I dedicate this thesis.



ABSTRACT

This thesis presents a comprehensive approach for the steady state stability analysis of AC-DC power systems. A new method is presented for the evaluation of the system state matrix which is then used to determine system stability and develop new algorithms for the stability analysis and control of large power systems.

The method exploits the powerful features of the Component Connection Method for power system modelling and overcomes the disadvantages of the earlier methods. The state matrix is formulated from two separate sets of equations. One set models the component subsystems whereas the other defines the interconnection between the subsystems. The main advantage of this is the great flexibility provided in the modelling of the power system components. As long as the input-output quantities are fixed the modelling complexity of the subsystems may be changed without affecting the interconnection equation. A compact interconnection equation has been derived relating machine voltages and currents in the presence of a multiterminal HVDC network. The subsystems retain their physical identity in this formulation and allow the derivatives of the system state matrix to be easily obtained. The power system operating point is determined by a new sequential AC-DC loadflow scheme. Any AC loadflow method can be

used. The DC network is solved using the Gauss-Siedel method and any HVDC network configuration and terminals control scheme can be accommodated. The DC network solution need not be repeated and the method ensures that a feasible HVDC system operating point is selected.

A new eigenvalue tracking algorithm has been developed based on the evaluation of the sensitivity of a matrix determinant. It iteratively updates the eigenvalues following any change in the system state matrix at one-third the cost of eigenvalue computation using the QR algorithm. Used together with the proposed state matrix formulation method, it is particularly useful for identifying the modes due to any particular subsystem.

Two new methods for decentralized pole placement have been developed. The first method assigns the given poles among the various subsystems and the elements of the feedback gain matrix are varied to cancel the effects of the system interconnection. The second method is based on the sensitivity of a matrix determinant and solves the decentralized pole placement problem as an inverse eigenvalue problem. Both methods are easy to implement and computationally efficient.

The methods presented in this thesis have all been verified by applying them to realistic power system models. These have included a single machine infinite bus system, a three-machine AC system with six buses and nine lines and a three-machine three-terminal AC-DC system. These applications include simulation, analysis and decentralized controller design.

LIST OF PRINCIPAL SYMBOLS

Generating Unit Model

v_d, v_q	- stator voltages in direct- and quadrature-axis circuits, respectively.
v_D, v_Q	- stator voltages in DQ synchronous reference frame.
v_t	- stator voltage.
i_d, i_q	- stator currents in direct- and quadrature-axis circuits, respectively.
i_D, i_Q	- stator currents in DQ synchronous reference frame.
λ_d, λ_q	- stator flux linkages in direct- and quadrature-axis circuits, respectively.
x_d, x_q	- synchronous reactances in direct- and quadrature axis circuits, respectively.
x_f, x_{kd}	- self reactances of field and direct-axis damper windings.
x_{kq}	- self reactances of quadrature-axis damper windings.
x_{af}	- stator field mutual reactance.
x_{ad}, x_{aq}	- stator-rotor mutual reactances with damper windings.
r_s	- stator resistance.
r_f, r_{kd}, r_{kq}	- field and damper winding resistances.

i_f, i_{kd}, i_{kq}	- currents in field and damper windings.
E_{fd}	- field voltage.
x_e	- total reactance between generator terminal and busbar.
r_e	- total resistance between generator terminal and busbar.
δ	- rotor angle.
ω_0	- angular frequency of infinite bus.
H	- inertia constant.
T_m	- input torque to generator shaft.
T_e	- generator output electrical torque.
ω	- angular speed of rotor.
P, Q	- active and reactive power.
E	- voltage behind synchronous impedance.
E_d'	- voltage proportional to quadrature-axis flux linkage.
E_q'	- voltage proportional to direct-axis flux linkage.
x_d'	- stator transient reactance.
τ_{qo}'	- quadrature-axis transient open-circuit time constant.
τ_{do}'	- direct-axis transient open-circuit time constant.
D	- damping coefficient.

Excitation System

V_R	- voltage sensor output.
V_l	- amplifier output voltage.

V_3	- stabilizer output voltage.
τ_R	- voltage sensor time constant.
τ_A	- amplifier time constant.
τ_F	- stabilizing loop time constant.
τ_E	- exciter time constant.
K_A	- amplifier gain.
K_F	- stabilizing loop gain
K_E	- exciter gain.
V_{ref}	- exciter reference voltage.

DC Terminal Controller

I_{DC}	- terminal DC current.
V_{DC}	- terminal DC voltage.
I_{REF}	- reference current.
V_{REF}	- reference voltage
V_{ST}	- stabilizing input.
α	- firing angle.
K_{AC}	- constant current controller amplifier gain.
K_{AV}	- constant voltage controller amplifier gain.
K_S	- stabilizing input gain.
τ_C	- current controller time constant.
τ_V	- voltage controller time constant.

DC Converter Stabilizer

K_{ST}	- stabilizer gain.
K_V	- voltage feedback gain.

K_w - speed feedback gain.
 K_δ - rotor angle feedback gain.
 τ_1, τ_2, τ_3 - lead-lag time constants.
 V_{ST} - output voltage.

Miscellaneous

Δ - prefix denoting incremental change.
 \cdot - superscript denoting differentiation with respect to time.
 T or t - superscript denoting matrix or vector transpose.
 -1 - superscript denoting matrix inverse.
 s - Laplace operator.

TABLE OF CONTENTS

	PAGE
ACKNOWLEDGEMENTS	iii
ABSTRACT	iv
LIST OF PRINCIPAL SYMBOLS	vi
LIST OF FIGURES	xiv
LIST OF TABLES	xvi
CHAPTER 1 INTRODUCTION	1
1.1 Dynamic Properties of Power Systems	1
1.2 Steady State Stability	3
1.3 The Role of HVDC	5
1.4 Objective of the Thesis	9
1.5 Thesis Structure	11
CHAPTER 2 A REVIEW OF METHODS FOR STEADY STATE ANALYSIS OF POWER SYSTEMS INCLUDING MULTITERMINAL HVDC LINKS	13
2.1 Introduction	13
2.2 Loadflow Analysis Methods for AC-DC Networks	14
2.2.1 Sequential Methods	16
2.2.2 Integrated Methods	17
2.2.3 Discussion	18
2.3 Steady State Stability Evaluation for AC Systems	18
2.3.1 Formulation of the State Matrices	20
2.3.2 Analysis Techniques	25
2.4 Inclusion of HVDC System	27
2.5 Summary	28

TABLE OF CONTENTS (continued)

	PAGE
CHAPTER 3 LOADFLOW ANALYSIS OF MULTITERMINAL AC-DC SYSTEM	29
3.1 Introduction	29
3.2 Converter Equations	31
3.3 DC Network Configurations	34
3.4 DC Converter Operating Modes	37
3.5 DC Loadflow Equations	40
3.6 AC Loadflow	41
3.7 AC-DC Loadflow Method	42
3.8 Test Results	45
3.8.1 A Nine-Bus, Three Terminal AC-DC Power System	45
3.8.2 A Six-Terminal Assymmetrical Bipolar HVDC Network	50
3.9 Summary	53
CHAPTER 4 STATE MATRIX FORMULATION OF AC POWER SYSTEMS	54
4.1 Introduction	54
4.2 The Component Connection Method	55
4.3 Advantages of the Formulation	60
4.4 Power System Modelling	61
4.4.1 Synchronous Machine Model	62
4.4.2 Mechanical Shaft Model	64
4.4.3 Exciter-Stabilizer and Turbine Governor Systems	65
4.5 AC Network	67
4.5.1 Static Network Representation	67
4.5.2 State Space Network Representation	71

TABLE OF CONTENTS (continued)

	PAGE
4.5.2.1 Single Phase Network State Space Representation	72
4.5.2.2 Two-Phase Network	74
4.6 Application to a Practical Power System	76
4.6.1 Single Machine - Infinite Bus AC System	76
4.6.2 Multimachine AC Power System	88
4.7 Summary	91
CHAPTER 5 STATE MATRIX FORMULATION FOR MULTITERMINAL AC-DC POWER SYSTEMS	95
5.1 Introduction	95
5.2 Modelling of the DC Terminal	96
5.3 Modelling of the DC Network	99
5.4 AC-DC Interface	100
5.5 AC-DC Interconnections	102
5.6 Test Examples	104
5.6.1 Single Machine - Infinite Bus System	104
5.6.2 Multimachine Multiterminal AC-DC System	111
5.7 Summary	115
CHAPTER 6 EIGENVALUE ANALYSIS AND DECENTRALIZED POLE PLACEMENT	118
6.1 Introduction	118
6.2 Eigenvalue Tracking	119
6.2.1 Mathematical Formulation	120
6.2.2 Algorithm Implementation	124
6.3 The Evaluation of the Derivative of the System State Matrix	125
6.4 Use of Eigenvalue Tracking in the Analysis of Power Systems	126

TABLE OF CONTENTS (continued)

	PAGE
6.4.1 Simplified Single Machine Infinite Bus System with a Single Time Constant Exciter	126
6.4.2 A Three-Machine, Three-Terminal AC-DC System	131
6.5 Some Practical Considerations in Eigenvalue Tracking	138
6.6 Decentralized Pole Placement	143
6.6.1 Pole Placement Using Direct Minimization	146
6.6.2 Newton Method	148
6.6.3 Conditions for Existence	152
6.7 Examples of the Use of Decentralized Pole Placement Algorithms	152
6.7.1 A Seventh Order System	152
6.7.2 A Three-Machine AC Power System	156
6.8 Discussion on the Pole Placement Methods	161
6.9 Summary	162
CHAPTER 7 CONCLUSIONS	164
REFERENCES	169
APPENDIX 1 PER UNIT SYSTEM	178
APPENDIX 2 SUBSYSTEM MODELS	180

LIST OF FIGURES

FIGURE	PAGE
3.1(a) Equivalent Bipolar DC Terminal Representation	32
3.1(b) Equivalent Monopolar DC Terminal Representation	32
3.2 DC Network - Multiple Pair Configuration	35
3.3 DC Network - Series Connected System	35
3.4(a) Parallel DC Network - Radial Interconnection	36
3.4(b) Parallel DC Network - Mesh Interconnection	36
3.5 A Nine-Bus, Three-Terminal AC-DC Power System	46
3.6 A Six-Converter Asymmetrical HVDC Network	52
4.1 Interconnected System Structure	56
4.2 Generator Input-Output Model	64
4.3 Shaft Input-Output Model	65
4.4 Exciter Input-Output Model	66
4.5 Turbine-Governor Input-Output Model	67
4.6 DQ-dq Reference Frame Transformation	69
4.7 Single Machine Infinite Bus AC System	77
4.8 Subsystem Interconnections for a Single Machine Infinite Bus System	83
4.9 Multimachine AC Power System	89
5.1(a) DC Converter - Constant Current Controller	98
5.1(b) DC Converter - Constant Voltage Controller	98

LIST OF FIGURES (continued)

FIGURE		PAGE
5.2	DC Converter Stabilizer	98
5.3	Single Machine Infinite Bus AC-DC Power System	105
5.4	Subsystem Interconnections for a Single Machine Infinite Bus AC-DC System	107
5.5	Three-Machine, Three-Terminal AC-DC System	112
6.1	Single Machine Infinite Bus System	128
6.2	Block Diagram of the Linearized Model of the Single Machine Infinite Bus System	129
6.3	Eigenvalue Locus for the Single Machine Infinite Bus System	130
6.4(a)	Movement of the Real and Imaginary Parts of Rotor Eigenvalues of Generator 1 as Function of Interconnection Coupling r	134
6.4(b)	Movement of the Real and Imaginary Parts of Rotor Eigenvalues of Generator 2 as Function of Interconnection Coupling r	135
6.5(a)	Movement of Real and Imaginary Parts of the Eigenvalues Corresponding to the Constant Current Controllers at Terminals R1 and R3 as a function of Interconnection Coupling	136
6.5(b)	Movement of the Eigenvalue Corresponding to the Constant Voltage Controller at Terminal I2 as a Function of Interconnection Coupling	137
6.6(a)	Movement of the Real and Imaginary Parts of Rotor Eigenvalues of Generator 1 as Function of Stabilizer Gain K_w	139
6.6(b)	Movement of the Real and Imaginary Parts of Rotor Eigenvalues of Generator 2 as Function of Stabilizer Gain K_w	140
6.7	Three-Machine AC Power System	158

LIST OF TABLES

TABLE		PAGE
3.1	AC Bus Data for Nine-Bus, Three Terminal Power System	47
3.2	AC Line Data for Nine-Bus, Three Terminal Power System	47
3.3	DC Terminal Data	48
3.4	DC Line Data	48
3.5(a)	Nine-Bus, Three-Terminal Network - AC Loadflow	49
3.5(b)	Nine Bus, Three-Terminal Network - DC Loadflow	49
3.6	Comparison of AC Line Flows	51
3.7	Comparison of AC Bus Voltages	51
3.8	Six-Converter Asymmetrical HVDC Network - DC Loadflow	52
4.1	Interconnection Matrix L_{11} for Single Machine Infinite Bus AC System	84
4.2	State Matrix for Single Machine Infinite Bus AC System	86
4.3	Generator Data	90
4.4	Interconnection Matrix L_{11} for Multimachine System	92
4.5	State Matrix for Multimachine AC System	93
5.1	Interconnection Matrix L_{11} for Single Machine Infinite Bus AC-DC System	108
5.2	Eigenvalues for Single Machine Infinite Bus AC-DC System	110
5.3	DC System parameters	114
5.4	Eigenvalues of Three-Machine, Three-Terminal AC-DC System	116
6.1	Eigenvalue Identification	133

CHAPTER 1.

INTRODUCTION

1.1 Dynamic Properties of Power Systems

An interconnected electric power system is an example of a large-scale multivariable system. It is spread over a wide geographical area with a large number of generating units supplying the electrical load through a transmission network. The analysis of a part of the power system may require that the whole interconnected system be considered.

An important question in power system operation is that of stability. Traditionally a system was considered stable if, following a disturbance, the individual generating machines remained in synchronism. The study of power system dynamics for the first one to two seconds following the disturbance was generally considered adequate for determining stability. However, increased system size and complexity, and the trend toward operating the system closer to its steady state, stability limit has resulted in system disturbances characterized by oscillations developing over several seconds. It is therefore necessary to study the system dynamics over a time span longer than that traditionally considered.

HVDC links are increasingly being considered for inclusion in AC power systems because they offer a number of economical and technical advantages. Of particular relevance to existing power systems is the role of HVDC for interconnecting AC networks. In a number of places it is extremely difficult to link two neighbouring AC networks because of stability considerations. The HVDC link provides a stable intertie by acting as a buffer between two AC networks transforming the AC to DC and the DC back to AC again. The inclusion of the HVDC link and its associated controls, however, contributes further to the system complexity and affects its dynamics.

Power system dynamics may be placed under three major categories [1],

- 1 - Prime mover energy supply dynamics and controls.
- 2 - System governing and generation controls
- 3 - Electrical machine and network dynamics.

Energy supply dynamics (e.g., boiler effects), usually last for many minutes. System governing and generation control dynamics last from several seconds to a few minutes while electrical machine dynamics are usually over in a few seconds. The appropriate level of detail in representing power system components - which include the transmission network, synchronous generators and control equipment - is determined by the type of phenomena judged to be important in a particular stability study. For example, for electrical machines and network transients, the machines, the network and the loads are required to be modelled in detail whereas the mechanical system including prime mover

and governing controls may be represented by a simple model. Again where the effects of significance are system frequency and interchange control, network representation is reduced with a corresponding increased emphasis on prime mover and energy supply representation [1].

One major area of concern has been the study of electrical machines and system dynamics, particularly where the instability may develop over several seconds. Analysis of this type of problem requires that the interaction between machines, excitation systems, turbine-governor systems, etc., must be carefully considered. This is further complicated by the inclusion of the HVDC network with its associated converter controls and requires an understanding of the relevant subsystem models.

Another modelling issue that is of great importance relates to the question of how much of the system external to the study area needs to be represented in order to obtain meaningful results. This question and related ones, such as the level of detail for the external system, can at present be answered only on the basis of experience and a system by system approach. This often requires that the system dynamics be studied for a number of cases with varying degrees of modelling detail, making it essential to have fast and computationally efficient tools for analyzing large power networks.

1.2 Steady State Stability

The steady state stability problem considers the dynamic behaviour of a power system which has been subjected to small

perturbations and has emerged as an important consideration in power system planning and operation only over the past two decades. Steady state stability is characterized by such phenomena as self-excitation, network torsional interactions, control system related oscillations, inter-machine (rotor - electromechanical) interactions, turbine governor related oscillations and monotonic instability associated with exceeding the steady state power transmission limits of the system. The potential for steady state instability has increased due to recent trends in the design and operation of power system. One major factor has been the use of fast response exciters to improve transient stability. This has resulted in decreased steady state stability because of their negative effect on the inherent damping of the synchronous machine rotor oscillations [2]. Again the machine may suffer oscillatory instability in the presence of a series compensated transmission line [3] or a HVDC converter controller [4]. Another source of instability is the decreased strength of transmission systems relative to the size of the generating stations [5].

In steady state stability analysis, the focus of the study is on small perturbations around a given operating point. For this purpose the non-linear differential equations describing the power system dynamic performance are linearized around the operating point and assembled together in state space form. This enables the use of linear system theory and the application of many control theory concepts thereby facilitating stability evaluation and also allowing the design of suitable controllers for improving system stability.

The introduction of HVDC links in an AC power system greatly influences the steady state and dynamic behaviour of the (AC-DC) power system. HVDC transmission systems are generally of significant size and their dynamic performance and controllability provide a significant capability for improving the AC-DC system dynamic response. The role of HVDC in present day power systems is reviewed in the following section.

This thesis is basically concerned with the study of steady state stability of AC-DC power systems with the aim of developing a computationally efficient tool capable of analyzing the wide variety of steady state stability aspects of AC-DC systems.

1.3 The Role of HVDC

Historically, it was DC that was used first for electric supply applications. The supply of power was however limited to short distances because of excessive voltage drops and power losses over long transmission lines. Long distance transmission became practicable only with the advent of AC which allowed higher voltage levels, thereby reducing line power losses, and which has now come to dominate electric supply and transmission systems. AC systems however, have their own disadvantages which have become more evident with the increase in system size and voltage level. The inherent difficulties of AC transmission are basically related to inductive voltage drop, corona discharge, charging current requirement and the need to keep generators operating in synchronism. These difficulties are not present in a DC system and the DC transmission line has emerged as a serious

alternative to AC for certain power transmission applications such as underground or underwater cables [6], very long overhead transmission lines [7] or asynchronous connections [8].

In an AC-DC power system, the HVDC network including its associated converters, can be basically considered as a special component of the AC transmission system. This component converts AC power to DC, transmits the DC and converts it back to AC at the receiving end. HVDC systems constructed so far have been two terminal links, which particularly for long distance bulk power transmission applications have had to compete with AC links primarily on the basis of costs. DC lines, towers, and rights of way are cheaper compared to those required for AC but the necessary converter stations are more expensive than AC substations. This for a long time resulted in the DC link being considered only above a certain "break-even" distance where the converter costs were offset by the cheaper cost for the DC line. However, for certain applications, technical considerations outweigh any cost factors and DC is the only practical alternative. Examples of this are the interconnection of asynchronous AC networks and long distance underground or underwater bulk power transmission. In the first case, an AC link is not possible because of stability considerations, while for the second case excessive charging current requirement poses a limit on the capacity of AC cables.

One significant feature of an HVDC system is that it is not passive, but must be controlled to function. The power flow on a DC line is much more easily and directly controlled than is the case for

the passive AC transmission line. However, when the AC network and DC line are combined the control of power flow on the HVDC line can be used to control the flow of power in the AC network. The DC line accomplishes this by extracting a controlled amount of power at one node from the AC system and simultaneously injecting it at a different point. Consequently, the DC line contribution to the short circuit power at the injected node is much less than the case for an AC line. This fact has been utilized in the King North line [9] which was installed to supply power to a dense inner city area primarily to limit the growth of short circuit power. The introduction of a multiterminal HVDC network consisting of a large number of HVDC lines would have a dominant influence on the power flow of the AC system since power flow distribution on the HVDC network may be used to control the AC line power flow.

Besides influencing the system steady state power flow, the HVDC link also affects the power system dynamic characteristics. This has been the subject of considerable research aimed at improving the system dynamic response by a proper control of its transient characteristics. For two terminal systems this has included power or voltage modulation [10], the use of classical control methods [11] or of modern control methods utilizing optimal control [12]. The effect of power modulation has been investigated in [13] using the linear model of a synchronous machine connected to an infinite bus by means of a bipolar HVDC link. Similar methods have been used in [14] for the case of a single machine connected to an infinite bus by a parallel AC-DC line.

The case of a parallel AC-DC line has also been considered in [15], where a number of methods have been used to construct optimal, suboptimal and conventional controls and their small and large signals performance evaluated.

Since 1954 when the first HVDC link was commissioned in Gotland, Sweden, a large number of DC links have become operational. Reference [16] lists the existing and planned systems for North America. In most cases the existing HVDC systems are equipped with controls to allow the links to enhance system performance [18]. In [18], a small signal model of the Pacific HVDC intertie has been developed and classical techniques used to design a controller to improve the damping on the parallel AC intertie. The controller has permitted a significant increase in the capacity of the AC intertie from 2100 MW to 2500 MW. The Nelson River HVDC System includes provision of damping to the receiving end and a reduction of transmitted power in the case of loss of AC tie lines to the U.S. [19].

As two-terminal HVDC systems have matured, interest has also been focused on interconnecting more than two terminal stations by means of a DC network. The more dispersed modulation capability of multiterminal HVDC appears to offer a greater potential for enhancing system behaviour. The first realistic operating strategy for multiterminal systems was given as early as 1963 [20] and similar to the case for two terminal schemes, various terminal characteristics have been proposed [16,21]. Centralized control principles for

multiterminal systems have been investigated in [22] and the feasibility of using on line computer control [23] has been shown.

For steady state stability studies simplified DC converter models are adequate. This has been verified by comparing simulation results from both simple and extremely detailed HVDC system models [24].

Approaches based on optimal and suboptimal control [25] as well as modal control [26] have been proposed for increasing system stability. A more recent approach using decentralized feedback has been presented in [27].

1.4 Objective of the Thesis

The steady state stability analysis of a modern day interconnected power system requires the solution of a large number of coupled differential equations which are linearized around a given operating point. Direct time domain solutions of system differential equations are possible, but the effectiveness of the approach is seriously limited because of the following practical considerations [28,29]:

- 1) Time responses are dependent on the choice of disturbance as well on the variables selected for observation. An incorrect choice of disturbance may not provide the appropriate excitation of the critical modes. Further the observed time response contains many modes and the poorly damped modes may not be immediately apparent. To get an indication of the growing oscillation it is therefore

necessary to carry out the simulation over a period of 10 to 15 seconds. Such simulations are costly because of the extensive computational effort required.

- ii) Time responses do not provide adequate information about the source of instability and yield little insight as to the parameters that must be adjusted to make the system stable.

The attention has therefore focused on using linear system techniques for predicting system stability.

The basic approach followed is to arrange the differential equations of the system into state space form. Steady state stability is then determined from the eigenvalues of the system state space matrix. The advantage of this method is that all the modes are clearly separated and identified by the eigenvalues. The eigenvalues indicate the frequency and damping of the oscillatory modes as well as the rate of decay of the non-oscillatory modes. A further assessment of the degree of stability is carried out by means of eigenvalue sensitivity analysis, essentially to determine whether system stability is compromised in the event of any changes in system parameters.

The formulation of the system differential equations into state space form can be easily performed for small systems. Analysis of practical power systems, however, involves a large number of systems which interact together in a complex manner. Formulation of the overall system matrix in this case requires an understanding of the different subsystems as well as of the interconnection between them.

A number of approaches have been employed for the formulation of the state matrices for large power systems. The main disadvantage shared by most of the existing techniques is that the formulation process requires the inversion or elimination of matrices. However an efficient approach for AC power systems has been presented in [5]. It does not suffer from this disadvantage and further retains the system parameters explicitly in the state space matrix. This latter feature is particularly useful for system identification and parameter sensitivity analysis.

The major aim of this thesis is the development of a comprehensive approach for the steady state stability analysis of AC-DC power systems. An efficient computational method has been developed for the formulation of the system state matrix. This method is based on recent advances in linear system theory and is capable of handling wide variety of models representing the various subsystems in the power system. The method considerably simplifies the task of state matrix derivative evaluation since system parameters are retained explicitly. An eigenvalue tracking method has been developed which utilizes this derivative to analyze the system stability as its parameters are varied.

1.5 Thesis Structure

The thesis has a total of seven chapters. The first two chapters may be viewed as introduction and background information,

whereas the remaining develop and apply the proposed state matrix formulation for power systems steady state stability analysis.

Chapter 2 essentially serves to put present research in an appropriate perspective and reviews the previous research in this area.

An AC-DC loadflow is required for determining the system steady state operating point for subsequent stability analysis. Chapter 3 describes the loadflow program developed for this purpose.

Chapter 4 presents the state matrix formulation for AC power systems. Both single machine infinite bus and multimachine power systems are considered.

Chapter 5 extends the techniques of Chapter 4 to include multiterminal HVDC systems. It develops a simplified interconnection equation for the AC-DC transmission system and the HVDC network components are considered as additional subsystems in the overall formulation.

Chapter 6 uses the proposed state matrix formulation approach to develop new tools for power system analysis and control. A new and computationally inexpensive eigenvalue tracking method is presented which helps in analyzing system stability by determining root movement with respect to parameter variation. For power system control two simple and efficient decentralized pole placement algorithms are also presented.

Finally, Chapter 7 summarizes the specific contributions of the thesis followed by suggestions for future work.

CHAPTER 2

• A REVIEW OF METHODS FOR THE STEADY STATE ANALYSIS OF POWER SYSTEMS INCLUDING MULTITERMINAL HVDC LINKS

2.1 Introduction

The advent of HVDC has necessitated the development of appropriate computational tools for analyzing AC-DC power systems. From a system analysis viewpoint this requires the development of a suitable model for the converter station which is the only essentially new component; and the incorporation of models for HVDC transmission lines, converter stations and control equipment into existing AC power system analysis programs. This chapter reviews the progress which has been made in the adaptation of loadflow and stability analysis to include HVDC multiterminal systems.

Multiterminal HVDC (MTDC) networks have not yet come into existence but have nevertheless been proposed because of numerous advantages foreseen in power systems operation. Both series and parallel DC networks have been proposed and an excellent survey on MTDC systems is presented in [21] with an extensive list of references. Most work on MTDC systems is concentrated on the parallel connected system because it is superior to the series connected system in terms of minimum transmission line loss, ease of control and flexibility for

future operation [30]. The first MTDC system will most probably be formed by a parallel extension of an existing two-terminal link.

Section 2.2 reviews AC-DC loadflow methods. Section 2.3 reviews existing AC steady state stability analysis methods and Section 2.4 outlines the inclusion of HVDC networks in stability analysis programs.

2.2 Loadflow Analysis Methods For AC-DC Networks

The incorporation of HVDC systems in AC loadflow solutions has been continuing for a long time. Initial methods using network analyzers were presented by Uhlmann [31] and Horigomé and Reeve [32]. Horigomé and Ito developed a digital computer approach based on an equivalent circuit concept [33] which involved separating the system into parts but took no account of the method of control. Methods that developed following these early efforts can be divided into two groups. The first group of methods termed the Sequential Methods solve the AC and DC system equations alternately till convergence is obtained at the AC-DC system interface. The second group of methods are termed the Integrated Methods with the AC and DC system equations being combined and solved together. Before reviewing these methods, the loadflow problem will be defined and solution types introduced.

We consider first an "n" bus (node) power system network. At any node (i) in the network, the net injected complex power (S) must equal the power outflow through the network. Thus:

$$S_i^* = V_i^* \sum_{k=1}^n Y_{ik} V_k \quad (2.1)$$

where Y_{ik} are the elements of the bus admittance matrix describing the transmission network and V_i is the bus voltage. (The * denotes complex conjugate.) The net injected power is the difference between the generation and load connected at the bus. If all the S_i and Y_{ik} are known, equation (2.1) can be solved iteratively for V_i . The Gauss-Seidel form of solution requires a simple rearrangement of (2.1) to give

$$V_i^{v+1} = \frac{1}{Y_{ii}} \left\{ \left[\frac{S_i}{V_i^v} \right]^* - \sum_{\substack{k=1 \\ k \neq i}}^{k=n} Y_{ik} V_k^v \right\} \quad (2.2)$$

where $v = 0, 1, 2, \dots$ denote the iteration step. This method features simplicity of programming that is effective for low order problems.

The Newton-Raphson approach is more complicated but is generally more efficient on larger problems. The difference between the left and right hand sides of (2.1) is called the bus power mismatch and is non-zero unless an exact solution has been obtained. Since equation (2.1) is complex, it is separated into real and imaginary parts and written as a set of two real equations. In the polar form of solution the bus power mismatch function is formulated in terms of

changes in the bus voltage magnitudes and bus voltage angles. This is written as:

$$\begin{bmatrix} \Delta P \\ \Delta Q \end{bmatrix} = \begin{bmatrix} J \end{bmatrix} \begin{bmatrix} \Delta \theta \\ \Delta V \end{bmatrix} \quad (2.3)$$

where ΔP and ΔQ are the real and reactive bus power mismatch vectors and ΔV and $\Delta \theta$ denote the bus voltage magnitude and bus voltage angle change vectors. The matrix J is called the Jacobian and is the matrix of the derivatives of the mismatch function with respect to voltage magnitudes and angles. Equation (2.3) is used to obtain the corrections for the bus voltage and angles. Matrix J is sparse in typical loadflow applications and (2.3) is solved directly and rapidly using sparsity-programmed optimal order triangulation and back-substitution. The Newton method is very reliable and extremely fast in convergence for loadflow applications. An advanced version of this method using approximations to the Jacobian is called the Fast Decoupled method [34]. The approaches to AC-DC loadflow solutions are now described.

2.2.1 Sequential Methods

One approach has been to treat the DC link as a load for the AC network. This has been adopted both for two-terminal and multiterminal HVDC system analysis [35-41]. The method can be illustrated as follows. Using an estimate of the converter AC voltages, calculate the

real and reactive load of the HVDC link on the AC system assuming that converter parameters and DC currents are known. Run the AC loadflow with the above loads and obtain improved estimates of the AC voltages. Repeat these steps until convergence is obtained and desired DC conditions are consistent with AC conditions. Since the AC and DC systems are solved independently of each other, the HVDC system may consist of one or more two-terminal links or an arbitrarily connected multiterminal system. For multiterminal systems, the DC network itself can be solved easily using either the Gauss-Seidel approach employing R_{BUS} matrix [40,41] or by means of the Newton-Raphson method and employing the G_{BUS} [39] in the Jacobian. Both methods provide for different DC converter controls such as constant current, constant power or constant firing angle. The Gauss-Seidel method is particularly attractive because of its simplicity. Since the number of buses on the DC network is going to be fairly small, no advantage is gained from using the Newton-Raphson method.

2.2.2 Integrated Methods

Another approach to solve the HVDC loadflow problem is to incorporate the DC system parameters directly in the Jacobian for the AC network formed normally in the Newton-Raphson method. The Jacobian is expanded to contain entries associated with the converter and DC transmission line in addition to the usual AC system coefficients. This method can incorporate DC terminal controls [42,43] but an important shortcoming is its inability to handle converter transformer

tap limits. The AC fast decoupled method has also been similarly modified to include multiterminal HVDC system [44,45,46].

2.2.3 Discussion

Both approaches to AC-DC loadflow problem namely, the sequential and integrated, have their own advantages. The Newton-Raphson and fast decoupled integrated approaches can provide good computing efficiency but require rewriting the complete program. Also, new AC loadflow techniques may not be as easily accommodated. The sequential approach has the advantage that any existing loadflow program can be used so that the computational efficiency or convenience of a specific program can be retained. The sequential approach has the capability to handle converter transformer tap limits as well as discrete transformer taps [41] which is not possible with the integrated methods.

One further disadvantage of integrated methods is the increased computer storage required because the Jacobian size increases rapidly as the number of variables increases to account for the HVDC system.

2.3 Steady State Stability Evaluation of AC Systems

The dynamic behaviour of the power system may be described by a set of non-linear differential equations:

$$\begin{aligned} \dot{x}(t) &= f(x(t), u(t)) & x(t_0) &= x_0 \\ y(t) &= h(x(t), u(t)) \end{aligned} \tag{2.4}$$

Here $x(t)$, $u(t)$ and $y(t)$ denote the state, input and output vectors of the system and x_0 is the initial system operating point.

A steady state stability study investigates the system stability in the vicinity of the operating point x_0 . Since we are only interested in the system stability in the presence of small disturbances, equation (2.4) can be expressed in terms of deviations around the operating point. If the disturbance is assumed small enough, second order and higher terms are negligible in a Taylor series expansion. The equations therefore take on the linear form:

$$\begin{aligned}\dot{\Delta x} &= [A] \Delta x + [B] \Delta u \\ \Delta y &= [C] \Delta x + [D] \Delta u\end{aligned}\tag{2.5}$$

where A , B , C and D are real constant matrices of the appropriate dimensions. The entries of these matrices are function of all system parameters as well as the steady state operating condition.

Steady state stability may now be analyzed using different approaches. The first is to use direct numerical integration of the system differential equations (2.5). However, because of the longer time period of the phenomena of interest, integration can be computationally expensive. The second and better approach is to apply modern control theory techniques [47, 48].

The evaluation of steady state stability then basically involves two related aspects. One is to use a formulation which reduces the system equations to state space form. The other is the use of an appropriate analysis technique to assess system stability. Both these aspects are now covered for AC power systems.

2.3.1 Formulation of the State Matrices

The formulation of the system state matrices in equation (2.5) from the system equations (2.4) is a complex and difficult task. For small problems such as a single machine infinite bus, the number of differential and algebraic equations describing the system performance is relatively small. The reduction of these equations to state space form is simple and easily performed. Analysis of practical systems, however, involves a large number of subsystems and complicated interactions. Formulation of the overall system state matrices requires careful choice of what to include and how best to combine the parts. This has been the subject of much interest since the early works of Enns et al [49] and Laughton [50].

Enns et al suggested the so-called 'PQR' technique. In this method the linearized system differential and algebraic equations are arranged as:

$$P \begin{bmatrix} \Delta \dot{x} \\ \Delta y \end{bmatrix} = Q \Delta x + R \Delta u \quad (2.6)$$

where the state, output and input vector x , y and u are of the same dimensions as those of equation (2.5). P , Q , R are appropriately dimensioned matrices and are functions of system structure and operating point. Equation (2.6) can now be easily transformed to (2.5) by premultiplying by P^{-1} and appropriate partitioning. This gives:

$$\begin{bmatrix} \Delta \dot{x} \\ \Delta y \end{bmatrix} = [P^{-1} Q] \Delta x + [P^{-1} R] \Delta u \quad (2.7)$$

The approach of Enns et al has been used by Anderson [51,52] for multimachine systems and extended to include network and shaft dynamics by Nolan et al [53]. This technique was considerably improved by Alden and Zein El-din [54] where the organizational simplicity of the PQR technique was combined with an efficient sub-matrix buildup method.

The approach suggested by Alden and Zein El-din [54] avoided the inversion of a large matrix by ordering the state, algebraic and output variables of each individual machine in such a way so as to set up the P matrix in the quasi-block diagonal form. Equation (2.6) is then rewritten, after partitioning the matrices P , Q and R , as:

$$\begin{bmatrix} I & PA \\ 0 & PB \end{bmatrix} \begin{bmatrix} \Delta \dot{x} \\ \Delta y \end{bmatrix} = \begin{bmatrix} QA \\ QB \end{bmatrix} \Delta x + \begin{bmatrix} RA \\ RB \end{bmatrix} \Delta u \quad (2.8)$$

The state space form equation (2.5) can be now written as:

$$\begin{aligned} \Delta \dot{x} &= [QA - PA PB^{-1} QB] \Delta x + [RA] \Delta u \\ \Delta y &= [PB^{-1} QB] \Delta x + [PB^{-1} RB] \Delta u \end{aligned} \quad (2.9)$$

Alternatively Laughton [50] used a direct elimination technique to form the state matrix from the complete differential and algebraic equation for the whole system. Undrill [55] proposed using a submatrix buildup technique with emphasis on the efficiency that results by avoiding large blocks of null elements.

The method described by Muir [56] uses the elimination technique described by Laughton. The state matrix is formed by eliminating the algebraic variables of the complete system in a number of steps. Initially, the network equations are combined with the algebraic and differential equations of the first machine and written as:

$$\begin{bmatrix} 0 \\ \Delta u_1 \\ 0 \end{bmatrix} = \begin{bmatrix} W_1 \end{bmatrix} \begin{bmatrix} 0 \\ \Delta x_1 \\ 0 \end{bmatrix} + \begin{bmatrix} Z_1 \end{bmatrix} \begin{bmatrix} \Delta v_N \\ \Delta x_1 \\ \Delta y_1 \end{bmatrix} \quad (2.10)$$

where Δx_1 , Δu_1 and Δy_1 are the state, input and algebraic vectors of machine 1 and v_N is the network voltage vector. The algebraic variables y_1 and the two node equations corresponding to machine 1 are now eliminated resulting in the reduced equation:

$$\begin{bmatrix} 0 \\ \Delta u_1 \end{bmatrix} = \begin{bmatrix} W_{R1} \end{bmatrix} \begin{bmatrix} 0 \\ \Delta x_1 \end{bmatrix} + \begin{bmatrix} Z_{R1} \end{bmatrix} \begin{bmatrix} \Delta v_N^1 \\ \Delta x_1 \end{bmatrix} \quad (2.11)$$

The matrices W_{R1} and Z_{R1} are the reduced matrices corresponding to W_1 and Z_1 and v_N^1 is the reduced voltage vector after the elimination of the nodes for machine 1. The equations for machine 2 may now be combined with equation (2.11) to give:

$$\begin{bmatrix} 0 \\ \Delta u_1 \\ \Delta u_2 \\ 0 \end{bmatrix} = \begin{bmatrix} W_2 \end{bmatrix} \begin{bmatrix} 0 \\ \Delta \dot{x}_1 \\ \Delta \dot{x}_2 \\ 0 \end{bmatrix} + \begin{bmatrix} Z_2 \end{bmatrix} \begin{bmatrix} \Delta v_N^1 \\ \Delta x_1 \\ \Delta x_2 \\ \Delta y_2 \end{bmatrix} \quad (2.12)$$

In this equation Δx_2 , Δu_2 and Δy_2 are the state, input and algebraic vectors of machine 2. Again the algebraic variables may be eliminated giving:

$$\begin{bmatrix} 0 \\ \Delta u_1 \\ \Delta u_2 \end{bmatrix} = \begin{bmatrix} W_{R2} \end{bmatrix} \begin{bmatrix} 0 \\ \Delta \dot{x}_1 \\ \Delta \dot{x}_2 \end{bmatrix} + \begin{bmatrix} Z_{R2} \end{bmatrix} \begin{bmatrix} \Delta v_N^2 \\ \Delta x_1 \\ \Delta x_2 \end{bmatrix} \quad (2.13)$$

The remaining machines are added similarly resulting in the equation:

$$\begin{bmatrix} \Delta u_1 \\ \Delta u_2 \\ \Delta u_M \end{bmatrix} = \begin{bmatrix} W_{RM} \end{bmatrix} \begin{bmatrix} \Delta \dot{x}_1 \\ \Delta \dot{x}_2 \\ \Delta \dot{x}_M \end{bmatrix} + \begin{bmatrix} Z_{RM} \end{bmatrix} \begin{bmatrix} \Delta x_1 \\ \Delta x_2 \\ \Delta x_M \end{bmatrix} \quad (2.14)$$

The state equation for the M machine system is obtained as:

$$\dot{\Delta x} = - [W_{RM}]^{-1} Z_{RM} \Delta x + [W_{RM}]^{-1} \Delta u \quad (2.15)$$

where $\Delta x = [\Delta x_1^T, \Delta x_2^T \dots \Delta x_M^T]^T$

$\Delta u = [\Delta u_1^T, \Delta u_2^T \dots \Delta u_M^T]^T$

As seen from equations (2.9) and (2.15), these methods are costly in terms of the computational effort particularly in view of the matrix inversions required. The method proposed in this thesis and presented in Chapters 4 and 5 does not require any matrix inversion for AC systems and the inversion of a submatrix of order equal to the number of DC terminals, for the case of an AC-DC system.

An important aspect of state matrix formulation is the grouping of the state variables. These can be either:

1. Type Grouping where all states associated with the same process in each machine are grouped together, e.g., rotor angles of all machines, rotor speeds of all machines, etc.
2. Machine Grouping where all states associated with a particular machine are grouped together.

The first approach has been adopted in [5], [50] and [55], whereas the second approach has been used in [52], [53], [54] and [56]. The second scheme has a number of advantages in terms of savings in computational time and improved flexibility for subsequent stability

analysis [54,57]. It occurs naturally using the state matrix formulation method proposed here.

One other method for steady state stability analysis is that proposed by Larsen et al [58]. It is based on using a transient stability simulation program to construct the system matrix via numerical differentiation. The approach is attractive and easy to implement, however it may be susceptible to inaccuracy caused by numerical instability associated generally with the numerical differentiation process [59].

2.3.2 Analysis Techniques

Steady state stability may be determined directly from a numerical integration of the linearized system differential equation. However, as mentioned in the previous section it is uneconomical to perform numerical integration for steady state stability evaluation because of the necessity to continue the integration over a long time period.

Classical control theory techniques such as Routh-Hurwitz [60], Nyquist [61] and Root-locus [62] have all been utilized for analysing power system dynamics. The concepts of damping and synchronizing torques, based on a frequency response technique, has also been used for the analysis of synchronous machines and its excitation systems [2,63]. These methods while useful for the understanding of basic concepts are restricted to small systems such as a single machine infinite bus system.

The most promising and commonly used method is the use of eigenvalues of the system state matrix A of equation (2.5). The eigenvalues of A ($\lambda_i = \sigma_i + j\omega_i$, $i = 1, 2, \dots, n$) completely specify the nature of the modeled system's response to small disturbance. In the time domain the components of the incremental state Δx are expressed as linear combinations of the modes $e^{\lambda_i t}$. The oscillation frequency is given by $\omega_i/2\pi$ and σ_i define the decay characteristic. The system will be stable if all the σ_i are negative so that the oscillations decay with time. A positive σ_i denotes an unstable system.

The uncertainty in power system data, variation in system parameters, and inaccuracies in measurements mean that the elements of the system state matrix A are incorrect and therefore its eigenvalues may be different from that of the actual power system. It is therefore necessary to further characterize stability by evaluating the sensitivity of stability to these parameter variations. This is accomplished by means of eigenvalue sensitivity evaluation and has been used frequently for power system analysis [53,54,64,65,66]. Expressions for first order sensitivities have been derived using a number of methods [67,68,69]. These have been extended for second order [70] and n th order sensitivity evaluation [71].

Eigenvalue sensitivity is particularly useful for identifying which system parameters have a significant impact on damping of particular modes and can therefore be used to adjust these parameters to provide an adequate stability margin. This is accomplished by means of eigenvalue tracking, i.e., plotting the root-locus, as the system

control or design parameter is varied. A technique for tracking a subset of critical eigenvalues has been developed in [70]. It is useful in cases where only a few eigenvalues are sensitive to parameter variations.

A major characteristic and limitation of eigenvalue-based approach to system stability evaluation is the large amount of computer memory and time required for eigenvalue evaluation particularly for large systems. The tracking approach of [72] is particularly useful as it is more economical than repeated eigenvalue computations.

2.4 Inclusion of HVDC System

The development of the state matrix for an AC-DC power system started with the more simple systems representing a single machine connected to an infinite bus through a parallel AC-DC line [73,74]: Goudie [73] used the elimination method of [50] for the study of steady state stability of a parallel HVDC-AC system. A more general formulation was reported in [75] for an arbitrary multimachine system containing one or more point-to-point HVDC links. In this method detailed representation of generators, DC link and associated controllers was considered. The component models are formulated separately and interconnected using the network model obtained directly from the Jacobian found by the Newton-Raphson loadflow method. The state matrix is then found by the elimination of the algebraic variables.

Linearized models of AC networks containing multiterminal DC systems have also been reported. However, these formulations have used simplified models of the AC system and are basically attempts to solve a specific problem [76,77]. This deficiency is overcome in the proposed state matrix formulation method presented in Chapters 4 and 5 which has a number of significant advantages in terms of ease of formulation, inclusion of a wide variety of subsystem models and state matrix derivative evaluation for eigenvalue sensitivity calculations.

2.5 Summary

This chapter has presented a survey of the various existing techniques available for HVDC-AC systems for both loadflow and stability studies. While substantial digital simulation capacity exists there is a need for a general small signal model which includes a full representation of the AC system.

CHAPTER 3

LOADFLOW ANALYSIS OF MULTITERMINAL AC-DC SYSTEMS

3.1 Introduction

An AC-DC loadflow is required for the determination of the base operating point of the AC-DC system. The machines and DC converter equations are then linearized around this operating point for the evaluation of system dynamic stability. Since efficient AC loadflow techniques are available and also as the major part of a multiterminal AC-DC power system would be AC, it is natural to take advantage of these techniques and extend them to include the DC network for AC-DC loadflow studies.

In an HVDC transmission network, unlike the passive elements of the AC transmission system, the DC converters are active devices. They are equipped with a variety of controls to adjust the DC system voltage, current or power flow. Under normal steady state conditions there is further a converter transformer tap changer which keeps the converter firing angle close to some minimum value. All these controls are utilized to enhance the AC system operation by controlling the system power flows. It is therefore necessary for the AC-DC loadflow method to be able to accommodate the many different control modes.

There are two ways to solve the AC-DC loadflow problem. In the first approach the AC and DC system equations are combined together and solved using a Newton method [42]. The second approach is to treat the DC system as a load on the AC network and iterating back and forth between AC and DC systems to match the boundary conditions between the two systems [39,40,41]. Both types of methods have been discussed in Chapter 2. A new method based on the second or sequential approach is presented in this chapter. It has the following advantages:

1. The reactive power requirement of the DC system is estimated first prior to running any loadflow iteration. This ensures the selection of a feasible operating point for the HVDC system by checking that adequate reactive power support is available.
2. The DC network loadflow is not required to be repeated.
3. The Gauss-Seidel method is used with the conductance matrix to solve for the DC loadflow. This results in minimal storage compared to the use of the Newton method for solving the DC system.

The converter equations are presented in Section 3.2, followed by a description of the different DC network configurations in Section 3.3. Section 3.4 discusses the DC converter operating modes for multiterminal DC systems. Sections 3.5 to 3.8 presents the new AC-DC loadflow method and gives the results of loadflow analyses for two test examples.

3.2 Converter Equations

The following basic assumptions have been made to derive the converter equations [78,79,80]:

1. The AC source delivers a constant sinusoidal voltage. Three phase voltages and currents are balanced.
2. All higher harmonics of voltage and currents produced by the converters are filtered out and do not appear in the AC system.
3. The converter tap changing transformers are ideal with a series reactance.
4. Converter is lossless and has no arc drop.
5. The direct voltage and current are smooth.

The DC converter equations must mesh in with the AC system equations expressed in per unit system. There are a number of ways that this could be accomplished. One set of AC and DC per unit system adopted in the literature [39,40,41] is used here and is given in Appendix A1.

The converter equations which relate the DC system to the AC system are written with reference to Figure 3.1(a) which shows one equivalent converter per pole. For symmetrical operation this bipolar circuit may be replaced by the monopolar equivalent circuit in Figure 3.1(b). Any parallel or series converter configuration may be reduced to one of these two equivalents [39,80].

The terminal DC voltage of the converter is given by

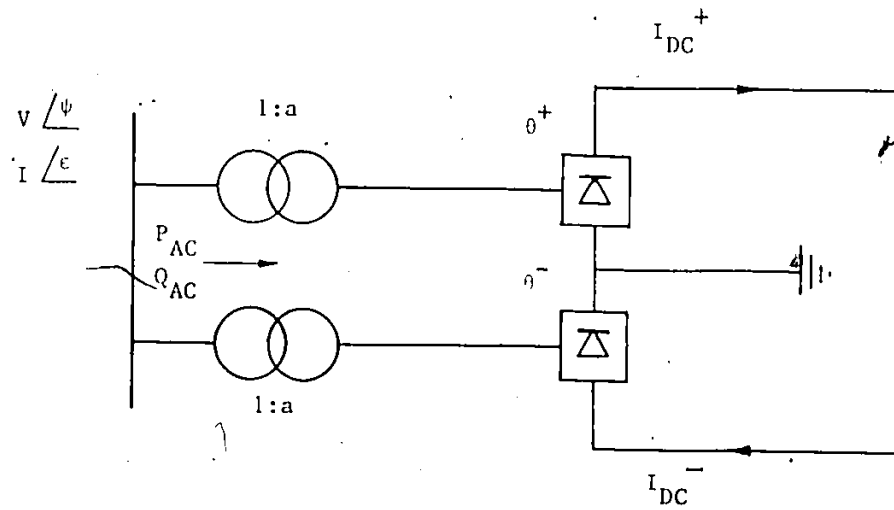


Figure 3.1(a) Equivalent Bipolar DC Terminal Representation

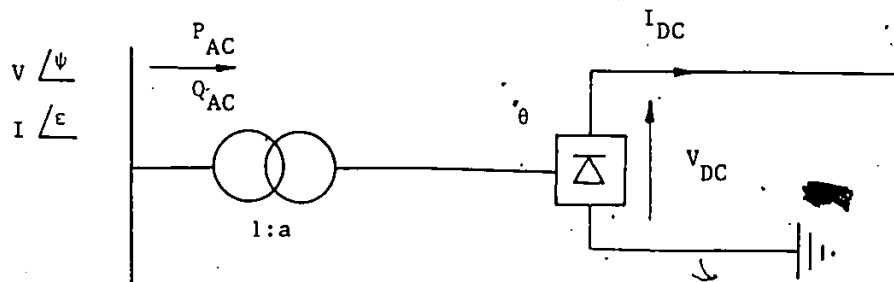


Fig. 3.1(b) Equivalent Monopolar DC Terminal Representation

$$V_{DC} = aV\cos\theta - R_C I_{DC} \quad (3.1)$$

where V_{DC} = Converter DC output voltage

I_{DC} = Converter DC current

R_C = Commutating resistance

a = Transformer tap ratio

V = AC bus voltage

θ = Converter firing angle

= α for Rectifier

= γ for Inverter.

Since a lossless inverter has been assumed

$$P_{DC} = P_{AC} \quad (3.2)$$

which gives

$$V_{DC} I_{DC} = aV I \cos(\psi - \xi) \quad (3.3)$$

where ψ and ξ are defined in Figure 3.1(a).

Since the AC and DC currents are equal in per unit we obtain

$$V_{DC} = aV \cos\phi \quad (3.4)$$

where $\phi = (\psi - \xi)$ denotes the power factor angle.

3.3 DC System Configuration

There are a number of possible DC system configurations. These are [21]:

1. Multiple pair.
2. Series connection.
3. Parallel connection.

The multiple pair connection is shown in Figure 3.2. It essentially requires double conversion and is strictly not a multiterminal system, being formed from separate but adjacent two terminal links.

The series connection is shown in Figure 3.3. The same current flows through the entire DC network which is grounded at one terminal only. One converter works in the constant current mode while the rest of the converters are operating in the constant voltage mode. The DC series system suffers from serious disadvantages such as severe reactive power requirement, difficulty in extending the network, large line losses and the impossibility of operating the system in case of a line outage.

The parallel connection includes both the radial and mesh configurations as shown in Figure 3.4(a) and (b). The DC network operates at nearly a constant voltage level with one converter determining the voltage and the rest of the converters operating either in constant current or constant power mode. The parallel connection overcomes the disadvantages of the series connected systems with the mesh interconnection resulting in the most flexible power interchange capability. It offers increased reliability and reactive power

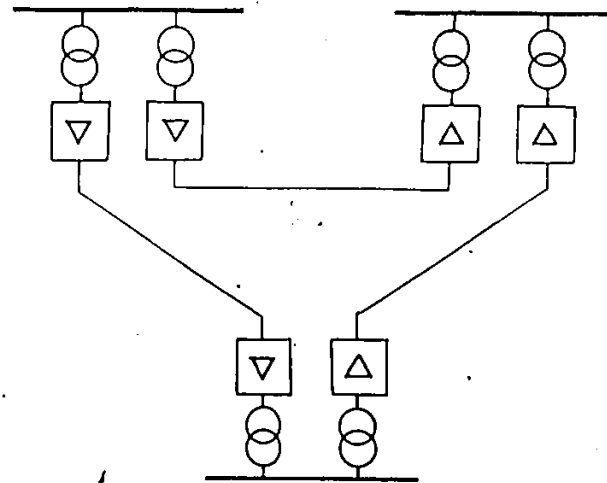


Figure 3.2 DC Network - Multiple Pair Configuration

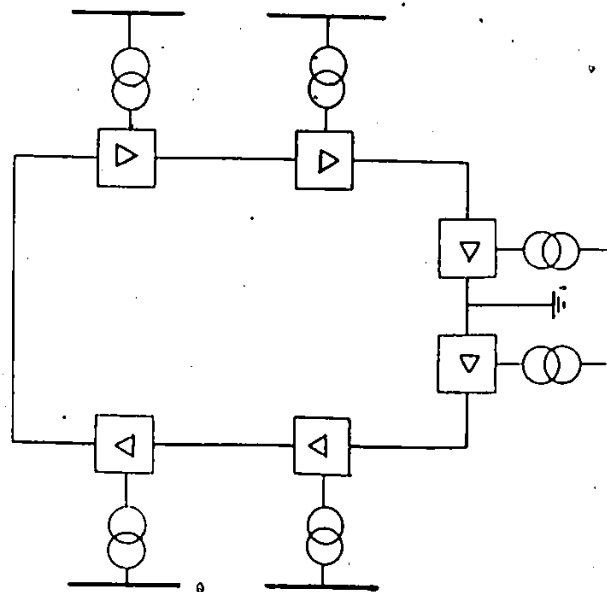


Fig. 3.3 DC Network - Series Connected System

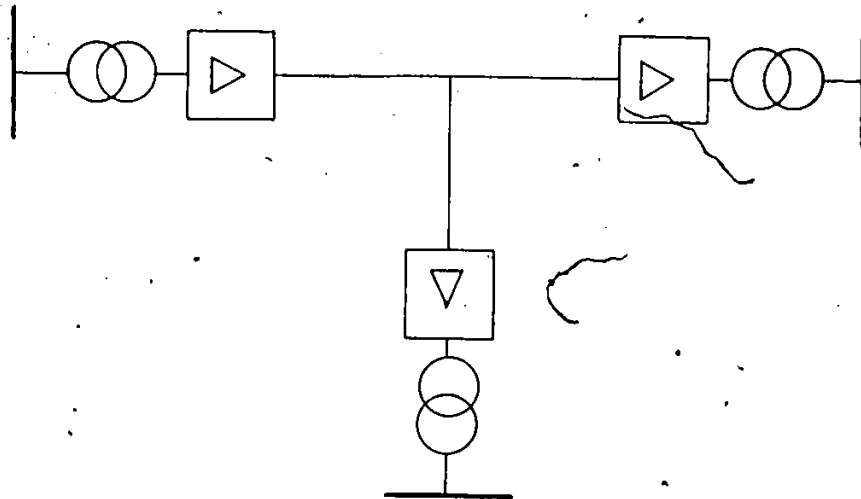


Figure 3.4(a) Parallel DC Network - Radial Interconnection

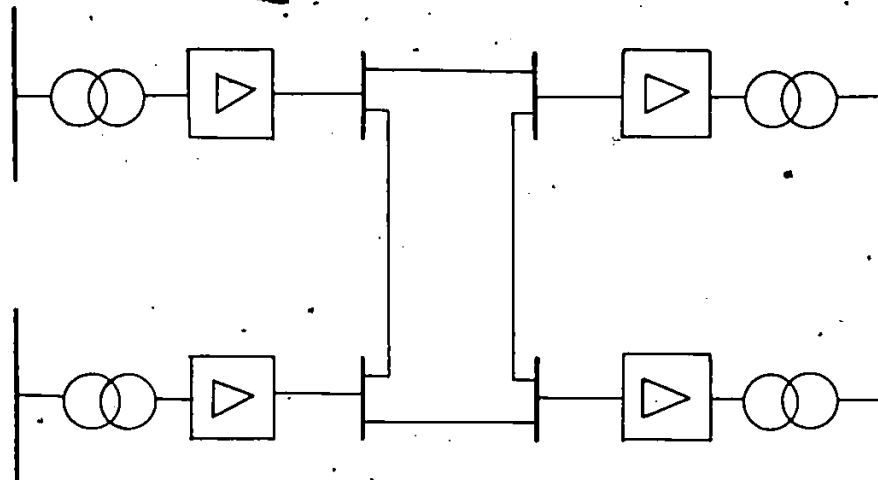


Fig. 3.4(b) Parallel DC Network - Mesh Interconnection

consumption is minimized because the converter operates at low values of control angles. Further, DC network losses are minimized because of natural DC load flows [21,29].

In the subsequent sections a parallel multiterminal system is assumed, since due to its inherent advantages it is likely that the first multiterminal HVDC system is of this type and therefore it has been studied extensively in the literature [21].

3.4 DC Converter Operating Modes <

It is assumed that there is a central dispatch control responsible for the current or power setting of the converters to implement a desired power interchange on the multiterminal HVDC network. One terminal determines the DC system voltage while the current or active power is fixed for the rest of the terminals. The power flow for a constant current converter will depend on the terminal voltage which is unknown at the beginning, hence such a scheme is not expected to provide accurate power dispatch at the constant current terminal.

The constant voltage DC terminal operates at either its minimum firing angle, α_{min} , if it is a rectifier or at its minimum extinction angle, γ_{min} , if it is an inverter. These may be expressed as:

$$V_{DC} = V_{DC}^{SPEC} \quad (3.5)$$

$$\theta = \theta_{MIN}^{SPEC} \quad (3.6)$$

where $\theta_{\text{MIN}}^{\text{SPEC}} = \alpha_{\text{MIN}}^{\text{SPEC}}$ for a rectifier
 $\quad \quad \quad = \gamma_{\text{MIN}}^{\text{SPEC}}$ for an inverter

and SPEC stands for specified.

For a converter with scheduled constant power or constant current operation it is necessary that the terminal operates at a DC voltage lower than its own firing angle or extinction angle characteristics. A 3% voltage margin is often provided [39] and is necessary to prevent normal fluctuation of AC voltages from causing mode changes. For a constant current terminal the converter control equations can therefore be written as:

$$I_{\text{DC}} = I_{\text{DC}}^{\text{SPEC}} \quad (3.7)$$

$$V_{\text{DC}} = 0.97 (aV \cos \theta_{\text{MIN}} - R_C I_{\text{DC}}^{\text{SPEC}}) \quad (3.8)$$

Similarly, for a constant power terminal

$$P_{\text{DC}} = P_{\text{DC}}^{\text{SPEC}} \quad (3.9)$$

$$V_{\text{DC}} = 0.97 (aV \cos \theta_{\text{MIN}} - R_C I_{\text{DC}}) \quad (3.10)$$

Considering that the converter voltage equation (3.1) is still applicable

$$V_{\text{DC}} = aV \cos \theta - R_C I_{\text{DC}}$$

and comparing with equations (3.8) and (3.10) we have

$$aV\cos\theta - R_C I_{DC} = 0.97 aV\cos\theta_{MIN} - 0.97 R_C I_{DC}$$

$$\text{or} \quad \cos\theta = 0.97 \cos\theta_{MIN} + 0.03 R_C I_{DC} / aV \quad (3.11)$$

This shows that the control angle is strongly dependent on θ_{MIN} and changes only slightly with a , V or I_{DC} . Therefore, rather than specifying a voltage margin we can fix the control angle for the constant current or constant power terminals. The converter voltage equations (3.8) and (3.10) are replaced by equation (3.1) with

$$\theta = \theta_{MARGIN} \quad (3.12)$$

where $\theta_{MARGIN} = \alpha_{MARGIN}$ for a rectifier
 $= \gamma_{MARGIN}$ for an inverter

For a rectifier taking a typical value of α_{MIN} to be between $5^\circ - 7^\circ$, α_{MARGIN} would lie between $14^\circ - 16^\circ$. In the case of the inverter where γ_{MIN} is around $16^\circ - 18^\circ$, voltage fluctuation may be taken into account by choosing γ_{MARGIN} between $21^\circ - 23^\circ$.

The loadflow method presented in the next section, therefore, considers the control angle to be fixed for constant current or constant power terminals.

3.5 DC Loadflow Equations

The DC network equation for mesh, radial, monopolar or bipolar, symmetrical or assymetrical network can be written as

$$I_{DC} = G V_{DC} \quad (3.13)$$

Since the number of DC buses in general will be small the Gauss-Seidel method is adequate for solving the DC loadflow. For a k terminal HVDC network where the kth terminal is the voltage controlled terminal and is taken as the reference, the voltage at the constant power terminal DC bus is given by

$$V_{DCi}^{(v+1)} = \frac{1}{g_{ii}} \left\{ \frac{P_{DCi}^{SPEC}}{V_{DCi}^{(v)}} - \sum_{\substack{n=1 \\ n \neq i}}^{k-1} V_{DCn}^{(v)} g_{in} \right\} \quad (3.14)$$

where v is the number of iterations (v = 0,1,2,...). For a constant current terminal

$$V_{DCi}^{(v+1)} = \frac{1}{g_{ii}} \left\{ I_{DC}^{SPEC} - \sum_{\substack{n=1 \\ n \neq i}}^{k-1} V_{DCn}^{(v)} g_{in} \right\} \quad (3.15)$$

The iteration is started by assuming

$$V_{DCi} = V_{DCk}^{SPEC} \quad (i = 1, 2, \dots, k-1) \quad (3.16)$$

The DC power of the current controlled terminals is evaluated from

$$P_{DC} = V_{DC} I_{DC} \quad (3.17)$$

For the reference voltage terminal

$$P_{DCK} = V_{DCK} \sum_{i=1}^{k-1} g_{ki} V_{DCi} \quad (3.18)$$

3.6 AC Loadflow

The primary advantage of sequential AC-DC loadflow methods is that any existing AC loadflow method may be employed. The DC network is simply considered as a load on the AC system. For an n bus power system the static loadflow equations are given by

$$P_{Gi} - P_{Di} = V_i \sum_{j=1}^n V_j (G_{ij} \cos \psi_{ij} + B_{ij} \sin \psi_{ij})$$

for $i = PQ$ and PV buses

(3.19)

$$Q_{Gi} - Q_{Di} = V_i \sum_{j=1}^n V_j (G_{ij} \sin \psi_{ij} - B_{ij} \cos \psi_{ij})$$

for $i = PQ$ buses

The Newton-Raphson method has been used here to solve equation (3.19) for bus voltage magnitude V and bus voltage angle ψ given the load demand P_{Di} , Q_{Di} and the system power generation P_{Gi} , Q_{Gi} . G_{ij} and B_{ij} are elements of the bus admittance matrix $Y = [G + jB]$.

3.7 AC-DC Loadflow Method

The method is as follows:

1. Estimate the DC system reactive power requirement. This basically requires an approximation of the terminal power factor since the active power P is known from the desired interchange. The power factor is obtained using equations (3.1) and (3.4) and is given as

$$\cos\phi = \cos\theta - \frac{R_C I_{DC}}{aV} \quad (3.20)$$

Initially, both the transformer tap setting a and AC bus voltage V are taken as 1.0 pu. Also, I_{DC} is given for the current controlled terminal. For a constant power terminal

$$I_{DC} = \frac{P_{DC}^{SPEC}}{V_{DCk}^{SPEC}}$$

assuming that there is no voltage drop across the DC network and the k th terminal is on constant voltage control.

Again, the current for the constant voltage terminal is computed from:

$$I_{DC} = - \sum_{i=1}^{k-1} I_{DCi}$$

The control angle θ is taken equal to either θ_{MIN} or θ_{MARGIN} as mentioned earlier in Section 3.4 and depends on whether the terminal is a rectifier or inverter. The reactive power requirement of the i th terminal is given by

$$Q_{\text{DC}i} = P_{\text{DC}i} \tan \phi_1 \quad (3.21)$$

where the real power P_{DC} is given by

$$P_{\text{DC}} = \begin{cases} P_{\text{DC}}^{\text{SPEC}} & \text{for a constant power terminal} \\ V_{\text{DC}} I_{\text{DC}}^{\text{SPEC}} & \text{for a constant current terminal} \\ V_{\text{DC}}^{\text{SPEC}} I_{\text{DC}} & \text{for a voltage controlled terminal} \end{cases} \quad (3.22)$$

2. The AC loadflow is now carried out using the equivalent AC loads for each DC terminal determined in Step 1.

3. If the AC system voltage profile is satisfactory, a DC loadflow is carried out. This gives the exact power and current flow in the DC network, which is used to update the AC equivalent loads calculated in Step 1.

4. The AC loadflow is repeated using the updated DC system loads. The AC bus voltages obtained in Step 2 are used as the initial values. This results in quick convergence, within two or three iterations, of the AC loadflow because the exact and estimated AC

equivalent loads are quite close and the voltages V 's obtained in Step 2 lie near the AC loadflow solution.

5. The AC bus voltages determined above is used to calculate the transformer tap ratio. Rewriting equation (3.4) gives

$$a = V_{DC} / V \cos \phi \quad (3.23)$$

If the transformer tap changers are within limits, the problem is solved. Usually no tap limit violation will be found in the normal operating range. However, in case of tap-limit violation, if either of the upper or lower limits has been exceeded, the voltage at the voltage controlling converter is rescheduled and Steps 3 to 5 are repeated. The new voltage can be determined using

$$V_{DC}^{SPEC} = \begin{cases} V_{DC}^{SPEC (OLD)} * \frac{a^{lower}}{a} & a < a^{lower} \\ V_{DC}^{SPEC (OLD)} * \frac{a^{upper}}{a} & a > a^{upper} \end{cases} \quad (3.24)$$

If there is more than one upper tap limit violation or more than one lower tap limit violation, the largest (a^{limit}/a) is used to change V_{DC}^{SPEC} . If there are simultaneously lower and upper tap violation there is no feasible solution [39].

3.8 Test Results

This section presents the results of applying the AC-DC loadflow algorithm to two different examples. The first example shows a nine-bus, three-terminal AC-DC system which has been used in subsequent stability studies in Chapters 4 and 5. The second example has been chosen to demonstrate the versatility of the method for the case of an asymmetrical bipolar network.

3.8.1 A Nine-Bus, Three-Terminal AC-DC Power System

In this example a three terminal HVDC network is overlayed on a nine-bus nine-line AC power system as shown in Figure 3.5 [81]. The bus data and the transmission line data for the AC and DC systems is given in Tables 3.1 to 3.4.

Converters R1 and R3 operate as rectifiers in the constant current mode with converter I2 determining the DC system voltage and operating as an inverter. The operating point of the HVDC system has been chosen such that R1 and R3 extract power from AC buses 4 and 6 which is simultaneously injected by I2 at bus 1. The results of the AC-DC loadflow are given in Tables 3.5(a) and 3.5 (b).

Besides determining the system operating point for stability studies in Chapters 4 and 5, this example also serves to highlight some of the advantages of incorporating HVDC networks in AC power systems. The AC line flows for the AC-DC system are compared to the line flows for the AC system in Table 3.6. Note the effect of the DC network on rerouting AC power flows. The power flow on lines 2 and 7 is decreased

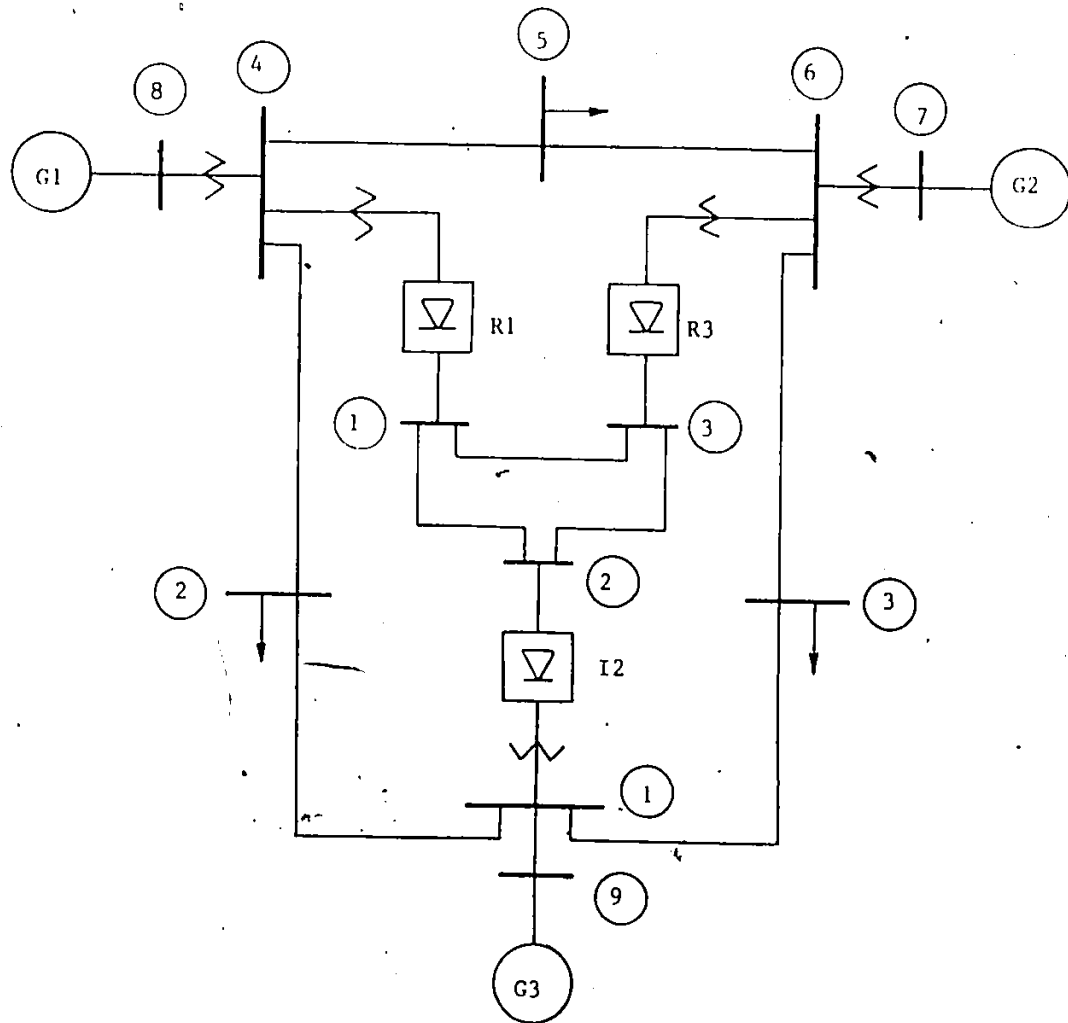


Fig. 3.5 A Nine-Bus, Three-Terminal AC-DC Power System

Table 3.1 AC Bus Data for Nine Bus, Three-Terminal Power System

Bus No.	Bus voltage	Generation		Load	
		P	Q	P	Q
1	-	0.000	0.000	0.000	0.000
2	-	0.000	0.000	1.250	0.500
3	-	0.000	0.000	0.900	0.300
4	-	0.000	0.000	0.000	0.000
5	-	0.000	0.000	1.000	0.350
6	-	0.000	0.000	0.000	0.000
7	1.025	0.850	-0.109	0.000	0.000
8	1.025	1.630	0.063	0.000	0.000
9	1.040	0.716	0.270	0.000	0.000

Table 3.2 AC Line Data for Nine-Bus, Three-Terminal Power System

Line No.	Bus		R	X	B
	To	From			
1	1	2	.01000	.08500	.0880
2	2	4	.03200	.16100	.1530
3	4	5	.00850	.07200	.0745
4	8	4	.00000	.06250	.0000
5	5	6	.01190	.10080	.1045
6	6	7	.00000	.05860	.0000
7	6	3	.03900	.17000	.1790
8	3	1	.01700	.09200	.0790
9	1	9	.00000	.05760	.0000

Table 3.3 DC Terminal Data for Nine-Bus, Three-Terminal Power System

DC Terminal No.	Connected To AC Bus No.	Control Mode	Current pu	Voltage pu	Control Angle Deg.	Commutating Resistance pu
1	4	Current	.25000	-	16.00	.05238
2	1	Voltage	-	0.966	16.00	.05238
3	6	Current	.25000	-	16.00	.05238

Table 3.4 DC Line Data for Nine-Bus, Three-Terminal Power System

Line No.	From Bus	To Bus	Resistance
1	1	2	.02304
2	2	3	.03073
3	1	3	.01119

Table 3.5 Results for AC-DC Loadflow

a) DC Loadflow Results

Terminal No.	DC Voltage	Power		Current	Tap	Control Angle	AC Bus Voltage
		P	Q				
1	.972	.243	.081	.250*	1.01	16.00	1.020
2	.966*	-.483	.182	-.500	1.01	16.00	1.020
3	.973	.243	.081	.250*	1.00	16.00	1.026

* denotes the control values

b) AC Loadflow Results

Bus No.	Bus Voltage		Power		Load	
	Magnitude	Angle	P	Q	P	Q
1	1.020	-2.19	.0000	.0000	-.4830	.1818
2	.992	-5.16	.0000	.0000	1.2500	.5000
3	1.008	-4.91	.0000	.0000	.9000	.3000
4	1.020	-3.32	.0000	.0000	.2431	.0812
5	1.010	-2.72	.0000	.0000	1.0000	.3500
6	1.026	-1.50	.0000	.0000	.2432	.0812
7	1.025	1.21	.8500	.0009	.0000	.0000
8	1.025	5.91	1.6300	.1628	.0000	.0000
9	1.040	.00	.7057	.3717	.0000	.0000

while being increased on lines 1 and 8. This capability of controlling AC line flows is an important advantage of multiterminal HVDC networks.

The bus voltages for the AC and AC-DC systems are compared in Table 3.7. While the bus voltage magnitude is decreased slightly because of the reactive power requirements of the DC terminals, the bus voltage angles at the generator buses 7 and 8 are significantly reduced in the AC-DC system. Thus the HVDC network is seen to strengthen the system. A parallel AC system could also have been employed for strengthening the system instead of using the HVDC network, but in this case line power flows could only be controlled by rescheduling the generators power outputs. This may result in uneconomic operation if generators operate away from their optimal power settings.

3.8.2 A Six-Terminal Asymmetrical Bipolar HVDC Network

The second example considers a six-terminal asymmetrical bipolar network tied into a large AC system and shown in Figure 3.6. This network was first presented in reference [42] and has been included here primarily to demonstrate the versatility of the proposed algorithm. Since AC network data was not available it is assumed that enough reactive power capability exists at each converter bus so as to be able to provide a constant AC voltage at each of the DC terminals. Here converters C2 and C4 set the DC network voltages, converters C1, C3 and C5 are on constant current control and converter C6 operates in a constant power mode. The results of the loadflow agree with those of reference [42] and are shown in Figure 3.8.

Table 3.6 Comparison of AC Line Flows

Line No.	From Bus	To Bus	AC Network		AC-DC Network	
			P	Q	P	Q
1	4	2	.40923	.22984	.64905	.18818
2	2	4	-.84288	-.11324	-.60528	-.17457
3	4	5	.76350	-.00795	.76913	-.00293
4	8	4	1.62935	.06647	1.62935	.16276
5	5	6	-.24087	-.24297	-.23536	-.24088
6	6	7	-.84966	.14954	-.84966	.03939
7	6	3	.60793	-.18072	.37036	-.15219
8	3	1	-.30526	-.16546	-.53443	-.10436
9	1	9	-.71612	-.23924	-.70545	-.33779

Table 3.7 Comparison of AC Bus Voltages

Bus No.	AC Network Voltage		AC-DC Network Voltage	
	Magnitude	Angle	Magnitude	Angle
1	1.026	-2.22	1.020	-2.19
2	.996	-3.99	.992	-5.16
3	1.013	-3.69	1.008	-4.91
4	1.026	3.72	1.020	.32
5	1.016	.73	1.010	-2.72
6	1.032	1.97	1.026	-1.50
7	1.025	4.66	1.025	1.21
8	1.025	9.28	1.025	5.91
9	1.040	0.00	1.040	0.00

Table 3.8 Six-Converter Example - DC Loadflow Solution

Terminal No.	Converter Voltage	Converter Current	Tap Setting	Control Angle	Converter P	Converter Load Q	AC Bus Voltage
1	0.9810	4.900*	1.022	16.0	4.807	1.599	1.012
2	0.9710*	-4.999	1.040	16.0	-4.854	1.622	0.984
3	-0.9808	-4.900*	1.021	16.0	4.806	1.599	1.012
4	-0.9710*	4.900	1.034	16.0	-4.758	1.585	0.990
5	0.9802	4.999	1.028	16.0	4.900*	1.635	1.005
6	0.9704	-4.900*	1.063	-22.5	-4.755	2.141	1.001

* denotes the control values

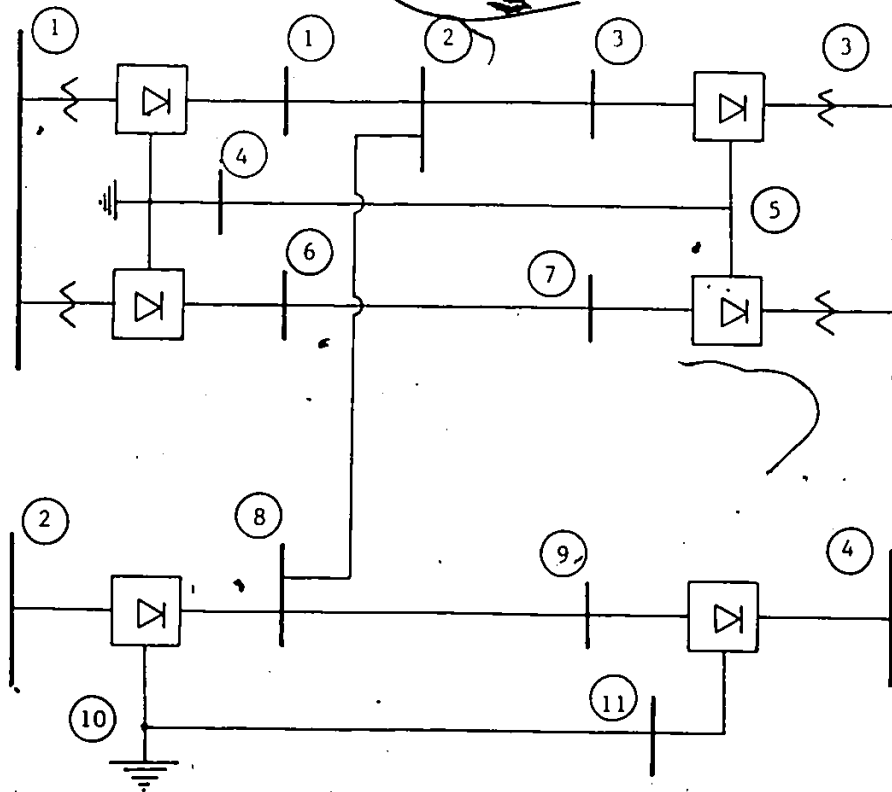


Fig. 3.6 A Six-Converter Asymmetrical HVDC Network

3.9 Summary

This chapter has presented a new sequential AC-DC loadflow method which has several significant advantages. The method estimates the reactive power requirements of the HVDC network and thereby ensures that a feasible DC system operating point has been selected. It uses the conductance matrix to solve the DC network using a Gauss-Seidel method. This results in the minimal storage requirements compared to the storage required for the elements of the Jacobian using the Newton method. The proposed method will accommodate a variety of converter control modes and the control on each converter can be specified independently of the other converters in the DC system. Again, any DC network configuration may be considered. However, as in all applications of powerflow, it is the user's responsibility to define a consistent set of terminal controls.

The method will be used in subsequent chapters for determining the base operating point for AC-DC steady state stability studies.

CHAPTER 4

STATE MATRIX FORMULATION OF AC POWER SYSTEMS

4.1 Introduction

The steady state or small signal stability analysis of a power system requires writing the linearized differential equations of the complete system in the state space form

$$\begin{aligned}\dot{x} &= Ax + Bu \\ y &= Cx + Du\end{aligned}\tag{4.1}$$

Once the equations have been obtained in this form, the eigenvalue of the state matrix A can be calculated and examined to obtain information of the dynamic behaviour of the system.

There are a number of methods for the formulation of the state matrix as reviewed earlier in Chapter 2. The main disadvantage of these methods is that they require costly matrix inversions. One important consequence of these inversions is that system parameters are no longer explicitly available in the overall system state matrix. This chapter presents a systematic approach for state matrix assembly which does not require any matrix inversions and is based on the

Component Connection method [82]. Each of the subsystems are represented in state space form and linked by an interconnection matrix. The formulation presented here is flexible enough to include network dynamics and any degree of complexity in subsystem modelling. The formulation in this chapter is confined to multimachine AC systems and is later extended to include power systems including HVDC links in the following chapter.

In Section 4.2 the Component Connection method is described. The practical advantages of using this technique over others in dynamic stability analysis are given in Section 4.3. Section 4.4 describes the various subsystems forming a large power system. Section 4.5 details the modelling of AC network. Lastly, Section 4.6 illustrates the use of the method. Two examples, a single machine infinite bus system and a multimachine system are presented.

4.2 The Component Connection Method

The Component Connection method details the formulation of the overall system state matrices from the state matrices of the different subsystems forming the overall system.

Assume an interconnected power system to consist of N subsystems (Figure 4.1) which are represented in state space form as

$$\begin{aligned}\dot{x}_1 &= A_1 x_1 + B_1 u_1 \\ y_1 &= C_1 x_1 + D_1 u_1\end{aligned}\tag{4.2}$$

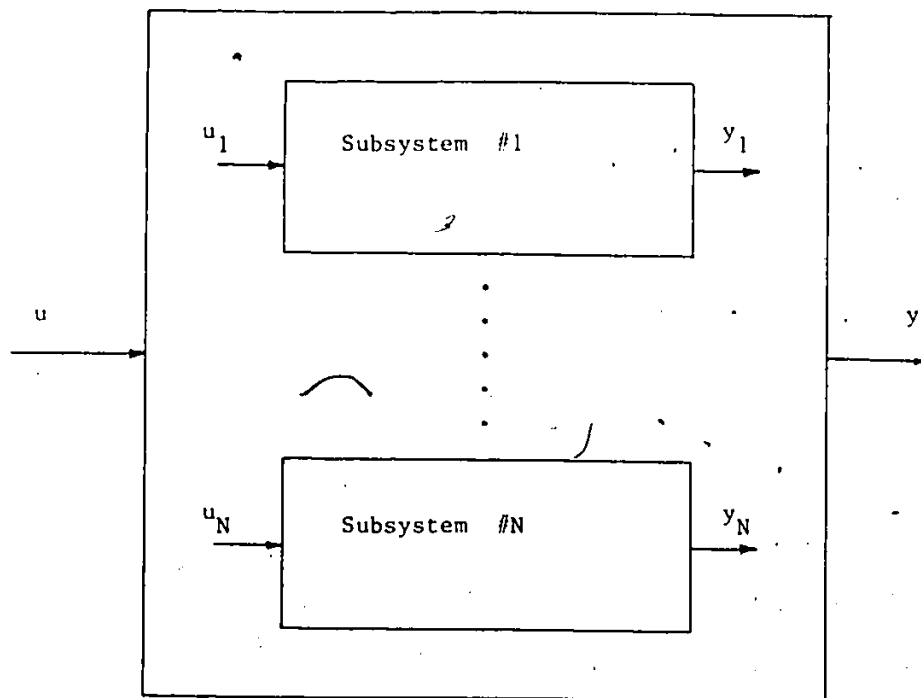


Fig. 4.1 Interconnected System Structure

where x_i , u_i and y_i represent the state, input and output vectors of the i th component subsystems. Let the interconnection between subsystems input and outputs and their relationship to overall system input and output be given by the algebraic equations

$$\bar{u} = L_{11}\bar{y} + L_{12}u \quad (4.3a)$$

$$y = L_{21}\bar{y} + L_{22}u \quad (4.3b)$$

$$\begin{aligned} \text{where } \bar{u} &= [u_1^T, u_2^T, u_3^T, \dots, u_N^T]^T \\ \bar{y} &= [y_1^T, y_2^T, y_3^T, \dots, y_N^T]^T \end{aligned}$$

and u and y are the overall system input and outputs.

For a decoupled system the overall state matrices are given by

$$\begin{aligned} \dot{\bar{x}} &= \bar{A}\bar{x} + \bar{B}\bar{u} \\ \bar{y} &= \bar{C}\bar{x} + \bar{D}\bar{u} \end{aligned} \quad (4.4)$$

where

$$\bar{x}^T = [x_1^T, x_2^T, x_3^T, \dots, x_N^T]^T$$

is the overall system state vector. Also

$$\bar{A} = \text{diag } [A_1, A_2, \dots, A_N]$$

$$\bar{B} = \text{diag } [B_1, B_2, \dots, B_N]$$

$$\bar{C} = \text{diag } [C_1, C_2, \dots, C_N]$$

$$\bar{D} = \text{diag } [D_1, D_2, \dots, D_N]$$

Substituting for \bar{y} in (4.3a) from (4.4) gives

$$\bar{u} = L_{11}\bar{C}x + L_{11}\bar{D}\bar{u} + L_{12}u$$

$$\text{or, } \bar{u} = (I - L_{11}\bar{D})^{-1}L_{11}\bar{C}x + (I - L_{11}\bar{D})^{-1}L_{12}u \quad (4.5)$$

Substituting equation (4.5) into (4.4) and combining with (4.3b) gives

$$\dot{x} = [\bar{A} + \bar{B}(I - L_{11}\bar{D})^{-1}L_{11}\bar{C}]x + [\bar{B}(I - L_{11}\bar{D})^{-1}L_{12}]u$$

$$y = [L_{21}\bar{C} + L_{21}\bar{D}(I - L_{11}\bar{D})^{-1}L_{11}\bar{C}]x + [L_{21}\bar{D}(I - L_{11}\bar{D})^{-1}L_{12} + L_{22}]u$$

which is rewritten as

$$\dot{x} = Ax + Bu$$

$$y = Cx + Du$$

(4.7)

with

$$\begin{aligned}
 A &= \bar{A} + \bar{B}(I - L_{11}\bar{D})^{-1}L_{11}\bar{C} \\
 B &= \bar{B}(I - L_{11}\bar{D})^{-1}L_{11}\bar{C} \\
 C &= L_{21}\bar{C} + L_{21}\bar{D}(I - L_{11}\bar{D})^{-1}L_{11}\bar{C} \\
 D &= L_{21}\bar{D}(I - L_{11}\bar{D})^{-1}L_{12} + L_{22}
 \end{aligned}
 \tag{4.8}$$

These expressions are considerably simplified if the \bar{D} matrix can be developed as a null matrix, i.e., subsystem output are dependent only on their states. In this case

$$\begin{aligned}
 A &= \bar{A} + \bar{B} \cdot L_{11}\bar{C} \\
 B &= \bar{B}L_{12} \\
 C &= L_{21}\bar{C} \\
 D &= L_{22}
 \end{aligned}
 \tag{4.9}$$

It follows then that once the subsystem state matrices and the interconnection matrices L_{11} , L_{12} , L_{21} and L_{22} are defined, the overall system matrix is easily computable. The main advantage, however, results from having $D_1 = 0$ for the various subsystems as the computation is considerably simplified. Again the subsystem model may be of any degree of complexity but as long as the input-output relationships are fixed, the interconnection remains the same.

4.3 Advantages of the Formulation

The main advantage of the method presented in the previous section lies in the formulation of the overall system state matrices from the state matrices of the component subsystems. If the subsystems are modelled such that $D_1 = Q$ in equation (4.8) then the state matrix A may be obtained simply by matrix multiplication and addition.

Other advantages may be summarized as

1. Flexibility in subsystem modelling. The subsystems may be modelled to any degree of detail as long as subsystem inputs and outputs remain the same, without necessitating any change in the interconnection matrix. This is particularly useful for the evaluation of different order models for a given system which requires the state matrix to be determined for each of the alternative models. The component matrices \bar{A} , \bar{B} , \bar{C} and L_{11} are extremely sparse and it is computationally inexpensive to obtain A using sparse matrix multiplication.
2. The system parameters are contained explicitly in the state matrix. Therefore system matrix derivatives are easily computed for use in eigenvalue sensitivity computations. From equation (4.9)

$$A = \bar{A} + \bar{B}L_{11}\bar{C}$$

therefore, the derivative with respect to any parameter ϵ is given by

$$\frac{dA}{d\epsilon} = \frac{dA}{d\epsilon} + \frac{d\bar{B}}{d\epsilon} L_{11} \bar{C} + \bar{B} \frac{dL_{11}}{d\epsilon} \bar{C} + \bar{B} L_{11} \frac{d\bar{C}}{d\epsilon} \quad (4.10)$$

The method is particularly attractive for state matrix derivative evaluation when compared to the previous methods described in Chapter 2. The state matrix derivative using the PQR method is obtained from equation (2.9) as

$$\frac{dA}{d\epsilon} = [I \ 0] [P^{-1}] \left[\frac{dQ}{d\epsilon} - \frac{dP}{d\epsilon} P^{-1} Q \right] \quad (4.11)$$

For the elimination approach the state matrix derivative is given by equation (2.15) as

$$\frac{dA}{d\epsilon} = -[W_{RM}]^{-1} \frac{dZ_{RM}}{d\epsilon} + [W_{RM}]^{-1} \frac{dW_{RM}}{d\epsilon} [W_{RM}]^{-1} Z_{RM} \quad (4.12)$$

Comparing equation (4.10) to equations (4.11) and (4.12) it is seen that the state matrix derivative is determined much more simply and at a lower computational cost using the proposed method.

4.4 Power System Modelling

The development of a power system model requires an understanding of the modelling and dynamic behaviour of its individual

subsystems. The extent to which a subsystem is modelled depends on the application as well as the computing facilities available. Often the machines in the area of interest are modelled in greater detail compared to others outside this area. The development of these individual subsystem models and subsequent analysis is by itself a formidable task and, fortunately available in the literature [81].

In this section it is proposed to present these models in the context of the Component Connection method. Essentially this requires defining the input and output quantities of these systems. The common power system components are:

1. Synchronous machine.
2. Mechanical shaft systems.
3. Exciter stabilizer systems.
4. Turbine-governor, boilers.
5. AC network.

Each of the above is now discussed, except for AC network which forms the subject of the next section. For simplification not all the components need to be modelled. Boiler-turbine governors may be eliminated by assuming constant mechanical input power. Exciter-stabilizer modelling may be omitted by assuming a constant field voltage. Some typical subsystem models are given in Appendix A2.

4.4.1 Synchronous Machine Modelling

A general model based on Park's equations has been used extensively in the literature [50-57]. Either the flux linkages or

currents may be considered as state variables. Irrespective of the choice of states the linearized generator state space model may be written as

$$\begin{aligned}\dot{x}_G &= A_G x_G + B_G u_G \\ y_G &= C_G x_G\end{aligned}\tag{4.13}$$

The matrices A_G , B_G and C_G are dependent on the type of generator model used. In the context of the subsystems interconnections approach used here the input-output vectors u_G and y_G need to be defined. These are

$$\begin{aligned}u_G &= [\omega, v_d, v_q, v_f]^T \\ y_G &= [T_e, i_d, i_q]\end{aligned}$$

The generator model is drawn as shown in Figure 4.2. The stator voltages and current are given by v_d , v_q and i_d , i_q , respectively, ω is the rotor speed, v_f is applied field voltage and T_e is the electrical torque produced by the machine. This choice of inputs and outputs ensures that no direct input-output connection is present in the model.

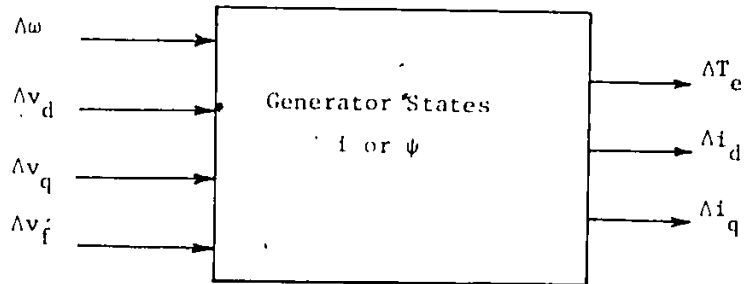


Figure 4.2 Generator Input-Output Model

4.4.2 Mechanical Shaft Model

The most common shaft representation is as a second order system called the SWING EQUATION

$$2H\omega_0\dot{\omega} = T_m - T_e - D\omega \quad (4.14)$$

where T_m and T_e are the mechanical and electrical torques, D is the damping coefficient, H is the inertia constant and ω is the rotor speed. This equation may be written in state space form as

$$\begin{aligned} \dot{x}_s &= A_s x_s + B_x u_s \\ y_s &= C_s x_s \end{aligned} \quad (4.15)$$

$$\begin{aligned} \text{with } u_s &= [T_m, T_e]^T \\ y_s &= [\delta, \omega]^T \end{aligned}$$

The shaft can be represented by a higher order system if subsynchronous effects are to be considered. However, regardless of modelling detail, the shaft subsystem can be viewed as in Figure 4.3 with electrical and mechanical torques as input and rotor speed and rotor angle as output.

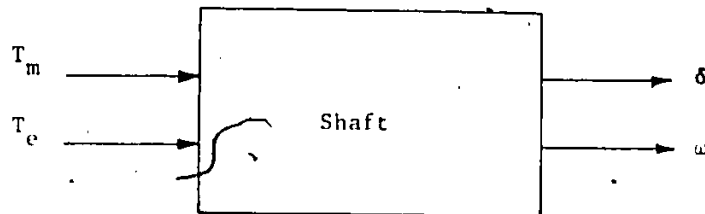


Figure 4.3 Shaft Input-Output Model

4.4.3 Exciter-Stabilizer and Turbine Governor Systems

The excitation and governor schemes are described in two IEEE committee reports [83,84]. For the excitation system the state equations are given by

$$\dot{x}_E = A_E x_E + B_E u_E$$

(4.16)

$$y_E = C_E x_E$$

The basic input-output model is shown in Figure 4.4.

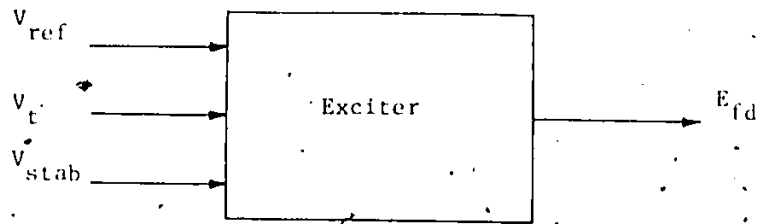


Figure 4.4 Exciter Input-Output Model

The inputs are the reference voltage V_{ref} , the machine terminal voltage V_t , the stabilizer output V_{stab} and the output is the field voltage E_{fd} . Again, the exciter itself can be modelled to any degree of detail.

Turbines-Governors can be represented similarly by

$$\dot{x}_{GT} = A_{GT}x_{GT} + u_{GT}$$

(4.17)

$$y_{GT} = C_{GT}x_{GT}$$

$$\text{with } u_{GT} = [\omega, P_{ref}]^T$$

$$y_{GT} = [P_m]$$

where ω is the speed, P_{ref} is the reference mechanical power and P_m is the turbine output power.

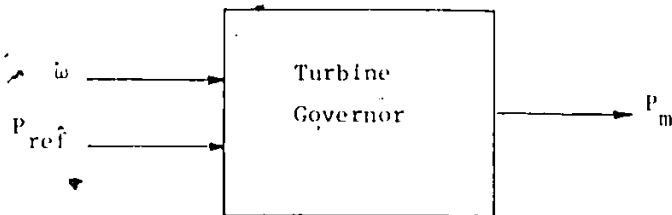


Figure 4.5 Turbine-Governor Input-Output Model

4.5 AC Network

Power systems AC networks may be represented in either of two ways. They could be described by a set of algebraic equations or alternatively, if stator transients are of interest, modelled in state space form.

4.5.1 Static Network Representation

For static representation the network is assumed to be completely described by the nodal admittance matrix equation

$$\hat{I}_N = Y_N \hat{V}_N \quad (4.18)$$

By treating all the loads as constant impedances, all load buses in the network can be eliminated. Under this assumption the reduced admittance matrix Y_R of an order equal to the number of system generator buses n is formed. This is converted to $2n$ real equations as proposed by Taylor [85],

$$I_N = Y_R V_N \quad (4.19)$$

where

$$Y_R = \begin{bmatrix} g_{11} & -b_{11} & & g_{1n} & -b_{1n} \\ b_{11} & g_{11} & & & \\ & & & g_{nn} & -b_{nn} \\ & & & b_{nn} & g_{nn} \end{bmatrix}$$

and $I_N = [i_{Q1}, i_{D1}, \dots, i_{Qn}, i_{Dn}]^T$

$$V_N = [v_{Q1}, v_{D1}, \dots, v_{Qn}, v_{Dn}]$$

The machine equations described in Section 4.4 and in Appendix A2, are expressed with reference to the perpendicular axis (d,q) rotating in synchronism with the machine rotor. In order to relate the internal quantities of the different machines, a reference frame (D,Q) which rotates at the angular frequency of the steady state network current is considered. The relationship between internal machine reference frame (d_1, q_1) and the general network reference frame (D,Q), is shown in Figure 4.6. The machine voltages in terms of the general reference frame are

$$\begin{bmatrix} v_{q1} \\ v_{d1} \end{bmatrix} = \begin{bmatrix} \cos \delta_1 & \sin \delta_1 \\ -\sin \delta_1 & \cos \delta_1 \end{bmatrix} \begin{bmatrix} v_{Q1} \\ v_{D1} \end{bmatrix} \quad (4.20)$$

or

$$v_{M1} = [T_{11}] v_{N1}$$

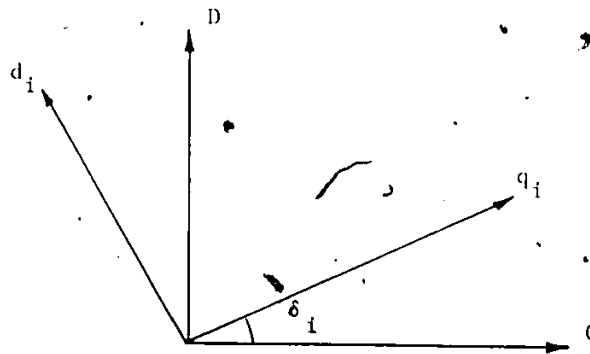


Figure 4.6 DQ-dq Reference Frame Transformation

For all machines connected to the network

$$V_M = [T]V_N \quad (4.21)$$

$$\text{where } V_M = [v_{q_1}, v_{d_1}, \dots, v_{q_n}, v_{d_n}]^T$$

$$V_N = [v_{Q_1}, v_{D_1}, \dots, v_{Q_n}, v_{D_n}]^T$$

$$T = \begin{bmatrix} T_{11} & & \\ & T_{22} & \\ & & \ddots \\ & & & T_{nn} \end{bmatrix}$$

For small perturbations, equation (4.21) is linearized and written as

$$\Delta V_M = [T_0] \Delta V_N + [T_1] \Delta \delta \quad (4.22)$$

where

$$T_1 = \begin{bmatrix} v_{d10} & & & \\ -v_{q10} & & & \\ & \ddots & & \\ & & v_{dn0} & \\ & & -v_{qn0} & \end{bmatrix}$$

and $\delta = [\delta_1, \delta_1, \dots, \delta_n]^T$

Similarly the linearized equation for machine currents can be written in terms of the reference frame currents as.

$$\Delta I_M = [T_0] \Delta I_N + [T_2] \Delta \delta \quad (4.23)$$

where $I_M = [i_{q1}, i_{d1}, \dots, i_{qn}, i_{dn}]^T$

and

$$T_2 = \begin{bmatrix} i_{d10} & & & \\ -i_{q10} & & & \\ & \ddots & & \\ & & i_{dn0} & \\ & & -i_{qn0} & \end{bmatrix}$$

Combining equations (4.20), (4.22) and (4.23) gives

$$\Delta I_M = Y_1 \Delta V_M + Y_2 \Delta \delta \quad (4.24)$$

where $Y_1 = [T_0 Y_R T^{-1}]$
 $Y_2 = [T_2 - T_0 Y_R T_0^{-1} T_1]$

Equation (4.24) is the desired relation needed between the machine voltages and currents if network transients are not modelled.

4.5.2 State Space Network Representation

The network may be represented in state space form if network dynamics are of interest. A full version of Park's Equation [81,86] includes stator flux linkages or currents as states. It would be inconsistent to combine a machine model incorporating these with a network model represented by algebraic equations. While this inconsistency leads to an erroneous prediction for the 60 Hz frequency modes, it does not affect the accuracy in predicting the other modes [87] and hence state space network models may be omitted. However, for subsynchronous resonance studies stator transients are of interest and network must be represented fully using differential equations.

The state space representation of a balanced three phase power network proceeds in two steps:

1. A single phase representation of the system.
2. The single phase equations are extended to a balanced uncoupled two-phase system and the equations transformed from a stationary to a synchronously rotating frame. This

ensures that the network equations are compatible with those of the rotating machines.

4.5.2.1 Single Phase Network State Space Representation

The single phase state representation of a power network is obtained by using the Component Connection method. Each inductive or capacitive element is treated as a subsystem. For an inductive element connected between node p and q, the state equations are given as follows:

$$\begin{aligned} \begin{bmatrix} \dot{i}_{pq} \end{bmatrix} &= \begin{bmatrix} -R_{pq} \\ L_{pq} \end{bmatrix} \begin{bmatrix} i_{pq} \end{bmatrix} + \begin{bmatrix} \frac{1}{L_{pq}} - \frac{1}{L_{pq}} \end{bmatrix} \begin{bmatrix} v_p \\ v_q \end{bmatrix} \\ \begin{bmatrix} i_{pq} \end{bmatrix} &= \begin{bmatrix} 1 \end{bmatrix} \begin{bmatrix} i_{pq} \end{bmatrix} \end{aligned} \quad (4.25)$$

Similarly the state equations for a capacitive element connected between node r and the ground are given as:

$$\begin{aligned} \begin{bmatrix} \dot{v}_r \end{bmatrix} &= \begin{bmatrix} 0 \end{bmatrix} \begin{bmatrix} v_r \end{bmatrix} + \begin{bmatrix} \frac{1}{C} \end{bmatrix} \begin{bmatrix} i_r \end{bmatrix} \\ \begin{bmatrix} v_r \end{bmatrix} &= \begin{bmatrix} 1 \end{bmatrix} \begin{bmatrix} v_r \end{bmatrix} \end{aligned} \quad (4.26)$$

The interconnection equations can be constructed from equation (4.3):

$$\begin{aligned} \bar{u} &= L_{11}\bar{y} + L_{12}u \\ y &= L_{21}\bar{y} + L_{22}u \end{aligned} \quad (4.3)$$

with $\bar{u} = [u_1^T, u_2^T \dots u_e^T]^T$
 $\bar{y} = [y_1^T, y_2^T \dots y_e^T]^T$

and where e is the total number of elements in the network.

For an inductive element connected between p and q

$$u_1^T = [v_p, v_q]$$

and $y_1 = [i_{pq}]$

For a capacitive element connected at node r

$$u_1 = [i_r]$$

and $y_1 = [v_r]$

The AC system state matrices \hat{A}_1 , \hat{B}_1 , \hat{C}_1 may then be obtained from

$$\hat{A}_1 = \bar{A}_1 + \bar{B}_1 L_{11} \bar{C}_1$$

$$\hat{B}_1 = \bar{B}_1 L_{12}$$

$$\hat{C}_1 = L_{21} \bar{C}_1$$

(4.27)

with A_i , B_i and C_i ($i = 1, 2, \dots, e$) obtained from equations (4.25) and (4.26).

4.5.2.2 Two-Phase Network Equations

The state equations for the single phase network may be extended to a two-phase rotating frame representation [88]. If the single phase representation is given as:

$$\begin{aligned}\dot{x}_1 &= \hat{A}_1 x_1 + \hat{B}_1 u_1 \\ y_1 &= \hat{C}_1 x_1\end{aligned}\tag{4.28}$$

The two-phase is then given simply as:

$$\begin{aligned}\dot{x}_2 &= \hat{A}_2 x_2 + \hat{B}_2 u_2 \\ y_2 &= \hat{C}_2 x_2\end{aligned}\tag{4.29}$$

$$\hat{A}_2 = \text{diag} [\hat{A}_1, \hat{A}_1]$$

$$\hat{B}_2 = \text{diag} [\hat{B}_1, \hat{B}_1]$$

$$\hat{C}_2 = \text{diag} [\hat{C}_1, \hat{C}_1]$$

$$x_2^T = [x_q^T, x_d^T]$$

$$u_2^T = [u_q^T, u_d^T]$$

$$y_2^T = [y_q^T, y_d^T]$$

where d and q denote the phases of the two-phase system.

The states can be transformed to a rotating reference frame using Kron's Transformation

$$x_2 = Tx_N \quad (4.30)$$

with

$$T = \left[\begin{array}{c|c} \cos\omega_0 t \, I & +\sin\omega_0 t \, I \\ \hline -\sin\omega_0 t \, I & \cos\omega_0 t \, I \end{array} \right] \quad (4.31)$$

$$x_N^T = [x_Q^T, x_D^T]$$

and I is an identity matrix of order e , where e is the number of elements in the system. Again Q and D denote a synchronously rotating reference frame. Then, from equation (4.30)

$$\dot{x}_2 = T\dot{x}_N - UTx_N$$

where

$$U = \left[\begin{array}{c|c} 0 & -\omega_0 \, I \\ \hline \omega_0 \, I & 0 \end{array} \right]$$

Substituting in equation (4.29) gives

$$\begin{aligned} \dot{x}_N &= [T^{-1}\hat{A}_2T + T^{-1}UT] x_N + T^{-1}\hat{B}_2T u_2 \\ y_N &= [T^{-1}\hat{C}_2T]x_N \end{aligned} \quad (4.32)$$

which may be written as

$$\dot{x}_N = A_{AN}x_N + B_{AN}u_N$$

(4.33)

$$y_N = C_{AN}x_N \quad (4.33)$$

The state equations given by equation (4.33) represent the network in a synchronously rotating reference frame. The network is now treated as a separate subsystem in the overall multimachine power system.

4.6 Application to Practical Power System

The advantages of the approach adopted in the previous section are now illustrated by applying to two different power systems. The case of a single machine connected to an infinite bus is presented first followed by a three-machine, nine-bus power system example.

4.6.1 Single Machine Infinite Bus AC System

The system to be studied is that of a single machine connected to an infinite bus through an AC transmission line. A single line representation of the system is shown in Figure 4.7 [81]. There are essentially two subsystems, namely the synchronous machine and the AC network. The machine itself is composed of three subsystems; the shaft, the generator and the exciter. The governor-turbine is not modelled and constant mechanical torque is assumed.

The synchronous machine to be studied is a 60 Hz synchronous machine with the following parameters:

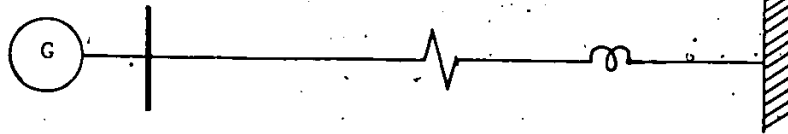


Figure 4.7 Single Machine Infinite Bus AC System

$x_d = 1.70$ pu	$x_l = 0.15$ pu
$x_q = 1.64$ pu	$r_s = 0.001096$ pu
$x_f = 1.65$ pu	$r_f = 0.000742$ pu
$x_{kd} = 1.605$ pu	$r_{kd} = 0.0131$ pu
$x_{kq} = 1.526$ pu	$r_{kq} = 0.0540$ pu
$H = 2.37$ secs	$D = 0.0$ pu
Rated MVA = 160 MVA	Power Factor = 0.85
Rated Voltage = 15 kV	Speed = 3600 rpm.

The machine is connected to an infinite bus through a transmission line having a line resistance $r_e = 0.02$ pu, line reactance $x_e = 0.4$ pu and shunt susceptance $x_c = 0.01$ pu. The infinite bus voltage is 1.0 pu. The machine loading is $P = 1.0$ pu at 0.85 power factor. Note: Resistance and reactance values are in per unit based on the machine ratings of 160 MVA and 15 kV.

The excitation system is represented by the fourth order IEEE Type 1 exciter described in Appendix A2.3. The exciter parameters are:

$\tau_R = 0.01$ secs	$K_R = 1.0$
$\tau_A = 0.05$ secs	$K_A = 40.0$
$\tau_E = 0.50$ secs	$K_E = -0.05$
$\tau_F = 0.715$ secs	$K_F = 0.04$

The exciter saturation is represented by the following non-linear function.

$$S_E = 0.0039 \exp (1.555 E_{fd})$$

The state matrices for the individual subsystems are now evaluated. The shaft subsystem is modelled as a second-order system with rotor angle and speed as the state variables. The state space equations for this system are presented in Appendix A2.2 and are evaluated at the system operating point. The state, input and output vectors x_S , u_S and y_S are as follows:

$$x_S = [\delta, \omega]^T$$

$$u_S = [T_m, T_e]^T$$

$$y_S = [\delta, \omega]^T$$

The matrices for the shaft subsystem are obtained as:

$$A_S = \begin{bmatrix} 0.0000 & 0.0000 \\ 0.0000 & 0.0000 \end{bmatrix}$$

$$B_S = \begin{bmatrix} 0.0000 & 0.0000 \\ 0.0006 & -0.0006 \end{bmatrix}$$

$$C_S = \begin{bmatrix} 1.0000 & 0.0000 \\ 0.0000 & 1.0000 \end{bmatrix}$$

The generator subsystem is modelled as a fifth order system. The currents are selected as the state variables and the model is

described in Appendix A2.1. The state, input and output vectors x_G , u_G and y_G for the generator model are as follows:

$$\begin{aligned} x_G &= [i_d, i_f, i_{kd}, i_q, i_{kq}]^T \\ u_G &= [v_d, v_f, v_{kd}, v_q, v_{kq}, \omega]^T \\ y_G &= [i_d, i_f, i_{kd}, i_q, i_{kq}]^T \end{aligned}$$

The state matrices for the generator subsystem are:

$$A_G = \begin{bmatrix} -0.0059 & 0.0014 & 0.0447 & -8.8798 & -8.0676 \\ 0.0021 & -0.0053 & 0.0671 & 3.0804 & 2.7986 \\ 0.0037 & 0.0038 & -0.1162 & 5.6007 & 5.0884 \\ 9.1817 & 8.3716 & 8.3716 & -0.0059 & 0.2848 \\ -8.9651 & -8.1740 & -8.1741 & 0.0058 & -0.3134 \end{bmatrix}$$

$$B_G = \begin{bmatrix} -5.4145 & 1.8783 & 3.4150 & 0.0000 & 0.0000 & -6.2247 \\ 1.8783 & -7.1826 & 5.1226 & 0.0000 & 0.0000 & 2.1593 \\ 3.4150 & 5.1226 & -8.8681 & 0.0000 & 0.0000 & 3.9261 \\ 0.0000 & 0.0000 & 0.0000 & -5.4011 & 5.2736 & 9.0499 \\ 0.0000 & 0.0000 & 0.0000 & 5.2736 & -5.8045 & -8.8363 \end{bmatrix}$$

$$C_G = \begin{bmatrix} 1.0000 & 0.0000 & 0.0000 & 0.0000 & 0.0000 \\ 0.0000 & 1.0000 & 0.0000 & 0.0000 & 0.0000 \\ 0.0000 & 0.0000 & 1.0000 & 0.0000 & 0.0000 \\ 0.0000 & 0.0000 & 0.0000 & 1.0000 & 0.0000 \\ 0.0000 & 0.0000 & 0.0000 & 0.0000 & 1.0000 \end{bmatrix}$$

The exciter system has been modelled by a fourth order model described in Appendix 2.3 and its state, input and output vectors x_E , u_E and y_E are as follows:

$$x_E = [v_R, v_1, v_3, E_{fd}]^T$$

$$u_E = [v_d, v_q, v_{ref}]^T$$

$$y_E = [v_f]$$

The state matrices for the exciter subsystem are obtained as:

$$A_E = \begin{bmatrix} -0.2653 & 0.0000 & 0.0000 & 0.0000 \\ 0.0000 & -0.0037 & 0.0000 & -0.0000 \\ -2.1220 & -2.1220 & -0.0531 & 0.0000 \\ 0.0000 & 0.0000 & 0.0053 & -0.0014 \end{bmatrix}$$

$$B_E = \begin{bmatrix} -0.0868 & 0.1266 & 0.0000 \\ 0.0000 & 0.0000 & 0.0000 \\ 0.0000 & 0.0000 & 2.1220 \\ 0.0000 & 0.0000 & 0.0000 \end{bmatrix}$$

$$C_E = \begin{bmatrix} 0.0000 & 0.0000 & 0.0000 & -0.0008 \end{bmatrix}$$

The AC network has also been modelled in state space form as described in Section 4.5. For the single transmission line network this results in a fourth order subsystem with its state, input and output vectors x_N , u_N and y_N given by:

$$x_N = [i_{Q\alpha}, v_{QM}, i_{D\alpha}, v_{DM}]^T$$

$$u_N = [i_{QM}, v_{Q\alpha}, i_{DM}, v_{D\alpha}]^T$$

$$y_N = [v_{QM}, v_{DM}]^T$$

The state matrices are obtained as:

$$\begin{aligned}
 \begin{matrix} A \\ N \end{matrix} &= \begin{bmatrix} -0.0500 & 2.5000 & 1.0000 & 0.0000 \\ -100.0000 & 0.0000 & 0.0000 & 1.0000 \\ -1.0000 & 0.0000 & -0.0500 & 2.5000 \\ 0.0000 & -1.0000 & -100.0000 & 0.0000 \end{bmatrix} \\
 \begin{matrix} B \\ N \end{matrix} &= \begin{bmatrix} 0.0000 & -2.5000 & 0.0000 & 0.0000 \\ 100.0000 & 0.0000 & 0.0000 & 0.0000 \\ 0.0000 & 0.0000 & 0.0000 & -2.5000 \\ 0.0000 & 0.0000 & 100.0000 & 0.0000 \end{bmatrix} \\
 \begin{matrix} C \\ N \end{matrix} &= \begin{bmatrix} 0.0000 & 1.0000 & 0.0000 & 0.0000 \\ 0.0000 & 0.0000 & 0.0000 & 1.0000 \\ 1.0000 & 0.0000 & 0.0000 & 1.9124 \\ 0.0000 & 0.0000 & 1.0000 & 0.0000 \end{bmatrix}
 \end{aligned}$$

The interconnections between the subsystems are shown in Figure 4.8 and the interconnection matrix L_{11} is given in Table 4.1. The reference frame transformation relating machine and network voltages and currents is included in the interconnection matrix.

The state matrix for the single machine infinite bus system is then given by

$$A = \bar{A} + \bar{B} L_{11} \bar{C} \quad (4.34)$$

where \bar{A} = block diag $[A_S, A_G, A_E, A_{AN}]$
 \bar{B} = block diag $[B_S, B_G, B_E, B_{AN}]$
 \bar{C} = block diag $[C_S, C_G, C_E, C_{AN}]$

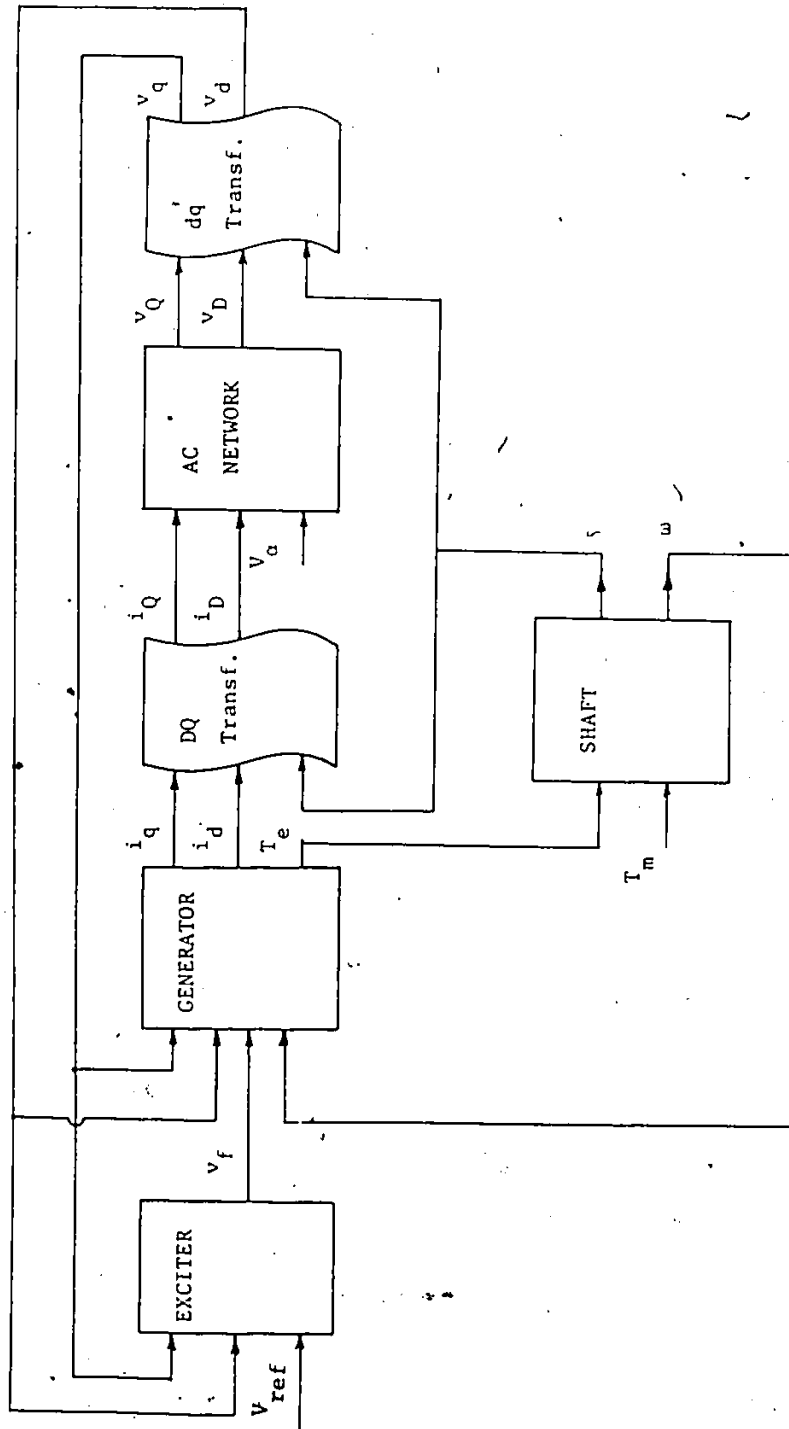


Fig. 4.8 Subsystem Interconnection for Single Machine Infinite Bus System

Table 4.1 Interconnection Matrix L_{11} for Single Machine Infinite Bus AC System

	δ	ω	i_d	i_f	i_{kd}	i_q	i_{kq}	T_e	v_f	v_{QM}	v_{DM}
T_m											
T_e								1			
v_d	E1								-E5	E6	
$-v_f$									-1		
v_{kd}											
v_q	E2								E6	E5	
v_{kq}											
ω		1									
v_d	E1								-E5	E6	
v_q	E2								E6	E5	
V_{ref}											
i_{QM}	E3		-E5			E6					
$v_{Q\alpha}$											
i_{DM}	E4		E6			E5					
$v_{D\alpha}$											

$E1 = -v_{q0};$
 $E2 = v_{d0};$
 $E3 = i_{q0} \sin \delta_0 - i_{d0} \cos \delta_0;$
 $E4 = i_{q0} \cos \delta_0 - i_{d0} \sin \delta_0;$
 $E5 = \sin \delta_0;$
 $E6 = \cos \delta_0.$

The matrix A evaluated for this system is shown in Table 4.2.

Apart from the ease of formulation of the state matrix one of the main advantages of using this method is in the evaluation of the derivative of the system state matrix. For example, we consider the evaluation of the state matrix derivative with respect to the amplifier gain K_A of the exciter. Applying equation (4.10) we get:

$$\frac{dA}{dK_A} = \frac{d\bar{A}}{dK_A} + \frac{d\bar{B}}{dK_A} L_{11} \bar{C} + \bar{B} \frac{dL_{11}}{dK_A} \bar{C} + \bar{B} L_{11} \frac{d\bar{C}}{dK_A} \quad (4.35)$$

where

$$\frac{d\bar{A}}{dK_A} = \text{block diag.} \left[\frac{dA_s}{dK_A}, \frac{dA_G}{dK_A}, \frac{dA_E}{dK_A}, \frac{dA_{AN}}{dK_A} \right]$$

$$\frac{d\bar{B}}{dK_A} = \text{block diag.} \left[\frac{dB_s}{dK_A}, \frac{dB_G}{dK_A}, \frac{dB_E}{dK_A}, \frac{dB_{AN}}{dK_A} \right]$$

$$\frac{d\bar{C}}{dK_A} = \text{block diag.} \left[\frac{dC_s}{dK_A}, \frac{dC_G}{dK_A}, \frac{dC_E}{dK_A}, \frac{dC_{AN}}{dK_A} \right]$$

Only the exciter subsystem matrices A_E and B_E are functions of the amplifier gain K_A . Therefore equation (4.34) can be rewritten as:

$$\frac{dA}{dK_A} = \frac{d\bar{A}}{dK_A} + \frac{d\bar{B}}{dK_A} L_{11} \bar{C} \quad (4.36)$$

where:

$$\frac{d\bar{A}}{dK_A} = \text{block diag.} \left[0, 0, \frac{dA_E}{dK_A}, 0 \right]$$

$$\frac{d\bar{B}}{dK_A} = \text{block diag.} \left[0, 0, \frac{dB_E}{dK_A}, 0 \right]$$

and:

$$\frac{dA_E}{dK_A} = \begin{bmatrix} 0 & 0 & 0 & 0 \\ -\frac{1}{T_A} & 0 & -\frac{1}{T_A} & 0 \\ 0 & 0 & 0 & 0 \\ 0 & 0 & 0 & 0 \end{bmatrix}$$

$$\frac{dB_E}{dK_A} = \begin{bmatrix} 0 & 0 & 0 & 0 \\ 0 & 0 & 0 & \frac{1}{T_A} \\ 0 & 0 & 0 & 0 \\ 0 & 0 & 0 & 0 \end{bmatrix}$$

It is seen that derivative evaluation is easily accomplished using matrix multiplication and is computationally inexpensive where $\frac{d\bar{A}}{dK_A}$, $\frac{d\bar{B}}{dK_A}$, L_{11} and \bar{C} have been stored in sparse form.

4.6.2 Multimachine AC Power System

The technique is next applied to a nine-bus three machine AC power system. The network is shown in Figure 4.9. It is the same as considered earlier in Section 3.8.1 but without the HVDC system. The bus and line data for the network is given in Tables 3.1 and 3.2. The data for the three machines is given in Table 4.3. In this example network dynamics have not been modelled and the machines have been represented by simplified models. Machines 1 and 2 are both represented by fourth order models formed by combining the second order shaft model with the two axis generator representation. Machine 3 is represented by the second order classical model.

The generator equations are as follows:

- Generators 1 and 2 (two axis model)

$$\tau'_{qoi} \dot{E}'_{qi} = -E'_{di} - (x_{qi} - x'_i) I_{qi}$$

$$\tau'_{qoi} \dot{E}'_{qi} = -E_{fdi} - E'_{qi} + (x_{di} - x'_i) I_{di}$$

(4.38)

$$2H_i \omega_0 \dot{\omega}_i = T_{mi} - D_i \omega_i - I_{doi} E'_{di} - I_{qoi} E'_{qi} - E'_{doi} I_{di} - E'_{qoi} I_{qi}$$

$$\dot{\delta}_i = \omega_i, \quad i = 1, 2$$

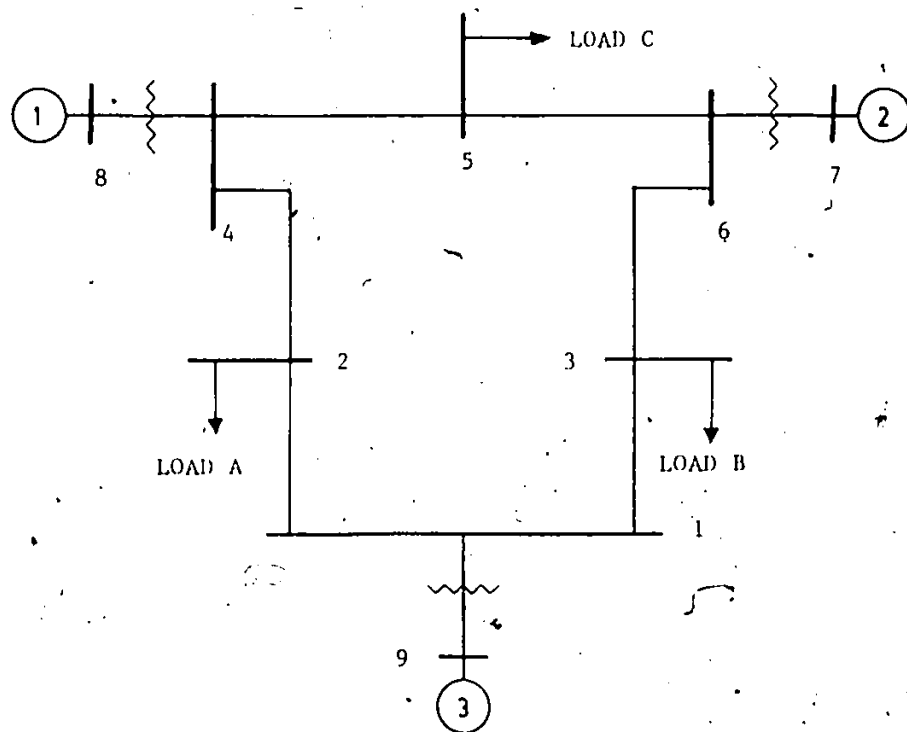


Figure 4.9 Multimachine AC Power System

Table 4.3 Generator Data [81]

Generator	1	2	3
Rated MVA	192	128	247.5
KV	18.0	13.8	16.5
Power factor	0.85	0.85	1.0
Type	Steam	Steam	Hydro
Speed	3600 rpm	3600 rpm	180 rpm
x_d	0.8958	1.3125	0.146
x'_d	0.1198	0.1813	0.0608
x_q	0.8645	1.2578	0.0969
x'_q	0.1969	0.25	0.0969
x_l	0.0521	0.0742	0.0336
τ_{do}	6.00	5.89	8.96
τ'_{qo}	0.535	0.6	0.0
E'_{qo}	0.7882	0.7679	-1.0558
E'_{do}	0.6940	0.6668	0.0419
I_{qo}	0.932	0.6194	-0.678
I_{do}	-1.2902	-0.5615	0.2872
H	6.4	3.01	23.64
D	1	1	1

Note: Reactance values are in pu on a 100-MVA base.
 All time constants are in sec.
 The inertia constants are in sec.

- Generator 3 (classical)

$$2H_3\omega_0\dot{\omega}_3 = T_{m3} - E_3I_{q3} - D_3\omega_3$$

(4.38)

$$\dot{\delta}_3 = \omega_3$$

Thus the system under study consists of ten first order differential equations and is represented by the following state variables: E_{q1} , E_{d1} , δ_1 , ω_1 , E_{q2} , E_{d2} , δ_2 , ω_2 , δ_3 and ω_3 . The system interconnection matrix is given in Table 4.4 and is formed using equation (4.24). The state matrix for the system is evaluated using equation (4.9) and is given in Table 4.5.

4.7 Summary

A procedure has been presented to form the linearized state variable model for a multimachine power system. The basic structure of equation (4.9) yields a number of advantages in the computational and conceptual process. The separation of subsystem representation ($\bar{A}, \bar{B}, \bar{C}$) and the interconnections (L_{11}, L_{12}, L_{21}) means that the assembly can be modularized. Given particular input-output quantities for the subsystems, the modelling complexity (order) within the subsystem can be changed and only the relevant coefficient matrices for the subsystem are affected. Several levels of assembly can be used to advantage.

[illegible]

Table 4.5 State Matrix for Multitachine AC System

-0.00166	0.00014	-0.00175	0.00000	0.00056	0.00004	0.00073	0.00000	0.00102	0.00000
-0.00132	-0.01569	-0.01188	0.00000	-0.00038	0.00526	0.00673	0.00000	0.00516	0.00000
0.00000	0.00000	0.00000	1.00000	0.00000	0.00000	0.00000	0.00000	0.00000	0.00000
-0.00061	-0.00027	-0.00107	-0.00044	0.00017	0.00023	0.00052	0.00000	0.00055	0.00000
0.00036	0.00012	0.00057	0.00000	-0.00138	0.00014	-0.00148	0.00000	0.00091	0.00000
-0.00127	0.00309	0.00371	0.00000	-0.00155	-0.01502	-0.00734	0.00000	0.00363	0.00000
0.00000	0.00000	0.00000	0.00000	0.00000	0.00000	0.00000	1.00000	0.00000	0.00000
0.00006	0.00013	0.00023	0.00000	-0.00038	-0.00007	-0.00055	-0.00021	0.00031	0.00000
0.00000	0.00000	0.00000	0.00000	0.00000	0.00000	0.00000	0.00000	0.00000	1.00000
0.00003	0.00003	0.00007	0.00000	0.00004	0.00004	0.00010	0.00000	-0.00017	-0.00006

For example, a generating unit model can be assembled from shaft, generator, turbine and exciter/governor control subsystems with interconnection matrices for the generating unit. With multiple choices of variables, these matrices are sparse and consist generally of ones and zeros. Later this generator is considered as a subsystem in an area within the overall interconnection and finally the areas can be combined.

The structure of the formulation process is thus compatible with the way power systems are conceptually developed and the degree of modelling complexity matched to the specific simulation problem. The restriction that the D matrices be null is also consistent with engineering modelling practices.

Two examples consisting of a single machine infinite bus system and a multimachine AC power system were included to illustrate the use of the method.

CHAPTER 5

STATE MATRIX FORMULATION FOR MULTITERMINAL AC-DC POWER SYSTEMS

5.1 Introduction

There is a significant impact of an HVDC system on the dynamic performance of the AC system. The HVDC system introduces a new degree of controllability which had not been previously available and current HVDC systems incorporate a variety of controls to enhance the performance of the integrated AC-DC power system [18].

The DC system performance may be considered under several distinct classifications. The steady state characteristics are determined from the AC-DC loadflow analysis. The dynamic response characteristics depend on the system response to large or small disturbances. The modelling of the HVDC system is dependent on the particular performance characteristics being considered. The steady state modelling for power flow purposes has been covered previously in Chapter 3. This chapter is concerned with the development of a linearized model of the integrated AC-DC power system to be used for determining the system response to small disturbances. It extends the formulation of the power system state matrix to include a multiterminal HVDC network.

The multiterminal HVDC system could either be of the parallel or series configuration. The parallel connection has been chosen here because of its advantages in terms of lower line losses, lesser reactive power requirement and greater reliability. All multiterminal studies envisage a central controller for the coordination of the current or power settings. In this chapter the central control is assumed to have a dispatching function only and is therefore not modelled for steady state stability study.

5.2 Modelling of the DC Terminal

The DC terminal has primarily three components, namely the converter itself, the converter firing angle controller and the converter tap changing transformer. The dynamics of the converter are much faster than those of the AC system and are usually not considered for the purpose of determining steady state stability. In this case the converter voltage equation rewritten on a single phase power basis is given by

$$V_{DC} = 3aV_{AC}\cos\alpha - R_C I_{DC} \quad (5.1)$$

With an appropriate selection of α , the converter acts as a rectifier for $V_{DC} \geq 0$ and as an inverter for $V_{DC} \leq 0$. All inverters are connected backwards in the DC system so that the rectifier deliver power to this network, whereas an inverter absorbs it (and delivers it

to the AC system). The inverter voltage can also be written in terms of the extinction angle γ as:

$$V_{DC} = 3aV_{AC}\cos\gamma - R_C I_{DC} \quad (5.2)$$

The DC terminal can function in either the constant angle, constant voltage or constant current modes. In all cases the controller is assumed to control the firing angle and is in general represented by a single lag time constant transfer function although more complex representations may be included if desired [89]. The converter controller model is represented in state space form as

$$\dot{x}_{DC} = A_{DC} x_{DC} + B_{DC} u_{DC} \quad (5.3)$$

$$y_{DC} = C_{DC} x_{DC}$$

with $x_{DC} = [\alpha]$

$y_{DC} = [\alpha]$

and u_{DC} is dependent on the type of control mode. The block diagrams of the converter controller for the different control modes are shown in Figure 5.1. Controller equations are given in the Appendix A2.4.

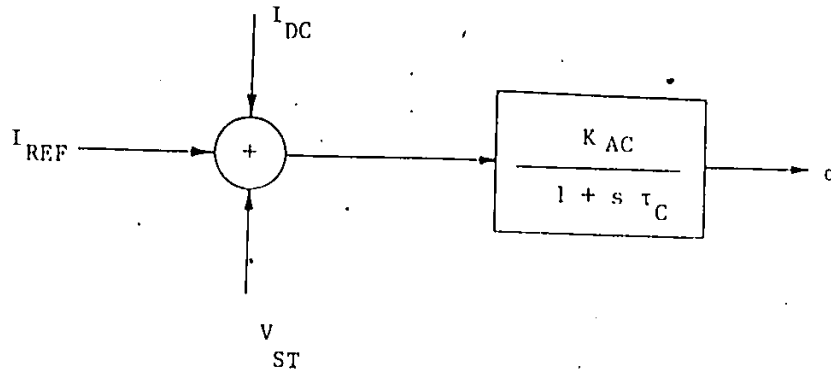


Fig. 5.1(a) DC Converter - Constant Current Controller

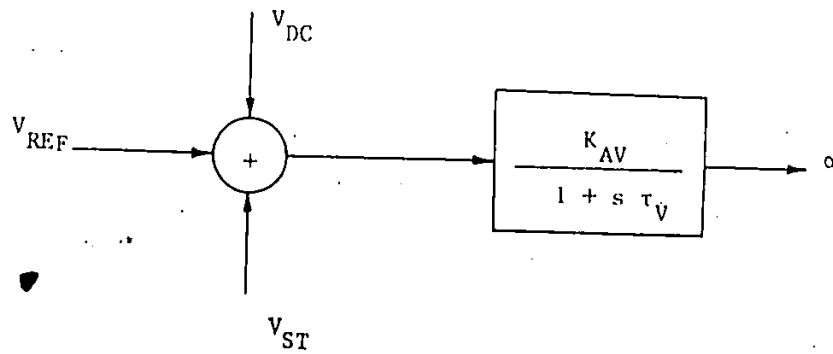


Fig. 5.1(b) DC Converter - Constant Voltage Controller

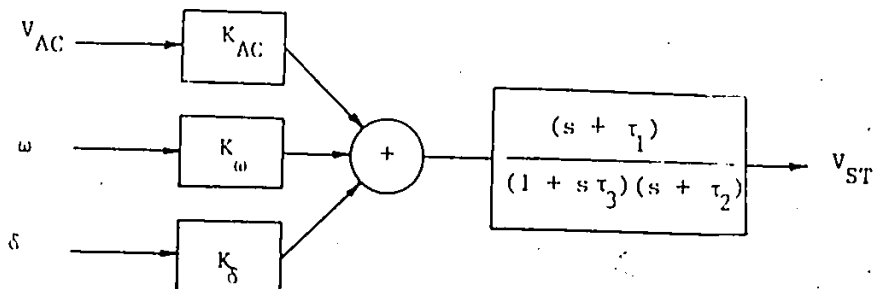


Fig. 5.2 DC Converter Stabilizer

The converter controller is also provided with an input signal from a supplementary stabilizer. This stabilizer provides for the modulation of the converter controller. The input signal for the stabilizers are selectable from various AC system quantities, such as power flow, voltage, frequency, phase angle, etc. [89]. Inputs from several independent sources may be required. The stabilizer model is shown in Fig. 5.2 and is represented in state space form as

$$\begin{aligned} \dot{x}_{ST} &= A_{ST} x_{ST} + B_{ST} u_{ST} \\ y_{ST} &= C_{ST} x_{ST} \end{aligned} \quad (5.4)$$

where $y_{ST} = V_{ST}$

and the states x_{ST} and inputs u_{ST} depend upon the stabilizer representation and the modulating quantities, respectively.

5.3 Modelling of the DC Network

The DC network is modelled in state space form. The method used is the same employed for the single phase state space representation of the AC network. For a k terminal network the state equations are

$$\begin{aligned} \dot{x}_{DN} &= A_{DN} x_{DN} + B_{DN} u_{DN} \\ y_{DN} &= C_{DN} x_{DN} \end{aligned} \quad (5.5)$$

where $u_{DN} = [V_{DC_1}, V_{DC_2} \dots V_{DC_k}]^T$
 $y_{DN} = [I_{DC_1}, I_{DC_2} \dots I_{DC_k}]^T$

V_{DCi} and I_{DCi} are the DC voltages and currents at the i th input node. The states x_{DN} are the currents in the line inductance or voltages across the shunt susceptance.

5.4 AC-DC Interface

The AC-DC interface equations define the relationships between the AC and DC quantities on both sides of the converter. This will enable the coupling of the AC and DC network.

The relation between the DC converter current and the corresponding AC components is

$$a^2 I_{DC}^2 = (i_D^2 + i_Q^2)/3 \quad (5.6)$$

The components of the terminal AC bus voltage in terms of the reference D-Q axes quantities is

$$V_{AC}^2 = (V_D^2 + V_Q^2)/3 \quad (5.7)$$

Assuming a lossless converter the input and output powers are equal

$$P_{AC} = P_{DC} \quad (5.8)$$

where $P_{AC} = v_D i_D + v_Q i_Q$

$$P_{DC} = 3aV_{AC}I_{DC}\cos\alpha - R_C i_{DC}^2$$

Linearizing equations (5.6) to (5.8) and solving for i_Q and i_D , gives for each converter

$$\begin{bmatrix} \Delta i_{Q1} \\ \Delta i_{D1} \end{bmatrix} = \begin{bmatrix} P_{11} & P_{21} & P_{31} & P_{41} \\ P_{51} & P_{61} & P_{71} & P_{81} \end{bmatrix} \begin{bmatrix} \Delta v_{Q1} \\ \Delta v_{D1} \\ \Delta \alpha_1 \\ \Delta i_{DC1} \end{bmatrix} \quad (5.9)$$

For a k terminal HVDC network this is written as

$$\begin{bmatrix} \Delta i_{Q1} \\ \Delta i_{D1} \\ \vdots \\ \Delta i_{Qk} \\ \Delta i_{Dk} \end{bmatrix} = \begin{bmatrix} P_{11} & P_{21} & & & \\ & P_{51} & P_{61} & & \\ & & & \ddots & \\ & & & & P_{1k} & P_{2k} \\ & & & & P_{3k} & P_{4k} \end{bmatrix} \begin{bmatrix} \Delta v_{Q1} \\ \Delta v_{D1} \\ \vdots \\ \Delta v_{Qk} \\ \Delta v_{Dk} \end{bmatrix} + \quad (5.10)$$

$$+ \begin{bmatrix} P_{31} & & & \\ P_{71} & & & \\ & \ddots & & \\ & & P_{3k} & \\ & & P_{7k} & \end{bmatrix} \begin{bmatrix} \Delta \alpha_1 \\ \vdots \\ \Delta \alpha_k \end{bmatrix} + \begin{bmatrix} P_{41} & & & \\ P_{81} & & & \\ & \ddots & & \\ & & P_{4k} & \\ & & P_{8k} & \end{bmatrix} \begin{bmatrix} \Delta i_{DC1} \\ \vdots \\ \Delta i_{DCk} \end{bmatrix}$$

Now equation (5.10) relates the AC currents injected in the DC network to the AC bus voltage, converter firing angle and currents.

5.5 AC-DC Interconnections

The relationship between machine voltages and currents when the machines are connected in an arbitrary AC network were given earlier in equation (4.24). The formulation is now expanded to include the presence of a multiterminal HVDC network in addition to the AC network already present. A static representation is assumed for the AC system.

Consider an AC-DC system with k terminals and r machines. The addition of the k terminals result in current injection at k AC buses apart from the original r AC buses where the machines are connected. Eliminating all load buses equation (4.19) can be expanded as:

$$\begin{bmatrix} I_{AC} \\ \hat{I}_M \end{bmatrix} = \begin{bmatrix} Y_{11} & Y_{12} \\ Y_{21} & Y_{22} \end{bmatrix} \begin{bmatrix} V_{AC} \\ \hat{V}_M \end{bmatrix} \quad (5.11)$$

where I_{ACi} , V_{ACi} ($i = 1, 2, \dots, k$) are the currents and voltages at the AC buses at which the terminals are connected. Similarly, I_{mi} , V_{mi} ($i = 1, 2, \dots, r$) are the current and voltages at the machine buses.

The net injected currents in the AC network due to the DC system is now given by equation (5.10) rewritten as

$$\Delta I_{AC} = -[P_1 \Delta V_{AC} + P_2 \Delta \alpha + P_3 \Delta I_{DC}] \quad (5.12)$$

where α is the set of converter firing angle and I_{DC} the set of converter DC currents. Substituting (5.12) in equation (5.11) gives

$$\begin{bmatrix} 0 \\ \Delta \hat{I}_M \end{bmatrix} = \begin{bmatrix} (Y_{11} + P_1) & Y_{12} \\ Y_{21} & Y_{22} \end{bmatrix} \begin{bmatrix} \Delta V_{AC} \\ \Delta \hat{V}_M \end{bmatrix} + \begin{bmatrix} P_2 \\ 0 \end{bmatrix} \begin{bmatrix} \Delta \alpha \\ \Delta I_{DC} \end{bmatrix} + \begin{bmatrix} P_3 \\ 0 \end{bmatrix} \begin{bmatrix} \Delta \delta \\ \Delta V_M \end{bmatrix} \quad (5.13)$$

We now transform as before and then rearrange to obtain the following equation which is equivalent to equation (4.24) for the expanded AC-DC system

$$\begin{bmatrix} \Delta V_{AC} \\ \Delta \hat{I}_M \end{bmatrix} = \begin{bmatrix} L_1 & L_2 & L_3 & L_4 \\ L_5 & L_6 & L_7 & L_8 \end{bmatrix} \begin{bmatrix} \Delta \alpha \\ \Delta I_{DC} \\ \Delta \delta \\ \Delta V_M \end{bmatrix} \quad (5.14)$$

where

$$\begin{aligned} L_1 &= Y_* P_2 \\ L_2 &= Y_* P_3 \\ L_3 &= -Y_* Y_{12} T_0^{-1} T_1 \\ L_4 &= Y_* Y_{12} T_0^{-1} \\ L_5 &= T_0 Y_{21} Y_* P_2 \\ L_6 &= T Y_{21} Y_* P_3 \end{aligned}$$

$$\begin{aligned}
 L_7 &= T_2 - T_0 [Y_{22} + Y_{21} Y_* Y_{12}] T_0^{-1} T_1 \\
 L_8 &= T_0 [Y_{22} + Y_{21} Y_* Y_{12}] T_0^{-1} \\
 \text{and } Y_* &= -[Y_{11} + P_1]^{-1}
 \end{aligned}$$

It can be seen that one matrix inversion is required whose order is twice the number of DC terminals.

5.6 Test Examples

In this section the results of the previous section are applied to the single machine and multimachine test examples of Section 4.6.

5.6.1 Single Machine - Infinite Bus System

The single machine-infinite bus AC-DC power system is shown in Figure 5.3. It is formed by adding a parallel DC transmission line to the AC line in the single machine infinite bus system of Section 4.6.1. The parameters of the machine and AC transmission network have been given earlier in that section. The DC system consists of the rectifier and inverter terminals and the HVDC transmission line. The rectifier operates on constant current control with $I_{DCR} = 0.5$ pu. The inverter sets the system voltage and is on constant voltage control with $V_{DCI} = 1.0$ pu. Both the converters are equipped with single time constant controllers as shown in Figure 5.1. The parameters of the converter controllers are:

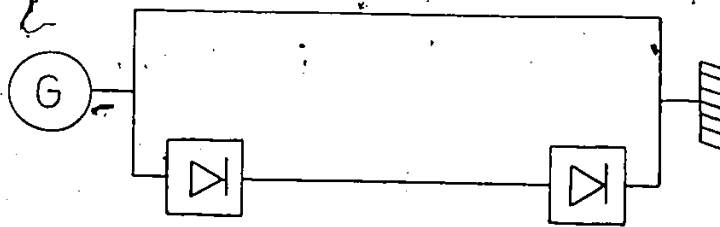


Fig. 5.3 Single Machine Infinite Bus AC-DC Power System

$$K_{AC} = 5.0 \quad K_{SC} = 1 \quad \tau_C = 0.01 \text{ secs}$$

$$K_{AV} = 5.0 \quad K_{SV} = 1 \quad \tau_V = 0.01 \text{ secs.}$$

The DC transmission line has a line resistance of 0.011 pu. The machine loading is $P = 1.0$ at 0.85 pf as before.

The state matrix of the AC-DC system is now formulated using equation (4.9). The two terminal controllers have been combined together to form a single subsystem. The state, input and output vectors for the combined DC terminal controller are:

$$x_{DC} = [\alpha_R, \alpha_I]^T$$

$$u_{DC} = [I_{REF}, V_{REF}, V_{STI}, V_{ACI}]^T$$

$$y_{DC} = [\alpha_R, \alpha_I]^T$$

DC line dynamics have been modelled with the line current as the state variable. The state, input and output vectors for the DC network subsystem are:

$$x_{DN} = [I_{DC}]$$

$$u_{DN} = [V_{QR}, V_{DR}, V_{QI}, V_{DI}, \alpha_R, \alpha_I]^T$$

$$y_{DN} = [I_{DC}]$$

The subsystems interconnections for this system are shown in Figure 5.4 and the interconnection matrix L_{11} is shown in Table 5.1.

The state matrix of the AC/DC system is given by:

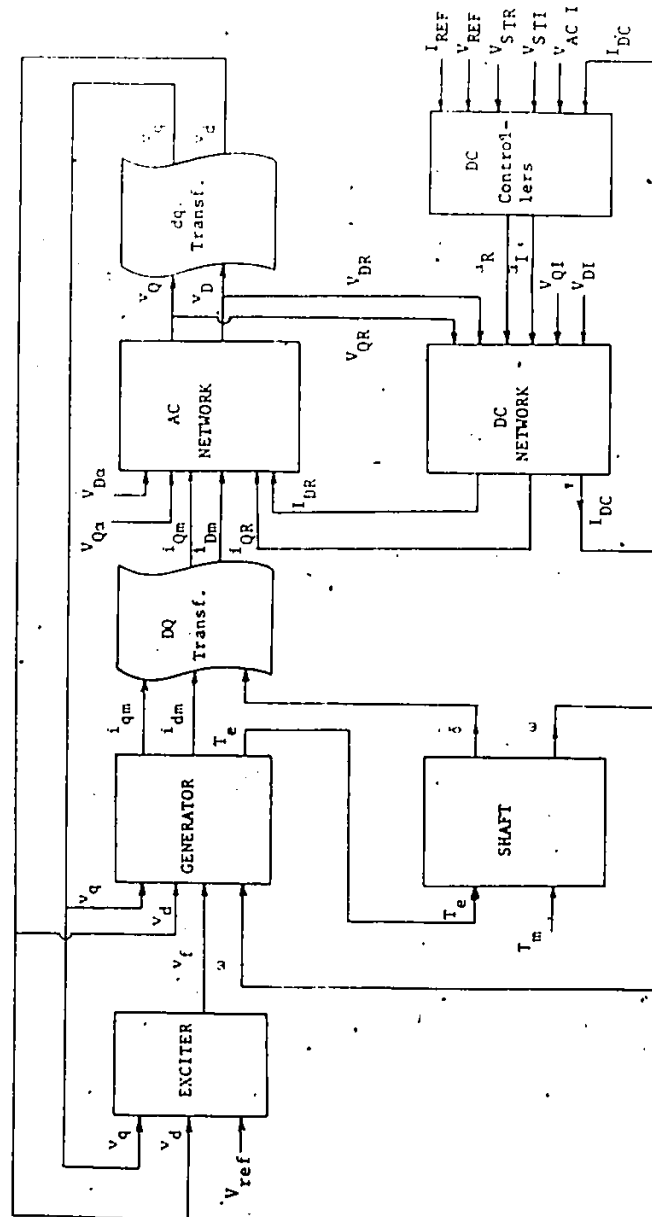


Fig. 5.4 Subsystem Interconnection for Single Machine Infinite Bus AC-DC System

Table 5.1. Interconnection Matrix L_{11} for Single Machine Infinite Bus AC-DC System

	δ	ω	i_d	i_f	i_{kd}	i_q	i_{kq}	T_e	$-v_f$	v_{QM}	v_{DM}	I_{DC}	α_R	α_I
T_m								1						
T_e														
v_d	E1									-E5	E6			
$-v_f$														
v_{kd}									1					
v_q	E2									E6	-E5			
v_{kq}														
ω		1												
v_d	E1									-E5	E6			
v_q	E2									E6	E5			
v_{ref}														
i_{QM}	E3		-E5			E6								
i_{QR}										P_{1R}	P_{2R}	P_{3R}	P_{4R}	
v_{Qa}														
i_{DM}	E4		E6			E5								
i_{DR}										P_{5R}	P_{6R}	P_{7R}	P_{8R}	
v_{Da}														
v_{QR}										1				
v_{DR}											1			
v_{QI}														
v_{DI}														
α_R													1	
α_I														1
I_{REF}														
V_{REF}														
I_{DC}												1		
v_{STR}			1											
v_{STI}														
v_{ACI}														

Note: E1 - E6 are defined in Table 4.1.
 P_{1R} - P_{8R} are given by equation (5.9).

$$A = \bar{A} + \bar{B} L_{11} \bar{C}$$

where

$$\begin{aligned}\bar{A} &= \text{block diag } [A_S, A_G, A_E, A_{AN}, A_{DN}, A_{DC}] \\ \bar{B} &= \text{block diag } [B_S, B_G, B_E, B_{AN}, B_{DN}, B_{DC}] \\ \bar{C} &= \text{block diag } [C_S, C_G, C_E, C_{AN}, C_{DN}, C_{DC}]\end{aligned}$$

and L_{11} is the interconnection matrix. The subscript DN and DC denote the DC controller and DC network subsystems, respectively.

The eigenvalues of the AC-DC system are shown in Table 5.2 and are given in rad/rad. For comparison the eigenvalues of the AC system of Section 4.6.1 are also given. Note that the HVDC system results in three extra eigenvalues corresponding to the DC controllers and DC line dynamics. The complex eigenvalue pair $(-0.8457 \pm j0.9272)$ is due to the interaction of the rectifier controller and DC line dynamics. The real eigenvalue (-0.2678) corresponds to the inverter controller. In both the AC-DC system and the AC system the transient response is dominated by two pairs of complex eigenvalues. For the AC-DC system these pairs are $(-0.0026 \pm j0.0307)$ and $(-0.0004 \pm j0.0056)$. The first pair corresponds to the rotor electromechanical oscillations which decay with a time constant of $1/(0.0026 * 377)$ or 1.02 secs and have a frequency of 1.78 Hz. The second pair represents the interaction between the field circuit and the exciter. For the AC system the corresponding pairs are $-0.0015 \pm j0.0289$ and $-0.0003 \pm j0.0064$, respectively. Note the rotor oscillations in the AC case have a decay

Table 5.2. Eigenvalues for Single Machine Infinite Bus AC-DC System

AC-DC System C = 0.20	AC System C = 0.01
-0.0360 ± j0.0998	-0.0359 ± j0.9983
-0.2653	-0.2652
-0.1046 ± j0.0096	-0.1215
	-0.0994
-0.0547	-0.0547
-0.0026 ± j0.0307	-0.0015 ± j0.0289
-0.0004 ± j0.0056	-0.0003 ± j0.0064
-0.0041	-0.0040
-0.3442 ± j7.7940	-0.0600 ± j29.12
-0.6399 ± j6.0024	-0.0648 ± j27.12
-0.8457 ± j0.9272	
-0.2678	

constant of 1.77 secs and a frequency of 1.73 Hz. Thus it is seen that the rotor damping is considerably improved in the presence of the DC system. The presence of the DC link has also resulted in increased damping of the field-exciter eigenvalue pair.

The eigenvalue $(-0.0360 \pm j0.9980)$ corresponds to a very fast transient of about 60 Hz which is damped with a time constant of 0.073 secs. This is the 60 Hz component injected into the rotor circuit to balance the MMF due to the stator DC currents and is little effected by the DC link. The complex eigenvalue pairs $(-0.3442 \pm j7.7940)$ and $(-0.6399 \pm j6.0024)$ essentially represent AC line dynamics and are different from those for the AC system since the line shunt capacitance is increased to include the terminal compensating capacitors in the DC case.

5.6.2 Multimachine Multiterminal AC-DC Power System

In this section the state matrix formulation approach is applied to the three machine - three terminal AC-DC system of Section 3.8.1. The power system has been redrawn in Figure 5.5. Machines 1 and 2 have been modelled by the fourth order two axis model described by equation (4.37) whereas generator 3 is modelled using the classical second order representation of equation (4.38). The AC system representation is the same as in Section 4.6.2, but additional subsystems to account for the HVDC network are added. There are two subsystems per converter terminal, one each for the converter controller and its associated stabilizer, respectively, and one

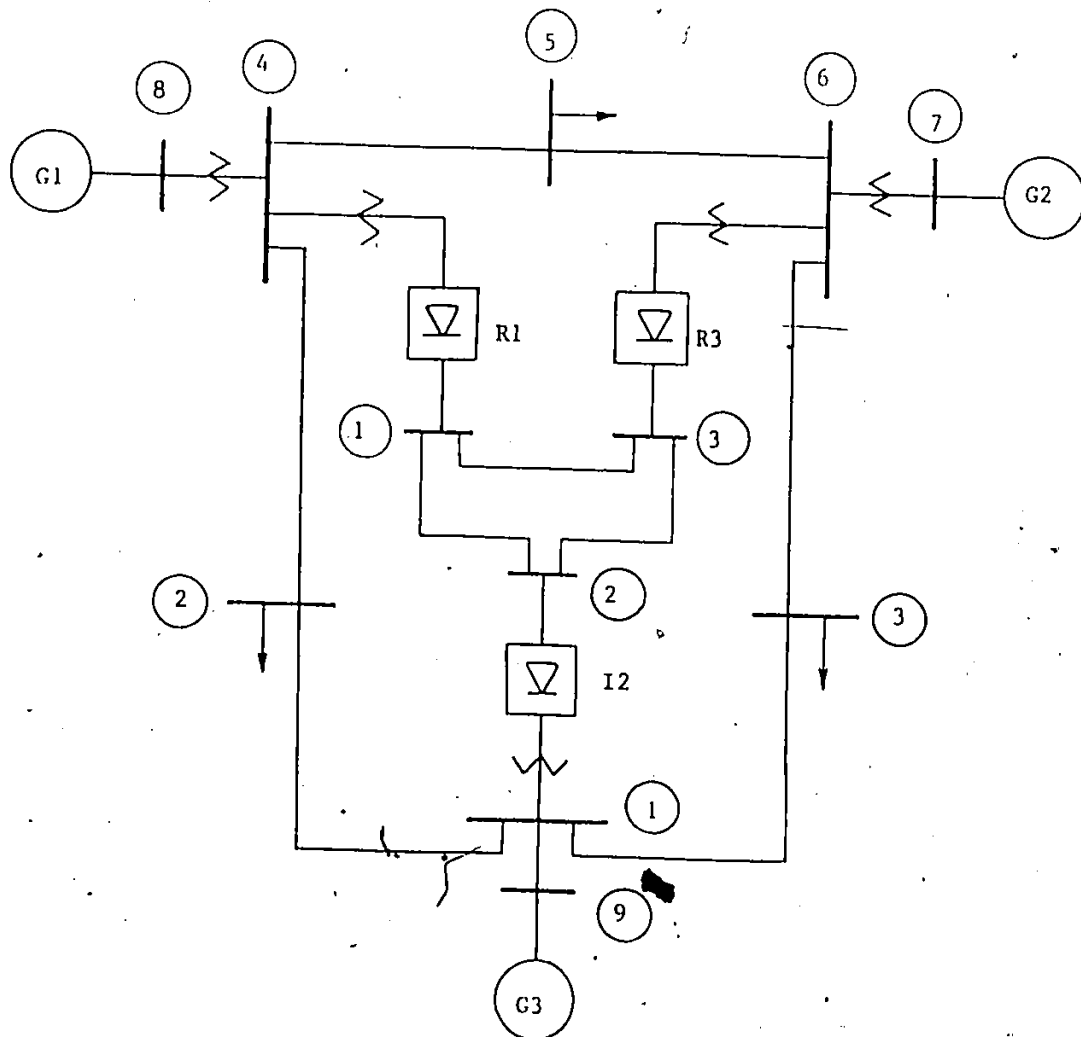


Figure 5.5 Three Machine - Three Terminal AC-DC System

subsystem representing the DC network. The DC terminal controllers are modelled by the first order lagging time constant transfer function representation of Figure 5.1. Each of the terminal stabilizers is represented by the lead-lag system of Figure 5.2 and its inputs are the converter bus AC voltage magnitude and the generator rotor speed and rotor angle. The parameters for the HVDC system controllers and stabilizers are given in Table 5.3. The state matrix is again given by equation (4.9) with

$$\bar{A} = \text{block diag } [A_{G_1}, A_{G_2}, A_{G_3}, A_{DC_1}, A_{DC_2}, A_{DC_3}, A_{DN}, A_{S_1}, A_{S_2}, A_{S_3}] \quad (5.15)$$

where the subscripts G_1 , G_2 and G_3 are for the three machines, DC_1 , DC_2 , DC_3 denote the converter controllers, DN denotes the DC network and S_1 , S_2 and S_3 denote the three converter stabilizers. The matrices \bar{B} and \bar{C} are constructed similarly replacing A by B or C in equation (5.15).

The AC-DC interconnection equation (5.14) is now used to construct the interconnection matrix. The coefficients of equation (5.14) form the entries of the expanded interconnection matrix L_{11} in equation (4.3) where

$$\bar{u} = [i_{q_1}, i_{d_1}, T_{m_1}, E_{fd_1}, i_{q_2}, i_{d_2}, T_{m_2}, E_{fd_2}, i_{q_3}, T_{m_3}, I_{REF_1}, i_{DC_1}, V_{ST_1}, V_{REF_2}, i_{DC_2}, V_{ST_2}, v_{q_2}, v_{d_2}, I_{REF_3}, i_{DC_3}, V_{ST_3}, v_{q_1}, v_{d_1}, v_{q_2}, v_{d_2}, v_{q_3}, \alpha_1, \alpha_2, \alpha_3, v_1, v_2, v_3]^T$$

Table 5.3. DC System Parameters

	Rectifier R1	Inverter I2	Rectifier R3
<u>Terminal Controllers</u>			
K_A	1.0	1.0	1.0
K_S	10.0	10.0	10.0
τ (secs)	0.05	0.05	0.05
<u>Terminal Stabilizers</u>			
K_{ST}	20.0	20.0	20.0
τ_1 (secs)	0.02	0.03	0.04
τ_2 (secs)	0.10	0.12	0.15
τ_3 (secs)	0.225	0.24	0.25
K_V	2.0	2.0	2.0
K_ω	15.0	15.0	15.0
K_δ	1.0	1.0	1.0

$$\bar{y} = [E'_{q1}, E'_{d1}, \delta_1, \omega_1, E'_{q2}, E'_{d2}, \delta_2, \omega_2, \delta_3, \omega_3, \alpha_1, \alpha_2, \alpha_3, \\ i_{DC1}, i_{DC2}, i_{DC3}, V_{ST1}, V_{ST2}, V_{ST3}]^T$$

The eigenvalues of the AC-DC system are given in Table 5.4. For comparison, the eigenvalues of the AC system alone have also been given. The two complex pairs of eigenvalues $(-0.00296 \pm j0.03685)$ and $(-0.00171 \pm j0.02736)$ correspond to the rotor oscillations of generators 1 and 2 with respect to generator 3, the reference machine. For the AC system the generators rotor oscillations are given by the eigenvalue pairs $(-0.00266 \pm j0.03648)$ and $(-0.00062 \pm j0.02298)$ and as for the case of the single machine infinite bus system the presence of the HVDC system is seen to contribute to the system damping. The dominant frequencies in both cases are between 1.4 Hz and 2.2 Hz. Another eigenvalue pair of interest is $(-0.06753 \pm j0.05598)$ and is due to the terminal controllers for rectifiers R1 and R3. It has a frequency of 3.5 Hz which lies within the range of turbine-generator shaft dynamics. A discussion on the other eigenvalues of the AC-DC system is delayed till the following chapter where a new eigenvalue tracking routine has been developed and is employed for identifying these eigenvalues.

5.7 Summary

This chapter has extended the state matrix formulation approach of Chapter 4 to include multiterminal HVDC systems. The DC system is

Table 5.4. Eigenvalues of Three-Machine, Three-Terminal AC-DC System

AC-DC System	AC System
-37.951	
-84.592	
-90.758	
-46.927	
-56.559	
-94.301	
-0.10000	
-0.63615	
-0.34796	
-0.06753 \pm j0.05598	
-0.14093	
-0.01410 \pm j0.00530	-0.01664
-0.00296 \pm j0.03685	-0.01037
-0.00171 \pm j0.02736	-0.00266 \pm j0.03455
-0.00042	-0.00062 \pm j0.02299
-0.00195	-0.00045
-0.00056	-0.000200 \pm j0.00013

represented as a group of additional subsystems within the overall component connection concept retaining all its advantages. The AC-DC interconnection has been developed in equation (5.14). While simplified DC subsystem models have been shown here, any level of modelling complexity can be included to include the various control functions of the HVDC terminal. The method was illustrated by means of two examples.

CHAPTER 6

EIGENVALUE ANALYSIS AND DECENTRALIZED POLE PLACEMENT

6.1 Introduction

The state matrix formulation approach presented in the previous two chapters is now utilized in developing a comprehensive approach for the stability analysis and control of a large-scale power system. In this chapter new methods are presented for eigenvalue tracking and for decentralized pole placement. Eigenvalue tracking is important for determining the behaviour of the power system as some control parameters vary. Decentralized pole placement methods helps in assigning the system eigenvalues to specified positions to meet a given design criteria.

A new eigenvalue tracking algorithm is presented in Section 6.2. Section 6.3 shows how to evaluate the derivative of the system state matrix. Section 6.4 and 6.5 presents some examples and a discussion on the practical applicability of the algorithm. Section 6.6 presents two decentralized pole placement methods with Section 6.7 and 6.8 containing examples and a discussion on the methods.

6.2 Eigenvalue Tracking

In dynamic stability studies of large interconnected power systems described in state space form the evaluation of system performance under a variety of operating conditions is necessary in both planning and operation. Since dynamic stability prediction of such systems is a direct function of the system state matrix eigenvalues, eigenvalue analysis techniques are receiving considerable attention in the analysis of power system dynamics [53,55,64,65,70,71,90,91].

The system eigenvalues are, in general, functions of all control and design parameters. A change in any of these parameters affects the system performance and is reflected as a shift in the whole eigenvalue pattern. In order to predict the system performance for different parameter settings, the eigenvalues are required to be recomputed for every parameter selection. For a power system, repeated eigenvalue computation becomes very expensive in terms of computer time and the usual approach is to employ eigenvalue sensitivities around the base case to estimate the eigenvalue. The new eigenvalue is given by

$$\lambda_{1\text{NEW}} = \lambda_{1\text{OLD}} + \left. \frac{\partial \lambda_1}{\partial \epsilon} \right|_{\epsilon_0} (\Delta \epsilon) + \frac{1}{2!} \left. \frac{\partial^2 \lambda_1}{\partial \epsilon^2} \right|_{\epsilon_0} (\Delta \epsilon)^2 + \dots \quad (6.1)$$

where $\Delta \epsilon$ is the change in the parameter around a nominal operating point ϵ_0 . This approach has been adopted in References [70,71] where expressions for second and higher order sensitivities have been

presented. This approach is however useful only if a few eigenvalues need to be tracked, otherwise the computational effort becomes greater than that required for the repeated application of the QR algorithm.

In this section an alternative approach is presented for updating eigenvalues following a parameter change. It is based on the determinantal approach to eigenvalue sensitivity evaluation [69]. The method converges rapidly to the exact eigenvalues and all the eigenvalues are simultaneously updated. The updated eigenvalue is considered as the new base value and the complete eigenvalue locus is traced as the parameter is varied.

The method requires the evaluation of the derivative of the system state matrix which is easily available if the state matrix formulation approach proposed in the previous chapters is used.

The following subsections show the development and use of the method. It is formulated to minimize the computational effort required.

6.2.1 Mathematical Formulation

Eigenvalue sensitivity has been expressed as [69,93]

$$\frac{\partial \lambda_i}{\partial \epsilon} = \{ \text{tr}[\text{adj}(\lambda_i I - A)]^{-1} \} \{ \text{adj}(\lambda_i I - A) * \frac{\partial A}{\partial \epsilon} \} \quad (6.2)$$

where $\frac{\partial A}{\partial \epsilon}$ = change in system matrix with respect to the parameter ϵ and can be obtained as outlined in the next Section 6.3. The $*$ denotes the inner product of two equally dimensioned square matrices

$$A * B = \sum_i a_i b_i \quad (6.3)$$

where a_i is the i th row of A and b_i is the i th column of B . Again the derivative of the determinant of matrix $[\lambda_i I - A]$ is given by

$$\frac{\partial}{\partial \epsilon} [\det(\lambda_i I - A)] = \text{adj}(\lambda_i I - A) * \frac{\partial A}{\partial \epsilon} \quad (6.4)$$

Combining (6.2) and (6.4) gives

$$\frac{\partial \lambda_i}{\partial \epsilon} = \{ \text{tr}[R(\lambda_i)] \}^{-1} \frac{\partial}{\partial \epsilon} \{ \det[\lambda_i I - A] \} \quad (6.5)$$

where

$$\text{adj}(\lambda_i I - A) \triangleq R(\lambda_i)$$

The change in eigenvalue $\Delta \lambda_i$ is then given by

$$\Delta \lambda_i = \{ \text{tr}[R(\lambda_i)] \}^{-1} \left\{ \frac{\partial}{\partial \epsilon} (\det[\lambda_i I - A]) \cdot \Delta \epsilon \right\} \quad (6.6)$$

The method proceeds by calculating $\Delta \lambda_i (i = 1, \dots, n)$ and updating $\lambda_i (i = 1, \dots, n)$ iteratively using

$$\lambda_i^{(k+1)} = \lambda_i^{(k)} + \Delta \lambda_i^{(k)} \quad (6.7)$$

where $k = 0, 1, 2, \dots$ and denotes the iteration step. The iteration is stopped when convergence is obtained.

Instead of calculating $\frac{\partial}{\partial \epsilon} \{\det[\lambda_1 I - A]\}$ in (6.6) using equation (6.4), we can write

$$\Delta\{\det[\lambda_1 I - A]\} = \det[\lambda_1 I - A] - \det[\lambda_1 I - (A + \frac{\partial A}{\partial \epsilon} \Delta \epsilon)]$$

but

$$\det[\lambda_1 I - A] = 0$$

therefore

$$\Delta\{\det[\lambda_1 I - A]\} = -\det[\lambda_1 I - (A + \frac{\partial A}{\partial \epsilon} \Delta \epsilon)] \quad (6.8)$$

Let

$$A + \frac{\partial A}{\partial \epsilon} \Delta \epsilon = A^*$$

and converting it to Hessenberg form

$$A^* = V A_H V^{-1} \quad (6.9)$$

where V is the product of Unitary Householder transformations. Now

$$[\lambda_1 I - A^*] = [\lambda_1 I - V A_H V^{-1}] = V[\lambda_1 I - A_H]V^{-1}$$

therefore,

$$\det[\lambda_1 I - A^*] = \det[\lambda_1 I - A_H] \quad (6.10)$$

because $\det(A.B) = \det A \det B$ and $\det V = 1$. Since $[\lambda_1 I - A_H]$ is in Hessenberg form its determinant can be easily evaluated using Hyman's method [67].

The use of equation (6.6) further requires the evaluation of $\text{tr}[R(\lambda_1)]$. This is now accomplished. The characteristic polynomial is

$$\det[\lambda I - A] = (\lambda - \lambda_1)(\lambda - \lambda_2) \cdots (\lambda - \lambda_n)$$

It can be shown [92] that

$$\text{tr}[R(\lambda)] = \frac{\partial}{\partial \lambda} \{\det[\lambda I - A]\} \quad (6.11)$$

therefore

$$\text{tr}[R(\lambda_1)] = \prod_{\substack{j=1 \\ j \neq 1}}^n (\lambda_1 - \lambda_j) \quad (6.12)$$

It is seen from equation (6.12) that equation (6.5) does not hold if two eigenvalues are equal. Therefore if the eigenvalue loci intersect

as the parameter changes equation (6.6) will not converge. Conversely a divergence indicates that the eigenvalue loci intersect and the QR method must be used directly to find the eigenvalues following the parameter change.

6.2.2 Algorithm Implementation

The algorithm is implemented as follows:

- Step 1: Compute base case eigenvalues using QR algorithm.
- Step 2: Convert $[A + \frac{\partial A}{\partial \epsilon} \Delta \epsilon]$ to Hessenberg form A_H .
- Step 3: Calculate $\text{tr}[R(\lambda_i)]$ $i = 1, \dots, n$ using equation 6.12.
- Step 4: Form the matrix $[\lambda_i I - A_H]$ and calculate its determinant for $i = 1, \dots, n$.
- Step 5: Find $\Delta \lambda_i$ using (6.6) for $i = 1, \dots, n$.
- Step 6: If $\Delta \lambda_i$ is greater than some convergence criteria, update λ_i using (6.7) for $i = 1, \dots, n$ and return to Step 3.
- Step 7: On convergence, the λ_i are a close estimate of the eigenvalues of $[A + \frac{\partial A}{\partial \epsilon} \Delta \epsilon]$.

Steps 1 through 7 are repeated for the next change $\Delta \epsilon$ after replacing A by $[A + \frac{\partial A}{\partial \epsilon} \Delta \epsilon]$. In this manner the eigenvalue locus can be plotted as a function of parameter values. If the eigenvalue loci cross (i.e., two eigenvalues become identical), the algorithm has to be restarted using the QR method.

6.3 The Evaluation of the Derivative of the System State Matrix

The eigenvalue tracking algorithm requires the determination of the derivative of the system state space matrix. The state matrix is given earlier as

$$A = \bar{A} + \bar{B} L_{11} \bar{C} \quad (6.15)$$

for the case where $D = 0$. Then

$$\frac{\partial A}{\partial \epsilon} = \frac{\partial \bar{A}}{\partial \epsilon} + \frac{\partial \bar{B}}{\partial \epsilon} L_{11} \bar{C} + \bar{B} \frac{\partial L_{11}}{\partial \epsilon} \bar{C} + \bar{B} L_{11} \frac{\partial \bar{C}}{\partial \epsilon} \quad (6.16)$$

The parameter of interest (ϵ) is usually contained in the subsystem state matrices A_1 , B_1 and C_1 from which the matrices \bar{A} , \bar{B} and \bar{C} are formed in accordance with equation (4.8). Thus the right-hand side of equation (6.16) is easily evaluated.

For the case of mode identification the system state matrix is assumed to be given by

$$A = \bar{A} + \bar{B} (r L_{11}) \bar{C} \quad (6.17)$$

where r denotes the amount of interconnection introduced. For the case $r = 0$ the system is completely decoupled, whereas $r = 1$ denote the interconnected system. The tracking of the eigenvalues as the system moves from the decoupled to the fully coupled state helps in

identifying the subsystem which contributes to any particular mode.

For this case

$$\frac{dA}{dr} = \bar{B} L_{11} \bar{C} \quad (6.18)$$

6.4 Use of Eigenvalue Tracking in the Analysis of Power Systems

The eigenvalue technique developed here is particularly useful for the analysis of power system dynamics. It can be used to examine the movement of the critical roots and then to adjust the design parameters in such a way as to achieve stability improvement. It provides the engineer with a good feel for the effect of different system parameters on the overall stability of the system.

This use of eigenvalue tracking in the analysis of synchronous machine dynamics is illustrated in this section by considering two examples. The first example examines the effect of the exciter gain parameter on the stability of a synchronous machine connected to an infinite bus where the machine is represented by a simplified third order model. The second example considers a larger multimachine system and demonstrates the use of eigenvalue tracking in both mode identification as well as stability determination with respect to parameter variation.

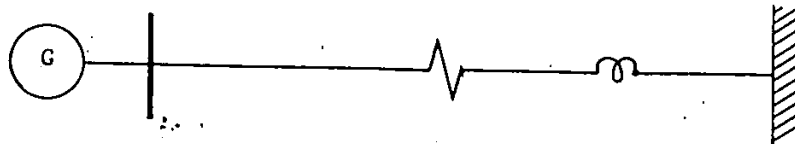
6.4.1 Simplified Single Machine Infinite Bus System with a Single Time Constant Exciter

In this example the effect of exciter parameter on the eigenvalues of a synchronous generator connected to an infinite bus are

studied. A single line diagram of the system is shown in Figure 6.1. The system data has been obtained from reference [81]. The AC machine is represented by a simplified third order model. This model neglects the effect of damper windings, stator resistance and network transients. The exciter is modelled as a single time constant regulator and constant mechanical torque is assumed. Under small perturbations the system can be represented by the block diagram shown in Figure 6.2. In spite of its simplicity, this model has been shown to be very useful in the analysis and design of machine excitation systems under a variety of conditions [2,94]. The block diagram coefficients ($k_1 - k_6$) are functions of the machine and transmission line parameters and the system operating conditions. The value of these coefficients for the loading conditions of Figure 6.1 are given along the block diagram in Figure 6.2.

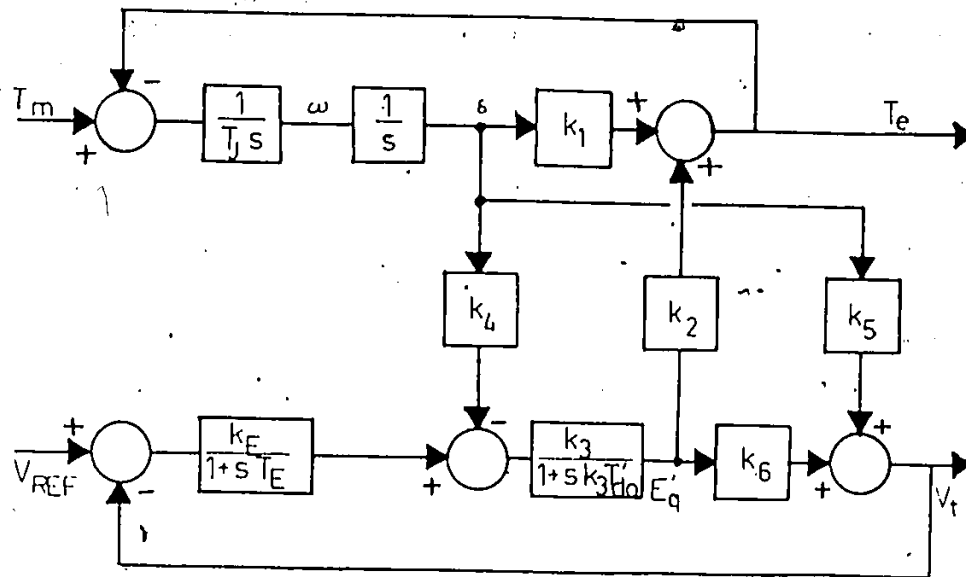
The machine and exciter together form a fourth order system whose state matrix can be written as:

$$\begin{bmatrix} \dot{E}_q \\ \dot{\delta} \\ \dot{\omega} \\ \dot{E}_{fd} \end{bmatrix} = \begin{bmatrix} -1/k_3\tau'_{do} & -k_4/\tau'_{do} & 0 & 1/\tau_{do} \\ 0 & 0 & 1 & 0 \\ -k_2/\tau_J & -k_1/\tau_J & 0 & 0 \\ -K_E k_6/\tau_E & -K_E k_5/\tau_E & 0 & -1/\tau_E \end{bmatrix} \begin{bmatrix} E_q \\ \delta \\ \omega \\ E_{fd} \end{bmatrix} + \begin{bmatrix} 0 \\ 0 \\ T_m/\tau_J \\ (K_E/\tau_E)V_{REF} \end{bmatrix}$$



$$\begin{aligned}
 x_d &= 1.70 \text{ pu} \\
 x_q &= 1.64 \text{ pu} \\
 r_s &= 0.001096 \text{ pu} \\
 \cos\phi &= 0.85 \text{ pu} \\
 v_t &= 1.0 \text{ pu} \\
 r_e &= 0.02 \text{ pu} \\
 x_e &= 0.40 \text{ pu} \\
 P &= 1.0 \text{ pu}
 \end{aligned}$$

Figure 6.1 Single Machine Infinite Bus System



$$k_1 = 1.076, k_2 = 1.258, k_3 = 0.307, k_4 = 1.712, k_5 = -0.041, k_6 = 0.497$$

$$\tau'_{do} = 5.90, \tau_E = 0.50, \tau_J = 2H\omega_0 \text{ where } H = 2.37, \omega_0 = 377.$$

Fig. 6.2 Block Diagram of the Linearized Model of the Single Machine Infinite Bus System

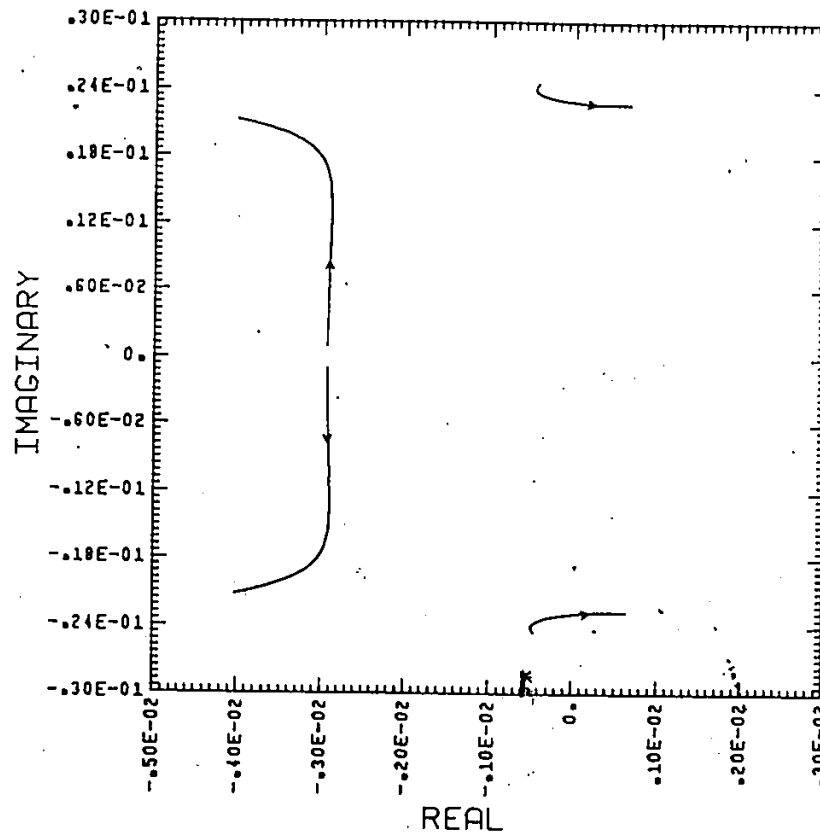


Fig. 6.3 Eigenvalue Locus for the Single Machine Infinite Bus System

The eigenvalues are plotted as exciter gain K_E is varied from 5 to 300 in steps of 5. The eigenvalue locus is given in Figure 6.3 and we note that the system becomes unstable as K_E is increased beyond 269. The eigenvalues obtained using the algorithm in Section 6.2 agree to five decimal places to those obtained using the standard IMSL library subroutine EIGRF.

6.4.2 A Three-Machine, Three-Terminal AC-DC System

In this section the eigenvalue tracking routine is used to analyse the performance of the three machine three terminal AC-DC system (Figure 5.5).

Machines 1 and 2 have been modelled using the fourth order two axis generator model and machine 3 has been represented by the second order classical model. Each of the three DC terminal controllers is represented by a single lag time constant transfer function. Again, each terminal controller is equipped with a second order stabilizer as shown in Figure 5.2. The input signals for the stabilizer are converter AC bus voltage magnitude, rotor speed and rotor angle. The gains K_V , K_ω and K_δ can all be individually set to control the composition of the stabilizer signal. Note that this system has been considered earlier in Section 5.6.2 and its eigenvalues are given in Table 5.4. Here the system performance is analysed by first identifying the eigenvalues and then determining the effect of parameter variation on system stability.

To identify the eigenvalues and to determine which subsystems contribute to a particular mode the eigenvalues are tracked as the interconnection or coupling parameter 'r' in equation (6.17) is varied from 0 to 1. The result is summarized in Table 6.1 which identifies the various eigenvalues of the AC-DC system.

The variation in the eigenvalues associated with a particular subsystem as r is varied is indicative of the degree of coupling of the subsystem with the other subsystems. A large movement of the eigenvalues mean that the subsystem is strongly coupled whereas a small change indicates that the subsystem is loosely coupled. Figure 6.4 shows the real and imaginary part of the rotor oscillation eigenvalues ($-0.002966 \pm j0.03465$ and $-0.00171 \pm j0.02734$) for machines 1 and 2 as a function of the interconnection. It is seen that both rotor damping and rotor oscillation frequency are extremely sensitive to the interconnection and that the subsystems corresponding to the two machines are strongly coupled. This is as expected since it is a three machine with a strong transmission system. The real and imaginary parts of the DC terminal controllers eigenvalues are plotted similarly in Figure 6.5. In this case while the damping remains almost constant the frequency of oscillation increases as the interconnection is introduced. The complex eigenvalue pair ($-0.06752 \pm j0.05598$) corresponding to the two rectifier terminals controller has an oscillation frequency of about 3.5 Hz ($0.05 * 60$). This frequency is within the frequency range of rotor oscillations and can lead to

Table 6.1. Eigenvalues Identification

Eigenvalue	Subsystem
-37.951 -84.592	Stabilizer - Terminal R1
-90.758 -46.927	Stabilizer - Terminal I2
-56.559 -94.301	Stabilizer - Terminal R3
-0.10000 -0.63615 -0.34796	DC Network
-0.06753 ± j0.05598	Constant Current Controller Terminals R1 and R2
-0.14093	Constant Voltage Controller Terminal I2
-0.00296 ± j0.03685	Rotor - Generator 1
-0.00171 ± j0.02736	Rotor - Generator 2
-0.01410 ± j0.00530	Field - Generators 1 and 2
-0.00042	Field - Generator 1
-0.00195	Field - Generator 2
-0.00056	Rotor Speed - Generator 3

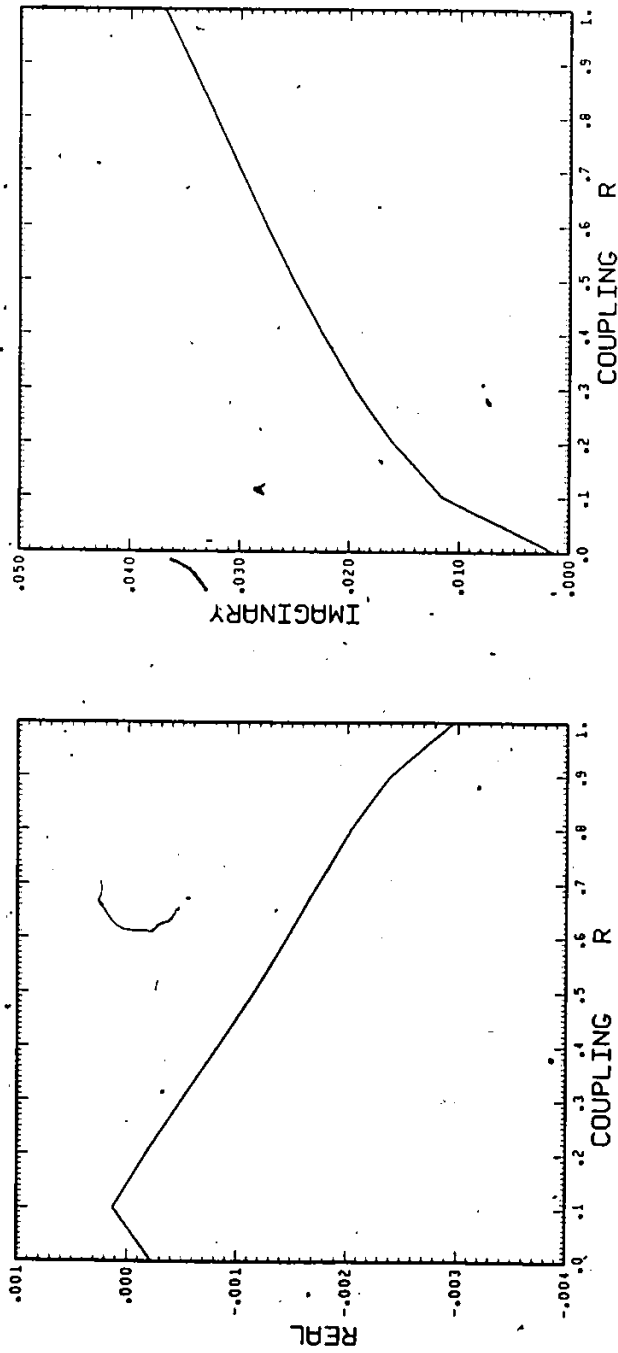


Figure 6.4(a) Movement of the Real and Imaginary Parts of Rotor Eigenvalues of Generator 1 as Function of Interconnection Coupling r

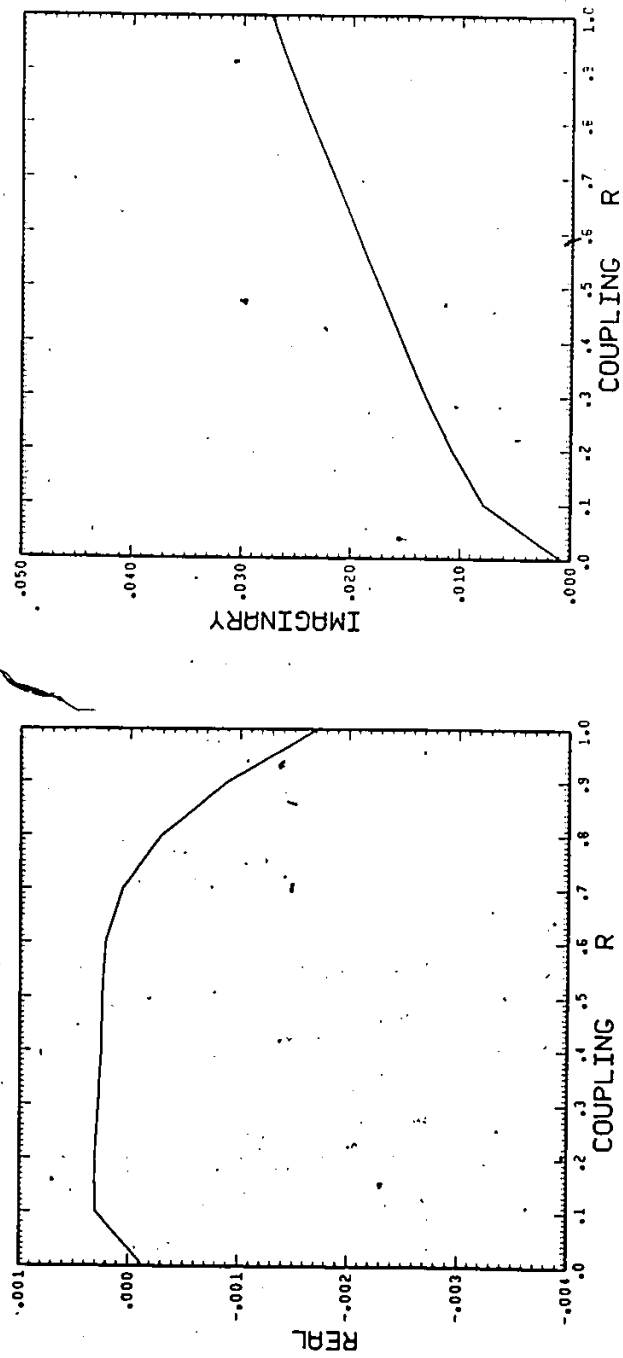


Figure 6.4(b) Movement of the Real and Imaginary Parts of Rotor Eigenvalues of Generator 2 as Function of Interconnection Coupling r

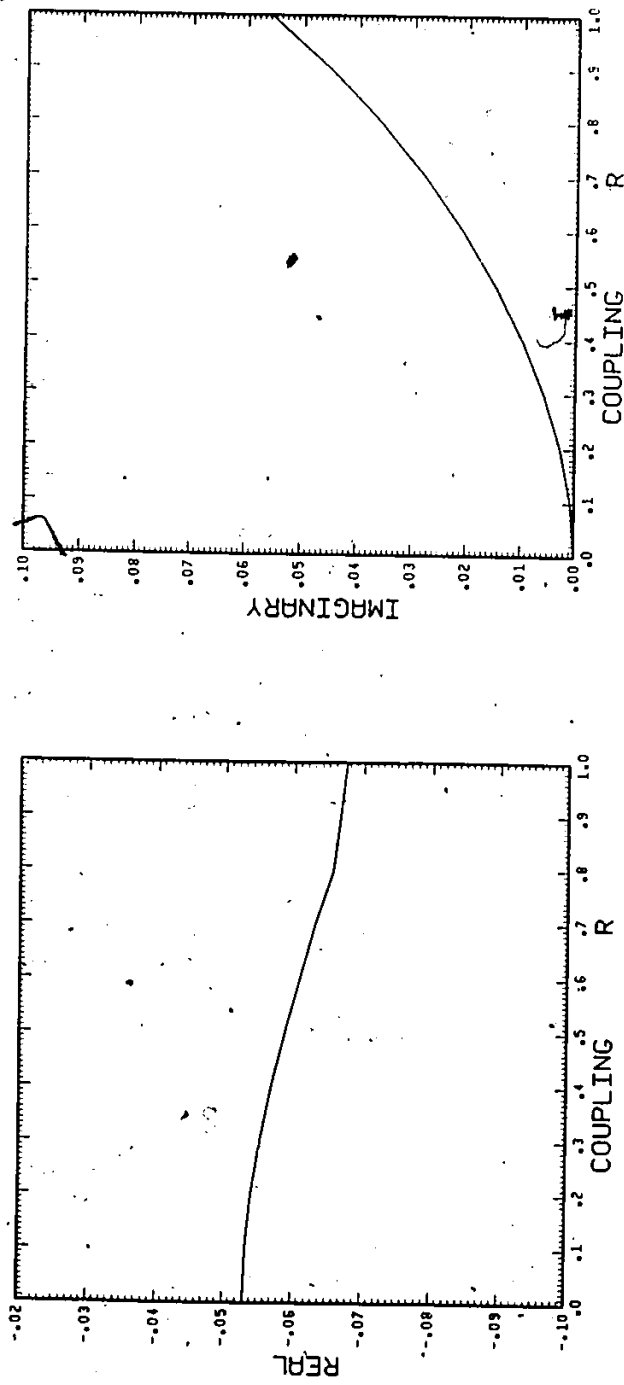


Figure 6.5(a) Movement of Real and Imaginary Parts of the Eigenvalues Corresponding to the Constant Current Controllers at Terminals R1 and R3 as a function of Interconnection Coupling

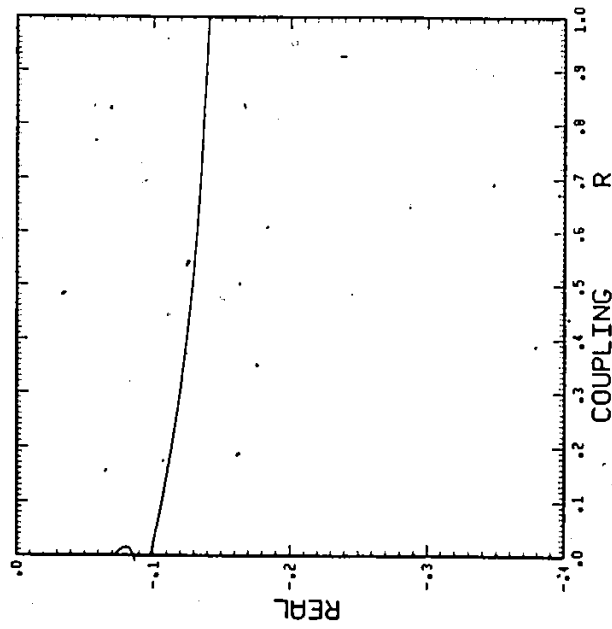


Figure 6.5(b) Movement of the Eigenvalue Corresponding to the Constant Voltage Controller at Terminal 12 as a Function of Interconnection Coupling

potential problems with HVDC terminal controllers interacting unfavourably with the generator rotor dynamics.

The effect of parameter variations on system eigenvalues is now illustrated. The parameter varied is the gain K_w of the stabilizer of rectifier R1 which is varied from $K_w = 15$ to $K_w = 100$ and the system eigenvalues are tracked. The movement of the rotor eigenvalues for machines 1 and 2 are shown in Figure 6.6 and it is seen that the speed feedback leads to a considerable improvement in the damping of rotor oscillations of both machines. This is similar to the case for AC networks where speed feedback is used for stabilizing purposes.

6.5 Some Practical Considerations in Eigenvalue Tracking

There are two practical aspects that need to be considered when programming this algorithm. The first relates to the calculation of the determinant and the second one to determining when two eigenvalues are equal and thus the algorithm needs to be restarted.

The determinant of a matrix can be very large or very small and very frequently its computation can cause an overflow or underflow on the computer. The determinant is usually evaluated as the product of a set of numbers. For example using the LU factorization approach, it is the product of the diagonal elements of the L and U matrices. If these elements are very large or very small, overflow or underflow will occur. This problem is circumvented by using logarithms to evaluate the product.

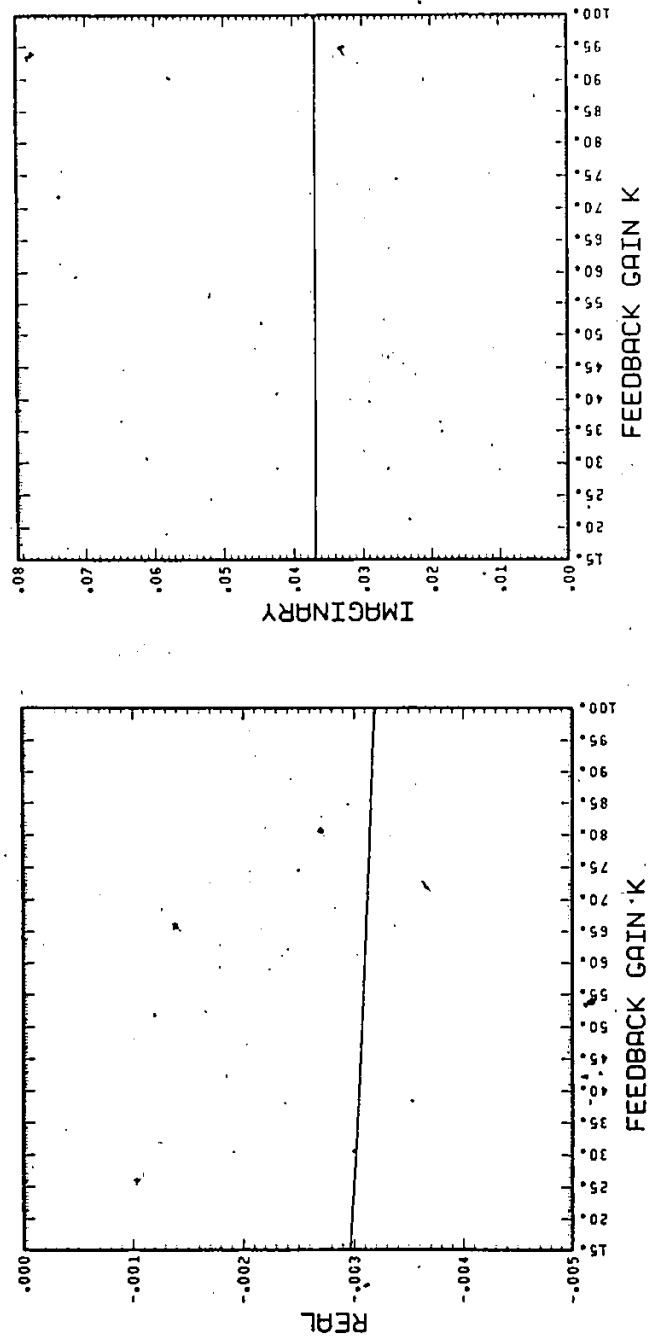


Figure 6.6(a) Movement of the Real and Imaginary Parts of Rotor Eigenvalues of Generator 1 as Function of Stabilizer Gain K_b

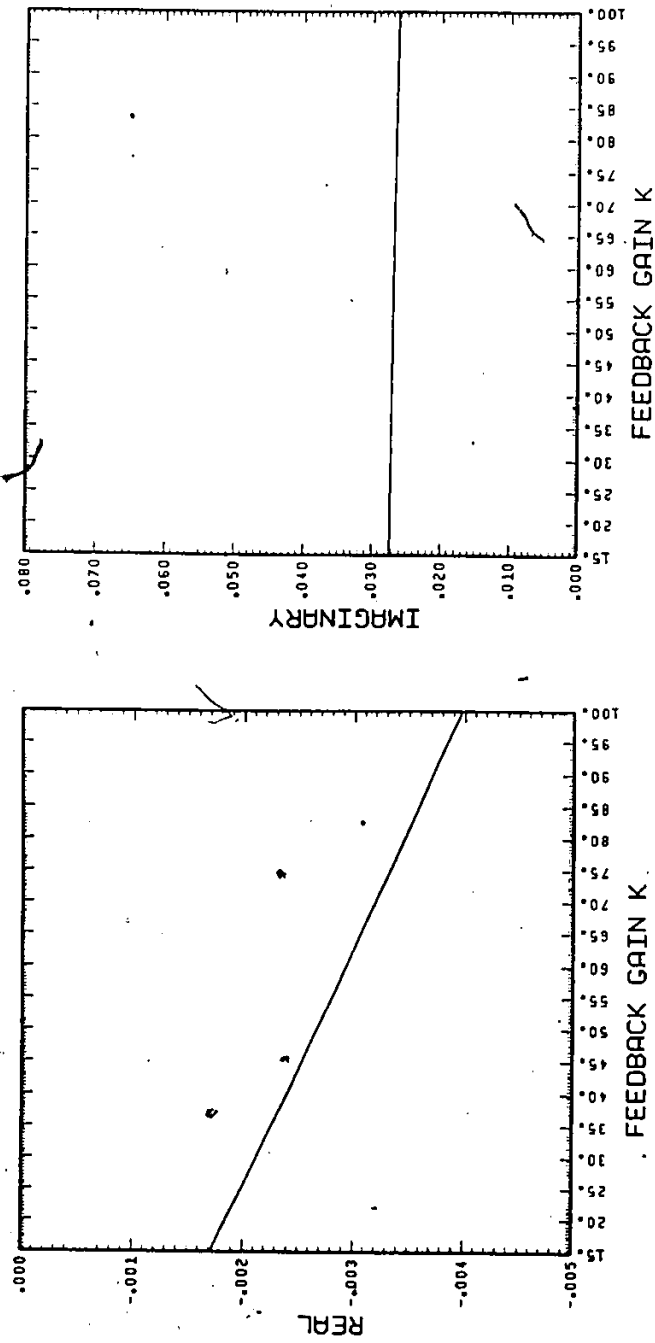


Figure 6.6(b) Movement of the Real and Imaginary Parts of Rotor Eigenvalues of Generator 2 as Function of Stabilizer Gain K_b

The main advantage of transforming $(\lambda_1 I - A)$ to Hessenberg form and using Hyman's method is the lesser number of operations required compared to direct LU factorization. Determinant evaluation using LU factorization of $(\lambda_1 I - A)$ requires $n^3/3$ operations for each $\lambda_1 (i = 1, \dots, n)$ resulting in a total of $n^4/3$ operations. Transforming $(\lambda_1 I - A)$ to Hessenberg form requires $5n^3/3$ evaluations and determinant evaluation of $(\lambda_1 I - A_H)$ requires $n^2/2$ operations for each $\lambda_1 (i = 1, \dots, n)$ resulting in a total of $(5/3 + 1/2)n^3$ operations. Thus Hyman's method is more economical for system orders greater than 6 and, in addition, is highly stable and single precision computation is considered adequate [67]. The accuracy of the method is proportional to 2^{-t_1} where $t_1 = t - 0.08406$ and t is the number of binary digits used for representing decimal fractions in the computer. Again n is the order of the matrix A . For most large computers, t is fairly large, e.g., $t = 48$ for the CDC Cyber 170 and $t = 24$ for the VAX11/750. This therefore ensures that no significant error is introduced with high order matrices and consequently the use of this method would tend to be constrained more by memory storage requirements than by considerations of numerical accuracy.

As mentioned earlier there is no need to explicitly determine when two eigenvalues become equal because equation (6.12) does not hold in this case. Due to this singularity the algorithm will not converge, even if the eigenvalues of A and $A + \Delta A$ are distinct, if the eigenvalue loci intersect when moving from A to $A + \Delta A$. A divergence therefore indicates that the algorithm needs to be restarted.

We now proceed to show that it is indeed computationally efficient compared to repeated eigenvalue computation. Let us consider a n th order system where the base case eigenvalues are known. An eigenvalue recomputation requires [67].

- (a) $(5/3)n^3$ operations to transform the system matrix to Hessenberg form.
- (b) $4n^2$ operations per QR iteration. Normally, 2-3 QR iterations are required per eigenvalue [67]. This, assuming an average of 2.5 iterations per eigenvalue, results in a total of $10n^3$ operations.

The total number of operations is then given by

$$N_R = (5/3)n^3 + 10n^3 = (35/3)n^3 \quad (6.19)$$

The tracking algorithm suggested here requires

- (a) $(5/3)n^3$ operation to convert A^* in equation (6.9) to Hessenberg form. This is required only once.
- (b) $(1/2)n^3$ operations per iteration to compute the determinants in equation (6.10) for $\lambda_i (i = 1, \dots, n)$.
- (c) $n(n-1) = n^2$ operations per iteration to compute $\text{tr}\{R(\lambda_i)\}$ using equation (6.12).

The number of iterations required depends on the parameter variation and the convergence criteria. For the example considered, four iterations were sufficient to bring $\Delta\lambda_i (i = 1, \dots, n)$ to less than 10^{-5} . The number of operations is then given by

$$N_A = (5/3)n^3 + 4[1/2)n^3 + n^2] = (11/3)n^3 \quad (6.20)$$

Comparing equations (6.19) and (6.20) it is seen that the algorithm requires less than one third of the computational effort as compared to repeated eigenvalue computation. As mentioned previously, the algorithm has to be restarted using the QR method, if the eigenvalue loci cross. The method tracks all the eigenvalues as compared to the methods reported in [71,72], which are designed to track a few eigenvalues to be economically advantageous.

For the analysis of power systems this method provides an efficient approach. It is to be noted that there is a limit to the order of the power system that can be handled by this method. This limit is dependent on the available memory on the computer used. While sparse matrix techniques may be employed to conserve storage, they cannot be used for eigenvalue evaluation as a sparse eigenvalue evaluation method has yet to evolve. The eigenvalue evaluation being required to initialize the method or to restart after two eigenvalues become identical.

6.6 Decentralized Pole Placement

While eigenvalue tracking helps in determining the system behaviour with respect to parameter variation, pole placement requires that the eigenvalues be moved to a desired set of locations in the complex plane in order to obtain good system response. In general this requires the availability of all state variables which are fed to all

of the inputs. However, spectrum assignment using centralized state feedback is impractical for many large distributed systems because of the difficulty in providing reliable and secure feedback between subsystems located far apart. For this purpose decentralized state feedback is advantageous since only local states are fed to local controllers. It may be noted that large engineering systems fall under the category of decentralized control with a group of controllers controlling local inputs and thereby indirectly controlling the large system. This is particularly true for electric power systems which are composed of interconnected but separately owned and operated utilities each of which contains a number of local areas, each with its own control center tied to an overall coordinating center. Within each area the tasks of coordination are repeated at a lower level where the area control center coordinates individual generating stations each of which is individually controllable.

The necessary conditions under which a set of local feedback laws exist were derived first by Wang and Davison [94] and later extended by Corfmat and Morse [95]. These imply that the fixed modes of the system cannot be assigned using local feedback. The concepts of fixed modes being a generalization of the uncontrollable mode concept occurring in centralized control. Subsequently Saeks [96] has shown that the fixed modes of the composite system coincide with the fixed modes of the component subsystems.

This section presents two methods for finding the decentralized feedback gains provided no fixed mode exists. The first

method is based on the Component Connection Method and uses a function minimization approach. The desired eigenvalues are assigned among the subsystems and the feedback gain matrix parameters are varied to keep the eigenvalues fixed as the interconnections are introduced. The method is different from [97] in the way the decentralized gains are obtained. In [97] a continuation approach has been adopted where the eigenvalue sensitivity is equated to zero as the system interconnections are introduced. It requires the repeated evaluation of the eigenvalues and the left and right eigenvectors of the system state matrix as the interconnections are introduced. In this thesis the gain matrix parameters are varied to minimize a cost function using standard minimization routines and requires, at most, the calculation of the system eigenvalues. The advantages are that the problem is easier to program and is computationally less expensive.

For the case of a strongly interconnected system the introduction of the interconnection moves the eigenvalues considerably far from the decoupled subsystem eigenvalues. This would require that the interconnections be introduced slowly which will result in increased computation time. Further the minimization routines may not converge due to the accumulation of numerical errors. In such a case an alternative second method is proposed. This views the decentralized feedback gain problem as an inverse eigenvalue problem. A Newton iteration process is used to arrive at a solution [98]. In this method the eigenvalues of the composite systems are moved directly to the desired location instead of the subsystems eigenvalues being moved

first and then held fixed at the desired values as the interconnections are introduced.

6.6.1 Pole Placement Using Direct Minimization

Eigenvalue assignment requires the evaluation of the feedback gain matrix K such that

$$\sigma[A + BK] = \Lambda \quad (6.20)$$

Here A and B are the state and input matrices of the overall system, $\sigma[A + BK]$ denotes the set of eigenvalues of $(A + BK)$ and Λ denotes the desired eigenvalue spectrum $(\lambda_1, \lambda_2, \dots, \lambda_n)$. For decentralized feedback with local states only as local inputs we must have

$$\sigma[A + \bar{B} \bar{K}_d] = \Lambda \quad (6.21)$$

Here \bar{K}_d = block diagonal $[K_{d1}, K_{d2}, \dots, K_{dN}]$ and K_{di} ($i = 1, \dots, N$) is the feedback gain matrix for the i th subsystem.

Direct Minimization Method

The algorithm starts by assigning the desired spectrum Λ among the various subsystems assuming that the large system is completely decoupled. This can be done using any pole placement method since subsystems are usually of small order. Then

$$\sigma[\bar{A} + \bar{B} \bar{K}_d] = \Lambda \quad (6.22)$$

If the interconnections are now introduced

$$\sigma(\bar{A} + \bar{B}(I - rL_{11}\bar{D})^{-1}rL_{11}\bar{C} + \bar{B}\bar{K}_d) = \bar{\Lambda} \quad (6.23)$$

where $\bar{\Lambda}$ denotes the new eigenvalues which are shifted from the desired spectrum Λ due to introduction of the interconnection as r varies from 0 to 1. The elements of K_d may now be varied such that

$$\Lambda - \bar{\Lambda} = 0 \quad (6.24)$$

It is proposed to use function minimization for this purpose. Two different functions may be used. The first is to find

$$\min \|F_1\|_2 \quad (6.25)$$

where,

$$F_1 = \begin{bmatrix} \lambda_1 - \bar{\lambda}_1 \\ \vdots \\ \lambda_n - \bar{\lambda}_n \end{bmatrix}$$

where $\lambda_1, \lambda_2, \dots, \lambda_n$ are the eigenvalues of Λ and are functions of the elements of K_d .

This function however requires an eigenvalue computation at each function evaluation. This may be avoided by using the second alternative function.

$$\min \|F_2\|_2 \quad (6.26)$$

where,

$$F_2 = \begin{bmatrix} \det(A + \bar{B} \bar{K}_d - \lambda_1 I) \\ \vdots \\ \det(A + \bar{B} \bar{K}_d - \lambda_n I) \end{bmatrix}$$

The evaluation of the function F_2 may be considerably simplified if the matrix $[A + \bar{B} \bar{K}_d]$ is first transformed to Upper Hessenberg form. The determinant for different $\lambda_i (i = 1, \dots, n)$ can then be computed using Hyman's method. While computation of function F_1 also requires the Hessenberg transformation for eigenvalue calculations, the computation of F_2 avoids the need for subsequent QR iterations.

Either $\|F_1\|_2$ or $\|F_2\|_2$ are minimized with respect to the elements of the feedback gain matrix K_d . The minimization is accomplished using standard IMSL library subroutines ZXMIN or ZXSSQ based on quasi-Newton and Levenberg-Marquardt methods respectively. These have the advantage of not requiring function derivatives for minimization. The minimization is done for each value of r as it is increased for 0 to 1. This introduces a small amount of coupling at a time and ensures that $\bar{\Lambda}$ are close to Λ , thereby resulting in faster convergence of the minimization routine.

6.6.2 Newton Method

For a strongly interconnected system the introduction of the interconnection moves the eigenvalues of the composite system far from

the location occupied when the systems are assumed decoupled. If the desired eigenvalues are assigned among the subsystems, the interconnection coupling parameter r must be increased in smaller steps compared to the step required for a loosely coupled system. Since a minimization is carried out at each step, this will lead to an increase in computation time.

Consider such a strongly interconnected system where the desired eigenvalues lie close to the overall system eigenvalues. In this case, assigning the desired eigenvalues among the subsystems leads to large initial values of the decentralized gains; whereas, since the desired eigenvalues lie close to the overall system eigenvalues, low gains are required. The wide difference between the initial and final gains lead to a larger number of minimization steps and may cause numerical difficulties in convergence because of error accumulation.

In this situation an alternative formulation to directly move the composite system eigenvalues to the desired location is employed. We assume n constant matrices each premultiplied by a constant $c_i (i = 1, \dots, n)$ which when added to the composite system state matrix results in a new system matrix having the desired eigenvalues. This problem in general is termed the inverse eigenvalue problem and we may obtain the controller gains from the constants c_i and the n constant matrices. Mathematically the problem is formulated as follows.

Given the overall state matrix A and n constant matrices $K_i (i = 1, 2, \dots, n)$, find the constant $c_i (i = 1, \dots, n)$ such that the matrix

$$A(c) = A + B \sum_i c_i K_i = A + \sum_i c_i B K_i \quad (6.27)$$

has the desired eigenvalues λ_i ($i = 1, \dots, n$).

In this case F_2 may be written as

$$F_2(c) = \begin{bmatrix} \det(A(c) - \lambda_1 I) \\ \vdots \\ \det(A(c) - \lambda_n I) \end{bmatrix} = \begin{bmatrix} F_{2,1}(c) \\ \vdots \\ F_{2,n}(c) \end{bmatrix}$$

and c is a solution of equation (6.27) if $F_2(c) = 0$. The Newton method solution is given by

$$c^{m+1} = c^m - G(c^m)^{-1} F_2(c^m), \quad m = 0, 1, 2, \dots \quad (6.28)$$

where the elements of $G(c)$ are given by

$$g_{ij}(c) = \frac{\partial F_{2,i}(c)}{\partial c_j} = F_{2,i}(c) \operatorname{tr}[(A(c) - \lambda_i I)^{-1} B K_i]$$

The structure of the matrices K_i ($i = 1, \dots, n$) is the same and depends on the state variables. For decentralized feedback

$$K_i = \begin{bmatrix} K_{i1} & & & \\ & K_{i2} & & \\ & & \ddots & \\ & & & K_{iN} \end{bmatrix}$$

where N is the number of subsystems. The elements of K_i are arbitrarily selected (e.g., by a pseudo-random number generator) so that norm

$$\|A\| = \left\| \sum_{i=1}^n B K_i \right\|$$

For a complex conjugate eigenvalue pair ($\lambda_j = \lambda_1^*$) we choose $K_j = K_1^*$ and fix $c_j = c_1^*$ at each iteration.

The decentralized gain matrix K_d is then given by

$$K_d = \sum_{i=1}^n c_i K_i$$

$$\text{and } A = \bar{A} + \bar{B} L_{11} \bar{C}$$

$$\text{and } B = \bar{B} L_{12}$$

The success of the method is dependent on the initial values for the constants c_i ($i = 1, \dots, n$), which were taken equal to the desired eigenvalues.

6.6.3 Conditions for Existence

The general conditions for the minimization of F_1 or F_2 depends on the existence of K_d . This is guaranteed for three conditions [98].

- (1) Each subsystem is controllable and observable.
- (2) At most one subsystem is of odd order.
- (3) Complex eigenvalues are distinct and exist in conjugate pairs.

Condition 1 is necessary for eigenvalue assignment whereas (2) and (3) result in real feedback gains.

6.7 Examples of the Use of Decentralized Pole Placement Algorithms

Two examples are presented to illustrate the methods. The first is a mathematical example showing a seventh order system consisting of three subsystems taken from [97]. For this loosely coupled system it is shown that direct minimization is feasible and faster execution time achieved as compared to the continuations approach adopted in [97]. The minimization approach may be unsuccessful for a strongly interconnected system and this is seen for a three machine AC power system which forms the second example. This second example is solved successfully using the Newton method.

6.7.1 A Seventh Order System

This example represents a system consisting of three subsystems as follows:

Subsystem 1

$$\dot{x}_1 = x_1 + u_1$$

$$\dot{x}_2 = -2x_2 + u_2$$

Subsystem 2

$$\dot{x}_1 = -x_1 + x_2$$

$$\dot{x}_2 = -x_1 + u_2$$

Subsystem 3

$$\dot{x}_1 = x_3 + u_1$$

$$\dot{x}_2 = x_1 + u_2$$

$$\dot{x}_3 = x_2$$

The interconnection among the subsystems is given by the following system interconnection matrix L_{11} given below

$$\begin{bmatrix} 0 & 0 & 0 & 0 & 0 & 0 & 1 \\ 0 & 0 & 0 & 0 & 0 & 0 & 0 \\ 1 & 0 & 0 & 0 & 0 & 0 & 0 \\ 0 & 0 & 1 & -1 & 0 & 0 & 0 \\ 0 & 0 & 0 & 0 & 0 & 0 & 0 \end{bmatrix}$$

The eigenvalues of the original systems are

System 1. 1, -2

System 2 $-0.5 \pm j0.866$

System 3 $-0.5 \pm j0.866, 1$

To achieve a certain desired system response, it is assumed that the eigenvalues have to be shifted to the following desired values.

$$-2 \pm j, -1 \pm j, -0.5 \pm j0.5, -3.$$

As a first step we assign the desired eigenvalues among each of the three subsystems.

$$\lambda_1 = -2 \pm j$$

$$\lambda_2 = -1 \pm j$$

$$\lambda_3 = -0.5 \pm 0.5j, -3$$

This is accomplished by using any pole placement method. For simplicity K_{d1} , K_{d2} , K_{d3} are chosen as in [97]

$$K_{d10} = \begin{bmatrix} -10/3 & 1/3 \\ -10/3 & 1/3 \end{bmatrix}$$

$$K_{d20} = \begin{bmatrix} 0 & -1 \end{bmatrix}$$

$$K_{d30} = \begin{bmatrix} -1.5 & -2.5 & -1 \\ -1.5 & -2.5 & -1 \end{bmatrix}$$

Both functions F_1 and F_2 were formed and minimized using the standard IMSL subroutine ZXMIN based on the quasi-Newton method. In both cases $\|F_1\|_2$ and $\|F_2\|_2$ less than 10^{-5} were achieved in 10 secs on the CDC Cyber 815 computer. The feedback gain matrices obtained using both functions are now given.

Function F1

$$\|F_1\|_2 \leq 10^{-5}$$

$$K_{d1} = \begin{bmatrix} -3.326 & 0.364 \\ -3.337 & 0.348 \end{bmatrix}$$

$$K_{d2} = \begin{bmatrix} 0.103 & -0.893 \end{bmatrix}$$

$$K_{d3} = \begin{bmatrix} -1.575 & -2.507 & -0.981 \\ -1.474 & -2.552 & -1.045 \end{bmatrix}$$

Function F2

$$\|F_2\|_2 \leq 10^{-5}$$

$$K_{d1} = \begin{bmatrix} 3.200 & 0.401 \\ -2.834 & 0.230 \end{bmatrix}$$

$$K_{d1} = \begin{bmatrix} 0.113 & -0.900 \end{bmatrix}$$

$$K_{d3} = \begin{bmatrix} -1.600 & -2.574 & -0.854 \\ -1.449 & -2.528 & -1.001 \end{bmatrix}$$

This example was also solved using the Newton method. The solution time is dependent on the initial values chosen for $c_i (i=1, \dots, n)$. Selecting the c_i equal to the desired eigenvalues required about 10 CP seconds to compute the decentralized gains. The gains matrices obtained are:

$$K_{d1} = \begin{bmatrix} -3.126 & 1.260 \\ -1.915 & 0.094 \end{bmatrix}$$

$$K_{d2} = \begin{bmatrix} -0.6815 & 0.3084 \end{bmatrix}$$

$$K_{d3} = \begin{bmatrix} -2.415 & -3.182 & -7.423 \\ -2.093 & -2.860 & -3.618 \end{bmatrix}$$

For this example both the direct minimization and the Newton Method took essentially the same time. This was thirty percent faster than the 15 sec reported in [97] for solving the same problem using the continuations approach on the CDC 6500 computer which has the same speed as the CDC Cyber 815.

6.7.2 A Three-Machine AC Power System

This example considers the three machine AC power system of Chapter 4 which has been redrawn and modified to show two lines between

buses 2 and 4 with total line impedance remaining the same. This enables the convenient simulation of a line removal with attendant change of operating point. The power system is redrawn in Figure 6.7.

The generators 1 and 2 are represented by fourth order models while generator 3 is represented as a classical second order model. The state equations for the subsystems were given before in Chapter 4. The eigenvalues for the overall system are

$$\begin{aligned} & -0.002664 \pm 0.034648 \\ & -0.000622 \pm 0.022984 \\ & -0.000199 \pm 0.000129 \\ \lambda = & -0.016647 \\ & -0.010373 \\ & -0.000455 \\ & 0.0 \end{aligned}$$

If the system is moved to a new operating point because one of the two lines between bus 2 and bus 4 is opened, the eigenvalues change to

$$\begin{aligned} & -0.002782 \pm 0.034601 \\ & -0.000541 \pm 0.021439 \\ & -0.000191 \pm 0.000137 \\ \bar{\lambda} = & -0.016173 \\ & -0.009981 \\ & -0.000495 \\ & 0.0 \end{aligned}$$

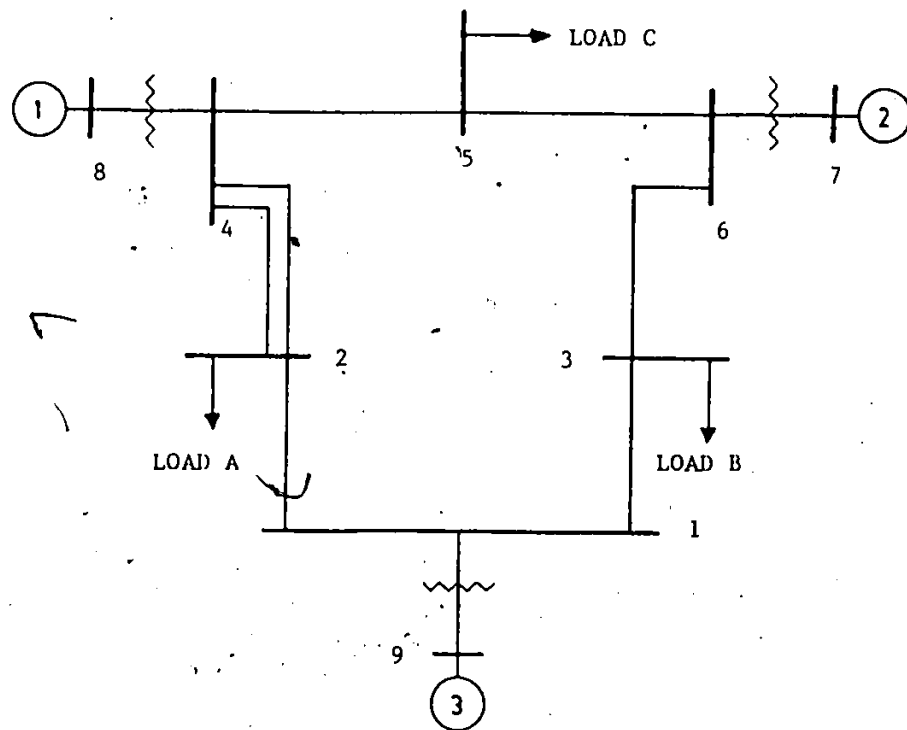


Fig. 6.7 Three-Machine AC Power System

It is desired to move the eigenvalues back to the original location.

The eigenvalues of the three decoupled generator subsystems are

System 1, 0.0
 -0.0.004421
 -0.000450
 0.000440

System 2 0.0
 -0.004958
 -0.000207
 -0.000442

System 3 0.0
 -0.0000561

We first attempt to assign the eigenvalues among the subsystems

$$\begin{aligned} \lambda_1 &= -0.002664 \pm 0.034648 \\ &\quad -0.016647 \\ &\quad -0.000455 \end{aligned}$$

$$\begin{aligned} \lambda_2 &= -0.000622 \pm 0.022984 \\ &\quad -0.010373 \\ &\quad 0.0 \end{aligned}$$

$$\Lambda_3 = -0.000199 \pm 0.000129$$

The gain matrices for the decoupled systems are

$$K_{d10} = \begin{bmatrix} 9569.14 & -1935.14 & -23.89 & -53412.55 \\ 9569.14 & -1935.14 & -23.89 & -53412.55 \\ 9569.14 & -1935.14 & -23.89 & -53412.55 \\ 9569.14 & -1935.14 & -23.89 & -53412.55 \end{bmatrix}$$

$$K_{d20} = \begin{bmatrix} 554.78 & -394.45 & 0.00 & -10812.68 \\ 554.78 & -394.45 & 0.00 & -10812.68 \\ 554.78 & -394.45 & 0.00 & -10812.68 \\ 554.78 & -394.45 & 0.00 & -10812.68 \end{bmatrix}$$

$$K_{d30} = \begin{bmatrix} 0.0026 & 15.85 \\ 0.0026 & 15.85 \end{bmatrix}$$

Note that the desired eigenvalues Λ are much closer to the coupled system eigenvalues $\bar{\Lambda}$ than to the eigenvalues of the decoupled subsystems. Therefore the actual decentralized gains would be smaller as compared to those given above by K_{d0} . Both subroutines ZXMIN and ZXSSQ failed to arrive at the minimum as the interconnections were introduced.

The alternative approach using the inverse eigenvalue based on equation (6.27) gave

$$K_{d1} = \begin{bmatrix} 0.41587 & 0.47010 & 0.10226 & -3.7313 \\ 0.67568 & -0.47228 & 0.56659 & -1.49504 \end{bmatrix}$$

$$K_{d2} = \begin{bmatrix} 0.72922 & -0.80143 & -0.67366 & 2.86279 \\ 0.85452 & -3.32070 & -1.74880 & 0.94660 \end{bmatrix}$$

$$K_{d3} = \begin{bmatrix} 0.49526 & 2.76366 \end{bmatrix}$$

The computation time required on the CDC Cyber 170/815 computer was about 45 seconds.

6.8 Discussion on the Pole Placement Methods

Two methods have been presented for pole placement using decentralized state feedback. The direct minimization method has the advantage that it is easy to program and advantage can be taken of optimization routines. The functions formed for minimization do not require the calculation of eigenvectors and if the second function is used, the calculation of eigenvalues is also not required. By setting the minimization objective the eigenvalues can be brought as close as desired to the specified values. There is little likelihood of the minimization routines converging to some local minima of $\|F_1\|_2$ and $\|F_2\|_2$. The fact that the interconnections are introduced in small

steps ensures that $\|F_1\|_2$ and $\|F_2\|_2$ are never far from their global minimum. The method works well for a loosely coupled system as seen in example in Section 6.7.1. However, for a strongly interconnected system where the system eigenvalues are far from the decoupled subsystem eigenvalues, it is less advantageous. A strongly coupled system necessitates introducing the interconnections in a greater number of steps and results at best, in additional, computation time and at worst, in convergence difficulties with the minimization routine because of round off errors.

The second method is based on formulating the decentralized control problem as an inverse eigenvalue problem. It uses the overall composite system state matrix and uses the Newton Method to calculate the feedback gains iteratively. This method is successful for both loosely and strongly coupled systems. Both decentralized state feedback methods can be easily adapted to include output feedback.

6.9 Summary

This chapter has presented new methods for the analysis and control of large systems. A new eigenvalue tracking method has been suggested which has been shown to be superior in terms of computational effort as compared to repeated eigenvalue computation. The method has been applied to power system examples to track eigenvalue movement with respect to parameter variations as well as identifying as to which modes are contributed by any particular subsystems.

This chapter has also presented new methods for designing decentralized state feedback controllers. Two methods have been suggested. The first is based on using direct minimization using standard optimization routines whereas the second method uses a Newton method to solve for the feedback gain. Both methods have been illustrated by means of examples.

CHAPTER 7

CONCLUSIONS

This thesis presents a comprehensive approach for the steady state stability analysis of AC-DC power systems. Steady state stability is usually determined from the eigenvalues of the system state matrix evaluated at the nominal operating condition. However a knowledge of the eigenvalues is usually not enough to completely characterize system stability. It is necessary to evaluate the degree of stability as a function of the system parameters and its operating point. Also it should be possible to stabilize the system, or if it is stable to improve its stability. A new method is presented for the evaluation of the system state matrix which is then used to develop new algorithms for the stability analysis and control of large power systems.

A review of existing stability analysis methods indicated a need for a state matrix formulation method which was simple to program and computationally efficient while at the same time retained sufficient flexibility to include a wide variety of power system models. The method presented here exploits the powerful features of the Component Connection Method for power system modelling and overcomes the disadvantages of the previous methods. It allows the system state


matrix to be formulated in an elegant yet simple and efficient way. Taking advantage of the nature of power system models, the state matrix for AC power systems is constructed without the need for any matrix inversions.

One feature of the method is that the state matrix is formulated from two separate sets of equations. One set models the component subsystems whereas the other defines the interconnection between the subsystems. The main advantage of this is the great flexibility provided in the modelling of the power system components. As long as the input-output quantities are fixed the modelling complexity of the subsystems may be changed without affecting the interconnection equation. Further, several levels of state matrix assembly may be employed. The state matrix of a generator system consisting of a number of subsystems (e.g., shaft, generator, exciter, etc.) may be constructed first and later the generator itself considered as a subsystem in the overall power system model. The structure of the formulation process is thus compatible with the way power systems develop and the degree of modelling complexity can be matched to the specific simulation problem.

A major advantage of the proposed state matrix formulation method is that it retains the physical identity of the subsystem models. This is extremely useful for analysing the degree of system stability using eigenvalue tracking since it permits the simple evaluation of the derivative of the system state matrix. As shown in Chapter 4 this is accomplished easily using matrix multiplication and

requires less computational effort as compared to the PQR or the elimination methods of state matrix formulation.

In Chapter 5, a compact interconnection equation has been derived relating machine voltages and currents in the presence of a multiterminal HVDC network. This has considerably simplified the state matrix formulation of AC-DC systems which at most requires the inversion of a matrix of the order of twice the number of DC terminals in the system. The HVDC network, the DC terminal controllers and stabilizers are simply treated as additional subsystems in the overall formulation. As before, any degree of modelling detail may be employed and derivatives of the system state matrix are easily obtained.



A major contribution of this thesis is the development of a new eigenvalue tracking algorithm. This algorithm is based on the evaluation of the sensitivity of a matrix determinant and iteratively updates the eigenvalues following any change in the system state matrix. It overcomes the disadvantage of excessive computational effort required particularly where eigenvalue computations are repeated to determine the effect of parameters variation on system stability. The algorithm updates all the system eigenvalues following a parameter change at one-third the cost of recomputing the eigenvalues using the QR algorithm. Used together with the proposed state matrix formulation method, it is especially useful for identifying the modes due to any particular subsystem. It provides the engineer with a flexible and cost effective tool to study the effect of different system parameters on the overall system stability.

The far reaching consequences of the proposed state matrix formulation method have been exploited in the development of two new methods for decentralized pole placement which are also presented in Chapter 6. The first method assigns the given poles among the various subsystems and the elements of the feedback gain matrix are varied to cancel the effects of the system interconnection. This method requires the evaluation of the system eigenvalues and has the advantage of being simple. It works well for a loosely coupled system using standard minimization routines. It is, however, unsuitable for a strongly coupled system which introduces extra computational effort for the minimization routines and may fail to arrive at a solution because of the accumulation of numerical errors. The second method based on the sensitivity of a matrix determinant is, however, well suited for both loosely and strongly coupled systems. The decentralized pole placement problem is considered as an inverse eigenvalue problem and the feedback gain matrix is found using the Newton method. Both methods are easy to implement and computationally efficient.

As part of the comprehensive approach to steady state stability analysis a new AC-DC loadflow scheme has been presented in Chapter 3. It is used to determine the base operating point of the system prior to the evaluation of the system state matrix. The sequential approach is employed and any AC loadflow method can be used. The DC network is solved using the Gauss-Seidel method and any HVDC network configuration and terminals control scheme can be accommodated. The main advantage of this method is that the DC network solution need not be repeated.

Further it ensures that a feasible DC system operating point is selected by comparing the reactive power requirements of the HVDC terminals with the supply capability of the connected AC system.

The methods presented in this thesis have all been verified by applying to realistic power system models, with the computer programs being written for specific system configurations. These have included a single machine infinite bus system, a three-machine AC system with six buses and nine lines and a three-machine three-terminal AC-DC system. These examples contribute significantly to an easier understanding of the various methods and are fairly general and indicative of the fact that the methods are easy to implement and applicable to large scale power systems. The publications [16,99-102] are related to the work reported in this thesis.

The work presented in this thesis provides some promising research directions for the future in the area of power systems stability. In particular, the specific topics which may be considered for further study are:

- (1) The extension of the proposed formulation to study transient stability, the system response to large disturbances.
- (2) the extension of the eigenvalue tracking approach to include systems with repeated eigenvalues.

REFERENCES

- [1] F.P. DeMello, "Power system dynamics - Overview", presented at the Symposium on Adequacy and Philosophy of Modelling: Dynamic System Performance at the IEEE PES Winter Power Meeting, N.Y., IEEE Publ. 75CH0790-4-PWR, Jan. 1975.
- [2] F.P. DeMello and C. Concordia, "Concepts of synchronous machine stability as affected by excitation control", IEEE Trans. PAS-92, pp. 316-329, April 1969.
- [3] IEEE Special Publication, "Analysis and control of subsynchronous resonance", No. 76-CH0066-0-PWR, presented at the IEEE PES Winter Meeting, N.Y. 1976.
- [4] M. Bahrman, E.V. Larsen, R.J. Piwko and H. Patel, "Experience with HVDC - turbine generator torsional interaction at Square butte", IEEE Trans. PAS-99, pp. 966-975, May/June 1980.
- [5] P. Kundur and P.L. Dandeno, "Practical applications of eigenvalue techniques in the analysis of power systems dynamic stability problems", presented at the 5th Power Systems Computation Conference, Cambridge, England, Sept. 1975.
- [6] "First HVDC underwater transmission links mainland and Vancouver Island", Electrical News and Engineering, Vol. 76, pp. 56-57, June 1967.
- [7] R. Banks and C.D. Clarke, "Early operating experience of the Nelson River HVDC Scheme", IEEE Conf Publication No. 107, pp. 232-236.
- [8] F.H. Ryder and F.G. Macloon, "The Eel River HVDC converter station and the development of electric utility interconnections in eastern Canada and U.S.A.", Can. Elec. Assoc. Eng. Op. Div. Meeting, Vancouver, B.C., May 22-25 1971.
- [9] F.H. Lasr, P. Gazzana Priaroggia and F.J. Miranda, "The underground HVDC link for the transmission of bulk power from the Thames Estuary to the Centre of London", IEEE Trans. PAS-90, pp. 1893-1901, July/Aug. 1971.
- [10] D.P. Carroll, J.A. Schassberger and R.A. Fernandes, "The use of voltage feedback in HVDC converter control", IEEE Trans. PAS-95, pp. 1579-1589, Sept./Oct. 1976.
- [11] K. Erikson, G. Liss and E. Persson, "Stability analysis of the HVDC control system transmission calculated Nyquist diagrams", IEEE Trans. PAS-89, pp. 733-740, May/June 1970.

- [12] M.S. Sachdev, R.J. Fleming and J. Chand, "Optimal control of a HVDC transmission link", IEEE Trans, PAS-92, pp. 1958-1965, Nov./Dec. 1973.
- [13] M.S. Sachdev and M.G. Bennett, "System Stabilization using HVDC transmission line control", Paper A 77 089-6, presented at the IEEE PES Winter Meeting, N.Y., Jan. 29 - Feb. 3 1978.
- [14] J.W. Klein, P.C. Krause and R.A. Fernandes, "Investigation of DC modulation of parallel AC-DC power systems", Paper A 78 235-4 presented at the IEEE PES Winter Meeting, N.Y., Jan. 29 - Feb 3 1978.
- [15] P.K. Dash, B. Puthal, O.P. Malik and G.S. Hope, "Transient stability and optimal control of parallel AC-DC power systems", IEEE Trans. PAS-95, pp. 811-820, May/June 1976.
- [16] R.T.H. Alden and F.A. Qureshy, "HVDC - A review of system analysis and applications", Canadian Electrical Engineering Journal, Vol. 9, No. 4, pp. 139-145, Oct. 1984.
- [17] IEEE AC/DC System Dynamic Task Force, "Dynamic performance characteristics of North American HVDC systems for transient and dynamic stability evaluations", IEEE Trans. PAS-100, pp. 3356-3364, July 1981.
- [18] R.L. Cresap and W.A. Mittelstadt, "Small signal modulation of the pacific HVDC intertie", IEEE Trans. PAS-95, pp. 536-541, March/April 1976.
- [19] C.V. Thio, "Nelson River HVDC bipole-two: Part 1 - System aspect", IEEE Trans. PAS-98, pp. 165-173, Jan./Feb. 1979.
- [20] U. Lamm, E. Uhlman and P. Danfors, "Some aspects of tapping HVDC transmission systems", Direct Current, Vol. 18, No. 5, pp. 124-129, May 1969.
- [21] J. Reeve, "Multiterminal HVDC power systems", IEEE Trans. PAS-99, pp. 729-737, May/April 1980.
- [22] G.K. Carter, C.E. Grund, H.H. Happ and R.V. Pohl, "The dynamics of AC-DC systems with controlled multiterminal HVDC transmission", IEEE Trans. PAS-96, pp. 402-413, March/April 1977.
- [23] J. Reeve, I.A. Rose and J. Carr, "Central computer controller for multiterminal HVDC transmission systems", IEEE Trans. PAS-96, pp. 934-944, May/June 1977.

- [24] B.K. Johnson, F.P. DeMello and J.M. Undrill, "Comparing fundamental frequency and differential equation representation of AC-DC", IEEE Trans. PAS-101, pp. 3379-3384, Sept. 1982.
- [25] A.M. Sharaf and R.M. Mathur, "Design of stabilizer loops for multiarea, multiterminal DC-AC Systems - 2. Stabilizing interconnected AC systems by frequency modulation of DC Controls", IEEE PES Summer Meeting, Paper A 79 457-3, Vancouver, B.C., 1979.
- [26] P.K. Dash, M.A. Rahman and P.C. Panda, "Dynamic analysis of power systems with multiterminal HVDC links and static compensators", IEEE Trans. PAS-101, pp. 1332-1341, June 1982.
- [27] L. Lefebvre, D.P. Carroll, R.A. DeCarlo, "Decentralized power modulation of multiterminal HVDC system", IEEE Trans. PAS-100, pp. 3331-3339, July 1981.
- [28] P. Kundur, D.C. Lee, H.M. Zein El-din, "Power system stabilizers for thermal units: Analytical techniques and on-site validation", IEEE Trans. PAS-100, Jan. 1981, pp. 81-95.
- [29] P. Kundur, "Evaluation of methods for studying power system stability", International Symposium on Power System Stability, Iowa State University, Ames, Iowa, May 13-15, 1985.
- [30] R. Foerst, G. Heyner, K.W. Kanngiesser and H. Waldmann, "Multiterminal operation of HVDC converter stations", IEEE Trans. PAS-88, pp. 1042-1052, July 1969.
- [31] E. Uhlmann, "Representation of an HVDC link in a network analyser", CIGRE, Paris, France, Paper 404, 1960.
- [32] T. Horigome and J. Reeve, "Equivalent circuits of interconnected AC-DC-AC power transmission systems", International Journal of Elect. Eng. Education, Vol. 1, pp. 503-509, 1964.
- [33] T. Horigome and N. Ito, "Digital computer method for the calculation of power flow in an AC-DC interconnected power system", Proc IEE, Vol. III, pp. 1137-1144, June 1964.
- [34] B. Stott and O. Alsac, "Fast decoupled loadflow", IEEE Trans. PAS-93, pp. 859-869, May/June 1974.
- [35] I.E. Barker and B.A. Carre, "Loadflow calculations for systems containing HVDC links", IEEE Conf. Publ. No. 22, UMIST, pp. 115-118, Sept. 1966.

- [36] G.D. Breuer, J.F. Luini and C.C. Young, "Studies of large AC-DC systems on the digital computer", IEEE Trans. PAS-85, pp. 1107-1116, Nov. 1966.
- [37] N.G. Hingorani and J.D. Mountford, "Simulation of HVDC systems in AC loadflow analysis, by digital computers", Proc. IEEE, Vol. 113, pp. 1541-1546, Sept. 1966.
- [38] H. Sato and J. Arrillaga, "Improved loadflow techniques for integrated AC-DC systems", Proc. IEEE, Vol. 116, pp. 525-532, April 1969.
- [39] J. Reeve, G. Fahmy and B. Stott, "Versatile loadflow method for multiterminal HVDC systems", IEEE Trans. PAS-96, pp. 925-933, May/June 1977.
- [40] C.M. Ong and A. Hamzei-Najad, "A general purpose multiterminal DC loadflow", IEEE Trans. PAS-100, pp. 3166-3174, July 1981.
- [41] H. Fudeh and C.M. Ong, "A simple and efficient AC-DC loadflow method for multiterminal DC systems", IEEE Trans. PAS-100, pp. 4389-4396, Nov. 1981.
- [42] D.A. Braunagel, L.A. Kraft and J.L. Whysong, "Inclusion of DC converter and transmission equation directly in a Newton power flow", IEEE Trans. PAS-95, pp. 76-88, Jan./Feb. 1976.
- [43] G.B. Sheble and G.T. Heydt, "Power flow studies for all systems with HVDC transmission", Proc. of the PICA Conference, pp. 223-228, New Orleans, 1975.
- [44] J. Arrillaga and P. Bodger, "Integration of HVDC links with fast decoupled loadflow solutions", Proc. IEE, Vol. 124, pp. 463-468, May 1977.
- [45] J. Arrillaga and P. Bodger, "ACDC loadflows with realistic representation in converter plant", Proc. IEE, Vol. 125, pp. 41-46, Jan. 1978.
- [46] M.M. El-Marsafawy and R.M. Mathur, "A new fast technique for loadflow solutions of integrated multiterminal DC-AC systems", IEEE Trans. PAS-99, pp. 246-255, Jan./Feb. 1980.
- [47] S.M. Shinnars, Modern Control System Theory and Application, Addison-Wesley Publishing Company, Reading, Mass., 1978.
- [48] B.C. Kuo, Automatic Control Systems, Prentice Hall, New Jersey, 1975.

- [49] M. Enns, J.E. Matheson, J.R. Greenwood and F.T. Thomson, "Practical aspects of state space methods", Joint Automatic Control Conference, Stanford, California, pp. 494-513, 1964.
- [50] M.A. Laughton, "Matrix analysis of dynamic stability in synchronous multimachine systems", Proc. IEE, Vol. 113, pp. 325-336, Feb. 1966.
- [51] J.H. Anderson, "Matrix methods for the study of a regulated synchronous machine", Proc. IEEE, Vol. 57, pp. 2122-2139, 1969.
- [52] J.H. Anderson, D.F. Leffew and V.M. Raina, "Dynamic modelling of an arbitrary number of interconnected power generating units", Paper C73-093-2 presented at IEEE PES Winter Meeting, New York, N.Y., Jan. 1973.
- [53] P.J. Nolan, N.K. Sinha and R.T.H. Alden, "Eigenvalue sensitivities of power systems including network and shaft dynamics", IEEE Trans. PAS-95, pp. 1318-1324, July/Aug. 1976.
- [54] R.T.H. Alden and H.M. Zein El-din, "Multimachine dynamic stability calculations", IEEE Trans. PAS-95, pp. 1529-1534, Sept./Oct. 1976.
- [55] J.M. Undrill, "Dynamic stability calculations for an arbitrary number of interconnected synchronous machines", IEEE Trans. PAS-87, pp. 835-844, March 1968.
- [56] M.J. Muir and V.J. Gosbell, "Computer formulation of state matrix for large power systems", IFAC Symposium, Melbourne, Australia, pp. 21-25, Feb. 1977.
- [57] H.M. Zein El-din and R.T.H. Alden, "An efficient multimachine formulation for power system dynamic stability studies including electrical transients", paper C85-242, presented at International Conference and Exposition, Toronto, Ont., Oct. 1975.
- [58] E.V. Larsen and W.W. Price, "Manstab/Possim power system dynamic analysis program - A new approach combining non-linear simulation and linearized state-space/frequency domain capabilities", Proc. of the PICA Conf., pp. 350-358, May 1977.
- [59] G. Dahlquist and A. Björck, Numerical Methods, Prentice Hall, New Jersey, U.S.A., 1974.
- [60] C. Concordia, "Steady state stability of synchronous machines as affected by voltage regulator characteristics", AIEE Trans., Vol. 63, pp. 215-220, May 1944.

- [61] D.N. Ewart and F.P. deMello, "A digital computer program for the automatic determination of dynamic stability limits", IEEE Trans. PAS-86, pp. 867-875, July 1967.
- [62] K. Bollinger, A. Laha, R. Hamilton and T. Harras, "Power system stabilizer using root-locus methods", IEEE Trans. PAS-94, pp. 1484-1488, Sept./Oct. 1975.
- [63] C. Concordia, "Synchronous machine damping and synchronizing torques", AIEE Trans., Vol. 70, pp. 731-737, 1951.
- [64] J.E. Van Ness, J.M. Boyle and F.P. Imad, "Sensitivities of large multiple-loop control systems", IEEE Trans. AC-14, pp. 308-315, July 1965.
- [65] A. Kasturi and P. Doraju, "Sensitivity analysis of a power system", IEEE Trans. PAS-92, pp. 1521-1529, Oct. 1969.
- [66] G. Gross, C.F. Imparato, P.M. Look, "A tool for the comprehensive analysis of power system dynamic stability", IEEE Trans. PAS-101, pp. 226-234, Jan. 1982.
- [67] J.H. Wilkinson, The algebraic eigenvalue problem, The Oxford University Press, 1965.
- [68] D.K. Faddeev and V.N. Faddeeva, Computational methods of linear algebra, Freeman, San Francisco, California, 1963.
- [69] B.S. Morgan, "Sensitivity analysis and synthesis of multivariable systems", IEEE Trans. AC-11, pp. 506-512, July 1966.
- [70] H.M. Zein Eldin and R.T.H. Alden, "Second order eigenvalue sensitivities applied to power system dynamics", IEEE Trans. PAS-97, pp. 1521-1529, 1977.
- [71] Z. El-razzaz and N.K. Sinha, "Dynamic stability analysis for large parameter variations: an eigenvalue tracking approach", Proc. IEE, Vol. 128, pp. 268-274, Nov. 1981.
- [72] H.M. Zein El-din and R.T.H. Alden, "A computer based eigenvalue approach for power system dynamic stability evaluation", Proc. of the PICA Conference, pp. 186-192, May 1977.
- [73] D.B. Goudie, "Steady state stability of parallel HV AC-DC power transmission systems", Proc. IEE, Vol. 119, pp. 216-224, Feb. 1972.

- [74] J.W. Klein, C.M. Ong, P.C. Krause and R.A. Fernandes, "Dynamic stability assessment model of a parallel AC-DC power system", IEEE Trans. PAS-96, pp. 1296-1304, July/Aug. 1977
- [75] K.R. Padiyar, M.A. Pai and C. Radhakrishna, "A versatile system for the dynamic stability analysis of power systems including HVDC links", IEEE Trans. PAS-100, pp. 1871-1880, April 1981.
- [76] A.M. Sharaf and R.M. Mathur, "Design of stabilizer loops for multi-area multiterminal DC-AC systems: Part I - Derivation of a small displacement linearized model", Paper A 79 456-5, presented at the IEEE PES Summer Meeting, July 15-20, Vancouver, B.C., 1979.
- [77] P.K. Dash, M.A. Rahman and P.C. Panda, "Dynamic analysis of power systems with multiterminal HVDC links and static compensators", IEEE Trans. PAS-101, pp. 1331-1341, June 1982.
- [78] C. Adamson and N. Hingorani, High Voltage Direct Current Power Transmission, London, Garraway Ltd., 1960.
- [79] E. Kimbark, Direct Current Transmission, Wiley - Interscience, New York, 1971.
- [80] J. Arrillaga, C.P. Arnold and B.J. Harker, Computer Modelling of Electrical Power Systems, Wiley - Interscience, New York, 1983.
- [81] P.M. Anderson and A.A. Fouad, Power System Control and Stability, Iowa State Univ. Press, Ames, Iowa, 1977.
- [82] Saeks and R.A. DeCarlo, "Interconnected dynamical systems", Marcel Dekker, N.Y., 1980.
- [83] IEEE Committee Report, "Excitation system dynamic characteristics", IEEE Trans. PAS-92, pp. 64-75, Jan./Feb. 1973.
- [84] IEEE Committee Report, "Dynamic models for steam and hydro turbines in power system studies", IEEE Trans. PAS-92, pp. 1904-1915, Nov./Dec. 1973.
- [85] D.G. Taylor, "Analysis of synchronous machines connected to power system networks", Proc. IEE, (London), Vol. 109, pt. C, pp. 606-610, 1962.
- [86] C. Concordia, Synchronous machines, John Wiley & Sons, New York, 1951.

- [87] J. Janischewskyj and P. Kundur, "Simulation of the non-linear dynamic response of interconnected synchronous machines", IEEE Trans. PAS-91, pp. 2064-2069, Sept./Oct. 1972.
- [88] P.J. Nolan, "Power system stability including shaft and network dynamics", Ph.D. Thesis, McMaster University, 1976.
- [89] IEEE Committee Report, "Functional model of two-terminal HVDC systems for transient and steady state stability", Paper 83 SM646-5, IEEE PES Summer Meeting, July 17-22, 1983.
- [90] R.J. Kuhler and V.J. Watson, "Eigenvalue analysis of synchronous machines", IEEE Trans. PAS-94, pp. 1629-1634, Sept./Oct. 1975.
- [91] J.H. Anderson, "The control of a synchronous machine using optimal control theory", Proc. IEEE, Vol 59, pp. 25-35, 1971.
- [92] P.N. Paraskevopoulos, C.A. Tsonis and S.G. Tzafestas, "Eigenvalue sensitivity of linear time invariant control systems with repeated eigenvalues", IEEE Trans. AC-19, pp. 610-612, Oct. 1974.
- [93] M.K. El-sherbiny and D.M. Mehta, "Dynamic system stability, Part I - investigation of different loadings and excitation systems", IEEE Trans. PAS-92, pp. 1538-1546, Sept./Oct. 1973.
- [94] S.H. Wang and E.J. Davison, "On the stabilization of decentralized control systems", IEEE Trans. AC, Vol. AC-18, pp. 473-478, Oct. 1973.
- [95] J.B. Corfmat and A.S. Morse, "Decentralized control of linear multivariable systems", Automatica, Vol. 12, pp. 479-495, Sept. 1976.
- [96] R. Saeks, "On the decentralized control of interconnected dynamical systems", IEEE Trans. AC, Vol. AC-24, pp. 269-271, April 1979.
- [97] S. Lefebvre, S. Richter and R. DeCarlo, "Eigenvalue assignment via decentralized state feedback", Proc. of the 18th Annual Allerton Conference on Communication, Control and Computing, pp. 909-918, Oct. 8-10, 1980.
- [98] F.W. Biegler-Konig, "A Newton iteration process for inverse eigenvalue problems", Numerische Mathematik, Vol. 37, pp. 349-354, April 1981.

- [99] R.T.H. Alden and F.A. Qureshy, "Application of the component connection method to power system calculations", Paper No. 83192, presented at the International Electrical and Electronics Conference and Exposition, Sept. 1983, Toronto, Ontario.
- [100] F.A. Qureshy and R.T.H. Alden, "Decentralized state feedback methods for spectrum assignment", Paper 84R364, presented at the IEEE International Symposium on Circuits and Systems, May 7-10, 1984, Montreal, Quebec.
- [101] F.A. Qureshy and R.T.H. Alden, "Multiterminal AC-DC loadflow method", Paper 068-027, presented at the Ninth IASTED Conference on Energy, Power and Environmental Systems, June 4-6, 1984, San Francisco.
- [102] R.T.H. Alden and F.A. Qureshy, "Eigenvalue tracking due to parameter variation", scheduled for publication, IEEE Transactions on Automatic Control, Vol. AC-30, No. 7, July 1985.

APPENDIX I

PER UNIT SYSTEM

In this Appendix the per unit systems followed in the thesis are presented. The per unit system for the AC-DC loadflow equations is based on three phase power as given in Appendix 1.1. The subsystems equations for stability studies however are based on a single phase power base because the power invariant modified Park transformation is used for representing the machines equations in d, q form.

1.1. Per Unit System for AC-DC Loadflow

For loadflow analysis it is customary to work in terms of three phase power as base. The same power base is chosen for AC and DC systems

$$P_{AC \text{ BASE}} = P \text{ MW (three phase power)}$$

$$V_{AC \text{ BASE}} = V \text{ KV (line to line)}$$

$$I_{AC \text{ BASE}} = \frac{P}{\sqrt{3}V} \times 10^3 \text{ A}$$

$$Z_{AC \text{ BASE}} = \frac{V}{\sqrt{3}I_{AC \text{ BASE}}} \text{ ohms}$$

For the DC side a current base is chosen such that

$$I_{DC \text{ BASE}} = \frac{\pi}{\sqrt{6}} I_{AC \text{ BASE}} \text{ A}$$

Now

$$P_{DC \text{ BASE}} = P_{AC \text{ BASE}} \text{ MW}$$

$$V_{DC \text{ BASE}} I_{DC \text{ BASE}} = \sqrt{3} V_{AC \text{ BASE}} I_{AC \text{ BASE}}$$

$$V_{DC \text{ BASE}} = \frac{3/2}{\pi} V_{AC \text{ BASE}} \text{ KV}$$

and

$$Z_{DC \text{ BASE}} = \frac{18}{\pi^2} Z_{AC \text{ BASE}}$$

1.2 Per Unit System for Stability Analysis

The per unit system was selected so as to use the power invariant Park transformation.

$$P_{\text{BASE}} = P \text{ MW} \quad (\text{single phase power})$$

$$V_{\text{BASE}} = V_{LN} \text{ KV} \quad (\text{line to neutral})$$

$$I_{\text{BASE}} = \frac{P_{\text{BASE}}}{V_{\text{BASE}}} = I_L \text{ A}$$

$$t_B = \frac{1}{\omega_{\text{BASE}}} \text{ secs}$$

APPENDIX II

SUBSYSTEM MODELS

The equations describing the performance of each subsystem are presented here. The models have been taken directly from the text by Anderson [81] with the equations have been rearranged in a matrix form.

2.1 Synchronous Machine

Synchronous machine modelling has been considered by many authors. Either stator and rotor currents referred to the machine rotor frame or stator and rotor fluxes referred to the machine rotor frame, may be chosen as states. In this Appendix stator and rotor currents have been selected as states, primarily because this approach allows a direct coupling between machine and network equations and the inclusion of stator transients.

The linearized differential equations for a synchronous machine are now given with the Δ prefix omitted for convenience. The state equation is obtained from

$$\begin{bmatrix} 1 & & & & \lambda_{q0} \\ & 1 & & & \\ & & 1 & & \\ & & & 1 & -\lambda_{d0} \\ & & & & 1 \end{bmatrix} \begin{bmatrix} v_d \\ -v_f \\ 0 \\ v_q \\ 0 \\ \omega \end{bmatrix}$$

$$= - \begin{bmatrix} r_s & & & \omega_0 x_q & \omega_0 x_{aq} \\ & r_f & & & \\ & & r_{kd} & & \\ -\omega_0 x_d & -\omega_0 x_{af} & -\omega_0 x_{ad} & r_s & \\ & & & & r_{kq} \end{bmatrix} \begin{bmatrix} i_d \\ i_f \\ i_{kd} \\ i_q \\ i_{kq} \end{bmatrix}$$

$$= \begin{bmatrix} x_d & x_{af} & x_{ad} & & & \\ x_{af} & x_f & x_{fd} & & & \\ x_{ad} & x_{fd} & x_{kd} & & & \\ & & & x_q & x_{aq} & \\ & & & x_{aq} & x_{kq} & \end{bmatrix} \begin{bmatrix} i_d \\ i_f \\ i_{kd} \\ i_q \\ i_{kq} \end{bmatrix} \quad (2.1)$$

The output equations are given by

$$\begin{bmatrix} \dot{i}_d \\ \dot{i}_q \\ T_E \end{bmatrix} = \begin{bmatrix} 1 & 0 & 0 & 0 & 0 \\ 0 & 0 & 0 & 1 & 0 \\ \frac{-\lambda_{q0} + x_d i_{q0}}{3} & \frac{x_{af} i_{q0}}{3} & \frac{x_{ad} i_{q0}}{3} & \frac{\lambda_{d0} - x_q i_{d0}}{3} & \frac{x_{aq} i_{d0}}{3} \end{bmatrix} \begin{bmatrix} i_d \\ i_f \\ i_{kd} \\ i_q \\ i \\ kq \end{bmatrix} \quad (2.2)$$

2.2 Shaft Subsystem

The generator shaft is modelled as a second order system with the state equation as:

$$\begin{bmatrix} \dot{\delta} \\ \dot{\omega} \end{bmatrix} = \begin{bmatrix} 0 & 1 \\ 0 & \frac{-D}{2H\omega_0} \end{bmatrix} \begin{bmatrix} \delta \\ \omega \end{bmatrix} + \begin{bmatrix} 0 & 0 \\ \frac{1}{2H\omega_0} & -\frac{1}{2H\omega_0} \end{bmatrix} \begin{bmatrix} T_m \\ T_e \end{bmatrix} \quad (2.3)$$

$$\begin{bmatrix} \delta \\ \omega \end{bmatrix} = \begin{bmatrix} 1 & 0 \\ 0 & 1 \end{bmatrix} \begin{bmatrix} \delta \\ \omega \end{bmatrix} \quad (2.4)$$

2.3 Excitation System

The IEEE Type 1 rotating exciter has been used in this thesis and is shown in Figure A.1. The exciter is represented in state space form as

$$\begin{bmatrix} \dot{V}_R \\ \dot{V}_1 \\ \dot{V}_3 \\ \dot{E}_{fd} \end{bmatrix} = \begin{bmatrix} -\frac{1}{\tau_R} & 0 & 0 & 0 \\ -\frac{K_A}{\tau_A} & -\frac{1}{\tau_A} & -\frac{K_A}{\tau_A} & 0 \\ 0 & \frac{K_f}{\tau_E \tau_F} & -\frac{1}{\tau_F} & -\frac{-K_R(K_E + S_E)}{\tau_F \tau_E} \\ 0 & \frac{1}{\tau_E} & 0 & \frac{-(K_E + S_E)}{\tau_E} \end{bmatrix} \begin{bmatrix} V_R \\ V_1 \\ V_3 \\ E_{fd} \end{bmatrix} + \begin{bmatrix} \frac{1}{\tau_R} & 0 \\ 0 & \frac{K_A}{\tau_A} \\ 0 & 0 \\ 0 & 0 \end{bmatrix} \begin{bmatrix} V_t \\ V_{ref} \end{bmatrix} \quad (2.5)$$

$$V_f = \begin{bmatrix} 0 & 0 & 0 & \frac{\tau_f/3}{\omega x_{af}} \end{bmatrix} \begin{bmatrix} V_R \\ V_1 \\ V_3 \\ E_{fd} \end{bmatrix} \quad (2.6)$$

2.4 Converter Controllers

The DC Converter Controllers are modelled by a single time constant circuit. The constant current converter is represented as

$$[\dot{\alpha}] = \left[-\frac{1}{\tau_c} \right] [\alpha] + \left[\frac{K_c}{\tau_c} - \frac{K_c}{\tau_c} - \frac{K_c}{\tau_c} \right] \begin{bmatrix} I_{DC} \\ I_{REF} \\ V_{ST} \end{bmatrix}$$

The constant voltage controller is represented as follows

$$[\dot{\alpha}] = \left[-\frac{1}{\tau_V} \right] [\alpha] + \left[\frac{K_V}{\tau_V} - \frac{K_V}{\tau_V} - \frac{K_V}{\tau_V} \right] \begin{bmatrix} V_{DC} \\ V_{REF} \\ V_{ST} \end{bmatrix}$$